AN ABSTRACT OF THE THESIS OF

Nicole S. Rogers for the degree of Master of Science in Sustainable Forest Management presented on July 31, 2013.

Title: Estimation of Leaf Area Index and Simulation of Evapotranspiration for Intensively Managed Douglas-fir Forests.

Abstract approved:

_____

Douglas A. Maguire

Understanding the tradeoff between water use and productivity is critical for modeling growth of intensively managed Douglas-fir forests in the Pacific Northwest. Evapotranspiration is closely linked to carbon dioxide intake during the process of photosynthesis. However, summer drought characterizing the growing season in this region imposes a limit on carbon dioxide intake due to plant responses that limit water loss to reduce potential for cavitation. Therefore, understanding or predicting the rate of water use and the effect of soil water potential and vapor pressure deficits on foliar exchange of both H_20 and CO_2 is important for simulating the net primary production of a given forest site. This project explores methods for estimating daily and seasonal evapotranspiration, compares estimates of evapotranspiration to soil water drawn down, and tests the relationship between water use and productivity.

A frequently used equation for simulation of forest evapotranspiration is the Penman-Monteith equation. Many forms of this equation can be found throughout the literature, covering a wide range of complexity. The performance of this equation depends on the accuracy of estimating its individual components, for example, Leaf Area Index (LAI). LAI is a key parameter of evapotranspiration equations because this index accounts for the surface area over which evapotranspiration occurs.

Three common methods of LAI estimation were compared to determine the most accurate value for simulating evapotranspiration. Methods explored included, LAI estimation through measure of light attenuation, sapwood area allometrics, and estimation from foliage mass measurements. Methods were employed across Douglas-fir (*Pseudotsuga menzsii*) stands in the Oregon Coast Ranges representing a range in structural characteristics, due to management and age. To best predict LAI in stands with structural and management variability, estimates of LAI from foliage mass were determined to be most appropriate. LAI from light attenuation consistently under predicted LAI, and estimates of LAI from sapwood allometrics were unable to capture appropriate estimates from stands with an LAI greater than eight.

Utilizing estimated LAI, seasonal and daily evapotranspiration was determined for the summer growing season of 2012. Evapotranspiration values were validated through comparison to soil water loss (m^3/m^3) measured throughout the growing season. Variability in stand and soil structural properties were thought to contribute to the range in measured soil water loss at both a daily and seasonal scale. Cumulative water loss over the growing season ranged from 0.0635 m^3/m^3 to 0.2706 m^3/m^3.

Variability in evapotranspiration calculated from a simple Penman-Montieth equation was also seen at each plot at both the daily and seasonal resolution. Cumulative evapotranspiration calculated at each study plot ranged from 0.2 to 1.0 m^3/m^3. A plot level comparison of calculated evapotranspiration and soil moisture at both daily and seasonal scales showed that simple measures of soil water loss cannot currently be used to validate evapotranspiration.

Estimation of Leaf Area Index And Simulation of Evapotranspiration in Intensively Managed Douglas-Fir Forests

by

Nicole S. Rogers

A THESIS

submitted to

Oregon State University

in partial fulfillment of
the requirements for the
degree of

Master of Science

Presented July, 31, 2013

Commencement June 2014

Master of Science thesis Nicole S. Rogers presented on July 31, 2013.

APPROVED:

Major Professor, representing Sustainable Forest Management

Head of the Department of Forest Engineering, Resources & Management

---

Dean of the Graduate School

I understand that my thesis will become part of the permanent collection of Oregon State University libraries. My signature below authorizes release of my dissertation to any reader upon request.

Nicole S. Rogers, Author

ACKNOWLEDGEMENTS

More people than I can count have been instrumental in completion of my master's degrees, but above all has been my advisor, Dr. Doug Maguire. I am incredibly grateful to have worked with Doug, who always had time for intelligent insight and equally as helpful, a good laugh.

I would also like to thank each of my committee members, Dr. John Becker-Bleese Dr. David Marshall, and Dr. Robin Rose. The time, feedback, and thoughtful perspectives they each gave to this project are greatly appreciated. In particular, I would like to thank David for taking the extra time to review data at every step and Robin for providing a wealth of academic and life advice.

A very sincere thank you is extended to George McFadden of the Bureau of Land Management who made sure this project had access to all the data and resources we could ask for.

To each member of the distinguished Maguire staff, thank you for all the support you have provided along the way, in particular Nate Osborne, Doug Mainwaring and Kristin Coons. Nate's funny stories and incredible work ethic made 600 tree cores fly by. Doug's quick wit and willingness to help out has certainly moved this research forward and even made hikes to Plot 314 bearable. Kristin has an uncanny ability to provide good conversation and a stroll by the river when they are needed most.

A very heartfelt thank you to each desk owner in Peavy 106. Our many laughs and utterly ridiculous conversations have made the time fly.

My master's degree could never have been completed without the love and encouragement of my family, friends, and dearly missed Maineiacs. My parents have continually reminded me of the value to be had a in a good work ethic and their unwavering confidence in me has repeatedly provided the motivation required to complete this degree. Just as important as confidence is the ability stay grounded, for

that I’m incredibly thankful to my sister, Jenn, who has never let me take myself too seriously with her truthful words and amusing mid-day phone calls. Kate provided a friendship that has kept me sane through her ability to deliver good conversation, a good laugh, and always, a well-timed pep talk. Finally, I would like to thank Mark whose go-with-the-flow attitude, patience, and unwavering love and support have made all the difference.

CONTRIBUTION OF AUTHORS

This thesis is a collective effort of many collaborators from different organizations and members of the College of Forestry. In Chapter 2, Doug Mainwaring performed the destructive sampling used to estimate leaf area index and David Marshall provided the quality control on tree re-measurement data used in this study. In Chapter 3, Dr. Jeff Hatten provided methodology for calculation of daily volumetric water content. In Chapter 4, Doug Mainwaring developed estimates of periodic annual increments used for growth assessments.

TABLE OF CONTENTS

TABLE OF CONTENTS (continued)

Page

LIST OF TABLES

LIST OF TABLES (continued)

Table Page

LIST OF FIGURES

LIST OF FIGURES (continued)

Figure Page

LIST OF FIGURES (continued)

Figure Page

LIST OF APPENDIX FIGURES

CHAPTER 1: INTRODUCTION

Forest Growth and Yield Models

Forest growth models provide forest managers and researchers with a unique opportunity to explore how a spectrum of actions may affect the future condition of forests. Early forest growth models date back to the 18th and 19th centuries when yield tables were used to predict expected stand volumes and other attributes under a given management regime (Monserud, 2003). Today, most forest models can be categorized as one of two general types, empirical or process-based (Korzukhin et al., 1996). Empirical models, similar to the early yield tables, use site specific data to provide detailed predictions of growth at the tree and stand level based on statistical models of varying sophistication. Process models are based on physiological principles and aim to explain the mechanisms which drive productivity, such as photosynthesis, respiration, and nutrient cycling (Monserud, 2003). Each model type presents several shortcomings, however. Empirical models, without a link to underlying growth processes necessarily assume static environmental conditions as represented by the recent past, while process models can be challenging to parameterize because many physiological relationships are still difficult to quantify and are poorly understood (Pinjuv et al., 2006; Makela et al., 2000). A proposed solution to the limitations of empirical and process models has been the creation of hybrid models, which combine the strengths of each (Kimmins et al. 1991; Landsberg, 2003; Weiskittel et al., 2009). Yet, to make useful and successful hybrid models, research is still needed to identify the key physiological processes and simulate the related components of forest productivity with sufficient accuracy and precision.

Evapotranspiration

One physiological process embedded in net gas exchange and essential to forest productivity is evapotranspiration, a process that forms a functional link between tree water use and intake of carbon dioxide for photosynthesis. Evapotranspiration is a combination of two processes, evaporation of water from the soil or vegetation surface

and stomatal transpiration of water vapor from leaves into the atmosphere. The extent to which each process contributes to total evapotranspiration is due largely to canopy cover; i.e., when canopies are open soil evaporation can contribute proportionately more to total evapotranspiration, but under closed canopies transpiration is the dominant component (FAO, 1998). Evapotranspiration is driven by climatic factors and physiological parameters. Climatic factors include solar radiation, air temperature, wind speed, humidity, and vapor pressure deficits. Evapotranspiration is controlled physiologically by leaf area index, stomatal conductance, and water uptake by roots (Taiz and Zeiger, 2006; Fitter and Hay, 2002). Solar radiation provides the energy needed to convert water from liquid state to vapor as the molecules move from the mesophyll cells to the substomatal cavities in leaves. Air temperature to a lesser extent can also provide energy by conduction and convection (Taiz and Zeiger; 2006, Monteith, 1965). During transpiration water vapor must diffuse through the stomatal pore to reach the surrounding air. During the diffusion of water vapor from leaves to the air, two forms of resistance can be encountered; resistance from the stomatal pore and resistance from the unstirred air of relatively high humidity lying near the leaf surface, known as the boundary layer. Boundary layer resistance can be reduced when wind moves the stagnant air of higher humidity. As water vapor moves from leaves to the immediately surrounding air, humidity increases in absence of air movement. If the surrounding air reaches its saturation point, transpiration will stop as diffusion is driven by a concentration gradient. However, if wind replaces the saturated air with air of lower humidity and higher evaporative demand, transpiration can continue until declining water potentials internal to the plant cause the stomata to close and thereby prevent desiccation of leaves. Evaporative demand is measured by the difference between actual moisture in the air and its potential moisture holding capacity, commonly referred to as the vapor pressure deficit. (Taiz and Zeiger, 2006; Waring and Running, 1998).

A tradeoff between water loss and growth is driven by the balance between stomatal regulation of evapotranspiration and associated intake of carbon dioxide during

photosynthesis. A very significant amount of water is lost for each carbon dioxide molecule absorbed, yet desiccation of leaves can often be prevented through closing of stomata at night and replenishment of water from the soil. Under water stressed conditions, if limited water is available from the soil, trees may also keep their stomata closed during the day to prevent cavitation and associated disruption of water flow through the xylem, thereby delaying resumption of gas exchange and tree growth until the water balance becomes more favorable (Fitter and Hay, 2002). In regions such as the northwestern United States that routinely experience drought conditions during the summer growing season, understanding controls on evapotranspiration is of particular importance (Waring and Franklin, 1979; Waring et al., 2008).

Many methods and models have been developed across a range of disciplines in an attempt to accurately estimate evapotranspiration. Methods used in forestry include sap flow measurements, soil water budgets, eddy correlation, the Bowen ratio, and detailed equations for simulating physiological processes (Spittlehouse, 1981; Wilson et al., 2001; Price and Black, 1989; Granier, 1986; Moore et al., 2011).

In relatively simple forest ecosystems, the Penman-Monteith equation is applied for estimation of evapotranspiration. H.L. Penman developed the first form of the equation in 1948 as a way to predict evapotranspiration from climatic variables (Penman, 1948; Allen, 1986). The equation was later modified by Monteith to include aerodynamic and canopy resistance (Monteith, 1965; Allen, 1986). Additional forms of the Penman-Monteith equation have been created throughout the years, but the variant that would potentially provide the best estimate of evapotranspiration for a given forest ecosystem remains unclear. However, through comparative analysis of model forms and improved estimates of individual components based on direct measurements, there is potential to improve the accuracy of simulating evapotranspiration from forest ecosystems.

Leaf Area Index

One key component driving Penman-Monteith equations is leaf area index, a unit-less measure of projected leaf area per ground area, i.e., m^2 m^{-2}. Leaf area is also a key physiological component in modeling forest growth given its strong influence on light interception, water loss, and carbon fixation. In short, leaf area is directly related to photosynthetic capacity and potential transpiration from a forest canopy (Bolstad and Gower, 1990; Gholz, 1982; Landsberg, 2003). Increasing foliage area means increasing surface area for trees to absorb the light energy needed for photosynthesis. Greater foliage surface area also translates into a larger number of stomata, the small pores on each leaf that regulate gas exchange of water and CO_2. Empirically, leaf area has been found to have high correlation with measures of productivity, such as net primary production (NPP), the amount of organic dry matter that plants store in excess of the amount released during construction and maintenance respiration (Gholz, 1982; Fitter and Hay, 2002).

The spectrum of variability in leaf area across a stand can make it a challenging parameter to estimate, but one that is crucial to obtain for process models (Jonckheere et al., 2003). Variability in leaf area can be attributed to climatic changes, such as water availability and temperature, management activities, natural disturbance history, and their net effect on stand structure (DeRose and Seymour, 2010; Medhurst and Beadle, 2000; Gholz, 1982).

Methods for measuring leaf area index fall into two categories, direct and indirect measurements. Direct measurements provide calibration for indirect methods, yet can be time consuming and hence expensive to collect. Methods of direct measurement include destructive sampling and leaf litter collection (Breda, 2003; Jonckheere et al., 2003). A variety of tools have been developed for indirect measurements of LAI, but common methods include: calculation of LAI through measurement of light attenuation (e.g., Li-Cor LAI-2200 Plant Canopy Analyzer) while assuming conformity to the Beer-Lambert law (Bolstad and Gower, 1990; Vose et al., 1995);

allometric relationships that predict LAI from tree diameter (Kittredge 1944) or sapwood area (Waring et al., 1982; Whitehead et al., 1984; Smith et al., 1991); and remote sensing using techniques such as satellite data (Nemani et al. 1993) or terrestrial LiDAR (Dewey et al., 2006; Breda, 2003; Jonckheere et al., 2003). Two commonly used methods of estimation that will be validated in this project are light attenuation with the Li-Cor 2200 Plant Canopy Analyzer and leaf area:sapwood area ratios.

Why Douglas-fir?

In the Pacific Northwest, Douglas-fir (*Pseudotsuga menziesii)* is the primary commercial conifer species and dominates the structure and function of many forested ecosystems; hence, it is frequently the target for improved models for predicting productivity under a variety of management and climate change scenarios. Douglas-fir is native to the region and has the largest latitudinal range of any commercial conifer species in western North America (U.S. Forest Service). Following an inverted "V" shape, Douglas-fir runs from British Columbia south along the Pacific Coast Ranges into California and down the Rocky Mountains in scattered concentrations to Mexico. Douglas-fir is especially important to the state of Oregon as it accounts for more of the annual board foot harvest of timber than any other species in the state (U.S. Forest Service, 2011). Douglas-fir also covers the largest area of forested ecosystems across public and private ownerships (U.S. Forest Service, 2007). The species' economic importance has sparked much interest in identifying management practices that optimize productivity across a range in site types. A study by Hermann and Lavendar (1999) found that thinning and fertilization tripled Douglas-fir yield to 643 m^3/ha compared to unmanaged stands with a yield of 174 m^3/ha at the end of a 50 year harvest rotation. However, timing of management practices and characteristics of the growing site can impact Douglas-fir productivity. Carter et al. (1997) found the inconsistent response of Douglas-fir to fertilizer across sites; rather, responses varied greatly depending on the site specific values of soil nitrogen and site index. Similarly, for Douglas-fir to achieve the desired response to management practices, many soil,

climatic, and stand structural variables must be taken into consideration. Through growth modeling, more informed decisions can be made about the management practices that will yield the desired future conditions and level of productivity on a given site.

Goals and Objectives

The overall goal of this project is to test mechanistic approaches to predicting productivity of intensively managed Douglas-fir under varying soil and climatic conditions. The proposed model will be developed by combining key ecophysiological processes and empirical relationships, with a major focus on estimating leaf area index and simulating evapotranspiration as a major control on overall gas exchange, including CO_2 fixation during photosynthesis. The working hypothesis is that a mechanistic growth model will help improve the prediction accuracy of productivity in Douglas-fir plantations under intensive management, in part by recognizing the interactions between silvicultural regime and soil and climatic attributes of the site. Successful quantification of these interactions will also facilitate more effective tailoring of silvicultural prescriptions to a given site.

The following three objectives provide the framework for the proposed research: (1) determine the most accurate and/or appropriate method for estimating LAI of intensively-managed stands; (2) quantify patterns in soil water loss on a daily and seasonal resolution and relate these patterns to site and climatic factors; and (3) validate the simulated evapotranspiration against continuously monitored soil moisture data and permanent plot growth measurements. Thesis chapters 2, 3, and 4 address these three respective objectives.

Literature Cited

Bolstad, P. V. & Gower, S. T. 1990. Estimation of leaf area index in fourteen southern Wisconsin forest stands using a portable radiometer. *Tree physiology* 7, 115–124.

Carter, R.E., McWilliams, E.R.G., Klinka, K., 1997. *Forest Ecology and Management* 107: 375-389.

Dewey, J. C., Roberts, S. D. & Hartley, I. 2006. A comparison of tools for remotely estimating leaf area index in loblolly pine plantations. *Proceedings of the 13th biennial southern silvicultural research conferenceGen. Tech. Rep. SRS* 92, 71–75.

Fitter, A.H., & Hay, R.K.M., 2002. Environmental Physiology of Plants: Third Edition. Academic Press.

Gholz, H. L., 1982. Environmental limits on aboveground net primary production, leaf area, and biomass in vegetation zones of the Pacific Northwest. *Ecology* 63, 469–481.

Granier, A.,1987. Evaluation of transpiration in a Douglas-fir stand by means of sap flow measurements. *Tree physiology* 3, 309–320

Hermann, R.K., Lavendar, D.P., 1999.Douglas-fir planted forests. *New Forests* 17: 53-70.

Jonckheere, I. *et al*,. 2004.Review of methods for in situ leaf area index determination: Part I. Theories, sensors and hemispherical photography. *Agricultural and Forest Meteorology* 121, 19–35.

Kimmins, J.P., Mailly, D., Seely B. 1999. Modeling forest ecosystem net primary production: the hybrid simulation approach used in FORECAST. Ecological Modeling. 122: 195–224.Kittredge, J. 1944. Estimation of the amount of foliage of trees and stands. Journal of Forestry 42:905-912.

Korzukhin, M. D., Ter-Mikaelian, M. T. & Wagner, R. G., 1996. Process versus empirical models: which approach for forest ecosystem management? *Canadian Journal of Forest Research* 26, 879–887.

Mäkelä, A. *et al.*,2000. Process-based models for forest ecosystem management: current state of the art and challenges for practical implementation. *Tree Physiology* 20, 289–298 (2000).

Medhurst, J. L. & Beadle, C. L., 2001. Crown structure and leaf area index development in thinned and unthinned Eucalyptus nitens plantations. *Tree Physiology* 21, 989–999.

Monserud, R.,2003. Evaluating Forest Models in a Sustainable Forest Management Context. *FBMIS* 1, 35-47.

Monteith, J. L., 1965. Evaporation and environment. in *Symp. Soc. Exp. Biol* 19, 4.

Nemani, R., L. Pierce, S. Running, and L. Band. 1993. Forest ecosystem processes at the watershed scale: Sensitivity to remotely-sensed leaf area index estimates. International Journal of Remote Sensing 14:2519-2534.

Phillips, N., Bond, B. J., McDowell, N. G. & Ryan, M. G., 2002. Canopy and hydraulic conductance in young, mature and old Douglas-fir trees. *Tree Physiology* 22, 205–211.

Pinjuv, G., Mason, E. G. & Watt, M., 2006. Quantitative validation and comparison of a range of forest growth model types. *Forest ecology and management* 236, 37–46.

Price, D. T. & Black, T. A., 1989. Estimation of forest transpiration and CO2 uptake using the Penman-Monteith equation and a physiological photosynthesis model. *Estimation of Areal Evapotranspiration, IAHS Publisher* 213–227.

Smith, F. W., Sampson, D. A. & Long, J. N., 1991. Notes: Comparison of Leaf Area Index Estimates from Tree Allometrics and Measured Light Interception. *Forest Science* 37, 1682–1688.

Taiz, L. & Zeiger, E. 2006. Plant Physiology: Fourth Edition. Sinauer Associates, Inc., Sunderland, Massachusetts, USA. 690 p.

Talbert, C., Marshall, D., 2005. Plantation productivity in the Douglas-fir region under intensive silvicultural practices; results from research and operations. *Journal of Forestry* 103:65-70.U. S. Forest Service. FIA Annual Inventories [Online] Available: http://www.fs.fed.us/pnw/fia/local-resources/pdf/tables/OR_table1-9.pdf [2012, February 7].

U. S. Forest Service. Douglas-fir: *Pseudotsuga menziesii* (Mirb.) Franco. [Online] Available: http://www.na.fs.fed.us/pubs/silvics_manual/volume_1/pseudotsuga/menziesii.htm [2012, February 7].

U. S. Forest Service Pacific Northwest Research Station. (2011, September, 01). West coast log, lumber exports soar in first half of 2011. [Online] Available:

http://www.fs.fed.us/pnw/news/3011/09/lumber-exports.shtml [2013, January 13].

Vose, J. M., Clinton, B. D., Sullivan, N. H. & Bolstad, P. V., 1995. Vertical leaf area distribution, light transmittance, and application of the Beer–Lambert Law in four mature hardwood stands in the southern Appalachians. *Canadian Journal of Forest Research* 25, 1036–1043.

Waring, R. H. & Franklin, J. F., 1979. Evergreen coniferous forests of the Pacific Northwest. *Science* 204, 1380–1386.

Waring, R. H., Thies, W. G. & Muscato, D., 1980. Stem growth per unit of leaf area: a measure of tree vigor. *Forest Science* 26, 112–117.

Waring, R.H. & Running, S.W.,1998. Forest Ecosystems and Analysis at Multiple Scales: Second Edition. Academic Press.

Waring, R. *et al.*, 2008. Why is the productivity of Douglas-fir higher in New Zealand than in its native range in the Pacific Northwest, USA? *Forest Ecology and Management* 255, 4040–4046.

Weiskittel, A. R., Maguire, D. A., Monserud, R. A. & Johnson, G. P., 2010. A hybrid model for intensively managed Douglas-fir plantations in the Pacific Northwest, USA. *European Journal of Forest Research* 129, 325–338.

Whitehead, D., Grace, J. C. & Godfrey, M. J. S., 1990. Architectural distribution of foliage in individual Pinus radiata D. Don crowns and the effects of clumping on radiation interception. *Tree Physiology* 7, 135–155.

CHAPTER 2: COMPARISON OF INDIRECT ESTIMATES OF LEAF AREA INDEX FOR INTENSIVELY MANAGED DOUGLAS-FIR

Nicole Rogers, Douglas Maguire, Douglas Mainwaring

Department of Forest Engineering, Resources, and Management, College of Forestry, Oregon State University, Corvallis, OR, 97330

Abstract

Leaf area index is an important parameter for physiological models in forest ecosystems. Two indirect estimates of LAI were assessed in comparison to direct estimates of LAI based on destructive sampling. Indirect estimates included LAI inferred from light attenuation measured by the Li-Cor 2200 Tall Plant Canopy Analyzer and application of leaf area:sapwood area ratios. LAI from light attenuation ranged between 1.64 and 5.29, values from the best performing allometric relationship were between 3.00 and 6.35, and estimated from destructive sampling ranged from 2.64 to 11.47. Indirect estimates were found to be inadequate for estimating LAI with sufficient accuracy without general calibration for Douglas-fir forests, and possibly local calibration for site-specific variation in structural attributes like the ratio of leaf to branch surface area.

Introduction

Leaf area index (LAI, m^2m^{-2}) is an important structural parameter for understanding forest productivity. LAI represents the photosynthetic surface area of a stand and its capacity for interception of solar radiation and exchange of both water vapor and CO_2 with the surrounding atmosphere (Grier and Running, 1977). Numerous methods have been explored for determining LAI in various plant communities. Two methods commonly employed in forestry include use of a ratio for conversion from sapwood area to leaf area based on the pipe-model theory (Waring et al. 1982), and estimation of LAI from light absorption (Chen et al., 1997; Dewey et al., 2006, Whitehead et al., 1984). These methods have been proposed to avoid the expensive and time consuming nature of direct measures of LAI in large and complex forest canopies (Breda, 2003; Jonckheere et al., 2003).

A key advantage of leaf area to sapwood area ratios (LA/SA) is the ease of measuring sapwood to estimate LAI. Additionally, patterns in LA/SA over a wide range of forest types have provided a relatively large information base about its variation among species, stands, trees within stands, and sites. Both linear and nonlinear regression

have been used in an attempt to capture the variability in this relationship (Waring et al., 1982; Smith et al., 1991). Ratios have also been developed for both breast height and crown base sapwood area, primarily because sapwood tapers from breast height to crown base and ratios of leaf area to sapwood area at crown base are generally considered more stable across stands of varying density.

Light attenuation as a measure of LAI has been proposed as an alternative to developing and applying allometric relationships. If the correlation between LAI and light attenuation is sufficiently strong, this approach offers a potentially cheap and effective approach to estimating LAI (Gazarini et al., 1990; Smith, 1992). Likewise, this approach eliminates the problem of destructive sampling on plots that are intended to be monitored for future productivity (Gower and Norman, 1991).

Increased interest in measurement of LAI from light attenuation has resulted in a variety of instruments that incorporate the Beer-Lambert Law or gap fraction theory to convert light absorption into LAI (Smith et al., 1991; Bolstad and Gower, 1990). The Li-Cor 2200 Plant Canopy Analyzer has been developed to estimate LAI from light attenuation for an assortment of canopy structures. Varying levels of success have been achieved with the Li-Cor in forested systems, in part because light attenuation is affected by not only LAI, but also by the spatial distribution of foliage and the amount and distribution of surface area in non-photosynthetic tissues, specifically branches and tree boles (Barclay and Trofymow, 2000).

Interest has also grown in the use of LiDAR remote sensing to estimate LAI at coarse spatial scales. LiDAR has been effectively used to estimate structural components of the forest, including canopy height, total basal area, and bole volume (Renslow et al., 2000; Means et al., 2000). Large footprint and small footprint LIDAR have been employed to estimate LAI with varying degrees of success (Richardson et al., 2009; Lefsky et al., 1999). Yet, constraints still exist for both LiDAR forms as a method to estimate LAI. Large footprint LiDAR is not as readily available and small footprint LiDAR requires nearly homogenous stand structure and reduced range in LAI

(Richardson et al., 2009). Further, calibration of LiDAR estimates requires detailed ground truthing (Means et al., 2000), which has received very limited attention to date.

The objective of this study was to evaluate the accuracy of two commonly used methods for estimation of LAI, specifically in the context of their application to intensively managed Douglas-fir stands. The two methods, leaf area to sapwood area ratios (LA/SA) and light attenuation were assessed by comparison to direct measurements obtained by destructive sampling. This assessment was motivated by the fact that LAI is a key stand attribute in the Penman-Monteith equation for estimating evapotranspiration from forest ecosystems.

Material and Methods

Study Site

Research for this project was conducted within the Panther Creek Watershed, located in the northern portion of the Oregon Coast Ranges within Yamhill County (Figure 2-1). Panther Creek covers just over 2500 hectares and comprises both public and private ownership. Elevation across the watershed ranges approximately between 170 and 700 m. Dominant vegetation includes Douglas fir (*Pseudotsuga menziesii*), western hemlock (*Tsuga heterophylla*), western red cedar (*Thuja plicata*), big leaf maple (*Acer macrophyllum*), and red alder (*Alnus rubra*), and the stands, in general, are under active management for timber production.

Climate within the study area can be characterized as having cool, wet winters and hot, dry summers. Periodic drought is common during summer months. Precipitation ranges from 1600 mm annually with average minimum January temperatures ranging from -2 to 2^{o} C and average maximum July temperatures from 20 to 28^{o}C (ClimateWNA).

Research plots across the watershed were established in two phases, Phase I for LiDAR ground-truthing and Phase II for soil research. Plots were circular with a 16m

radius. For this project research was confined to 22 Phase II plots with Douglas-fir basal area ≥ 80% of the total. This compositional threshold was established to focus on plots as close to pure Douglas-fir as possible. The ecophysiological and morphological information for other species on the site is relatively limited, and would add an uncertain level of variability in total LAI estimates, and complicate the opportunity to test the accuracy with which Douglas-fir LAI (and ultimately evapotranspiration) can be estimated.

Douglas-fir age on individual plots ranged between 21- and 139-years-old at breast height. Plot basal area and tree density ranged from 25.9 to 104.7 m^2/ha and 223 to 1255 trees/ha, respectively (Table 2-1). Nineteen of the twenty-two plots were naturally regenerated after clearcut harvesting, and the three remaining plots were planted.

Sampling Design and Field Measurements

Sapwood Area on Standing Trees

Sapwood area was measured on a subsample of trees on each of the 22 plots. At each plot between 15 and 20 trees were sampled. Two cores were extracted from opposite sides of each tree, i.e., separated by 180^o around the tree circumference. Cores were taken as close to breast height as possible and perpendicular to the slope of the ground. Sapwood width was measured to the nearest tenth of a centimeter and recorded in the field. If the distinction between sapwood and heartwood was not clearly visible, methyl orange dye was applied to accentuate the division between these two zones. Diameter at breast height (DBH) was also recorded to the nearest tenth of a centimeter using a diameter tape.

Sampled trees were pre-selected from a full tree inventory completed in 2009. Only trees with DBH ≥10cm were sampled to ensure that a measurable core could be extracted. The two smallest trees and the two largest trees with DBH ≥10cm from the 2009 inventory were sampled at each plot. The remaining 16 trees were evenly

distributed across the diameter range to ensure all diameter classes were well represented. The goal was to sample 20 trees in each plot. However, if field conditions or mortality of selected trees prevented all 20 trees from being sampled then a minimum of 15 trees was accepted. If a selected sample tree could not be cored, a new tree of similar DBH was selected as a replacement. Measurements were collected between mid-August 2012 and mid-September 2012 under the assumption that the vast majority of diameter growth for current growing season had finished and, therefore, that sapwood area and leaf area had reached equilibrium.

Sapwood Area on Felled Trees

Along with sapwood thickness measurements taken from cores, sapwood was also measured on disks from trees that were destructively sampled. Sampling was completed on 22 trees across the watershed outside of the soil plots. Selected trees represented approximately the 10th, 50th and 90th quantile by DBH of the Douglas-fir population measured on the 22 Panther Creek study plots. Disks were cut out of each tree at breast height and crown base. On each disk, heartwood diameter and total diameter inside bark were measured in to the nearest 0.1 cm on the longest axis and on the axis perpendicular to the longest. Sapwood area for each sample disk was estimated as the difference between heartwood area and total cross-sectional area inside bark, assuming an elliptical cross-section of each.

Li-Cor

Canopy light absorption was measured with the Li-Cor LAI 2200 Tall Plant Canopy Analyzer (Li-Cor Environmental, Lincoln, NE). The Li-Cor LAI 2200 Tall Plant Canopy Analyzer was designed to estimate LAI by comparing light intensity above and below the canopy. Readings were taken through a fish eye lens with five zenith angles to calculate intercepted blue light (320-490 nm). The instrument translates light interception into leaf area index by assuming a random distribution of foliage. If foliage is not randomly distributed, then adjustments can be made using a view cap to increase accuracy.

Li-Cor samples were collected between mid-August and mid-September 2012 to capture LAI after the completion of the summer growing season. Readings were taken on clear days before 9am to reduce variation from sun flecks. Two types of readings were collected at each plot, "A" readings that represent light above the canopy and "B" readings taken under the canopy. To avoid the challenge of elevating the instrument above the canopy, the A readings were taken in an opening as close to the plot of interest as possible. The point at which the A readings were taken needed to be at least two tree lengths from the nearest tree. The A readings were taken with the Li-Cor wand held facing west without any shadow covering the lens. A 45^{o} view cap was placed on the lens to ensure consistency among readings for the amount of sun blocked from the lens, to account for clumping and gaps in the canopy, and to ensure consistency among plots of varying slope. All A readings were taken every fifteen seconds for two minutes prior to taking B readings, and again following this same procedure immediately after taking the B readings.

The "B" readings were taken at thirteen points under the canopy on each plot. For B readings the wand was held at chest height. The first reading was taken at plot center, and subsequent readings were taken on the N, S, E, and W transects. Readings were taken five meters and ten meters away from plot center. On the NE, NW, SE, and SW transects readings were taken ten m from plot center (Figure 2-2). At each point a Li-Cor reading was taken with the wand pointing north, south, east and west.

When A and B readings were completed, the Li-Cor console provided an LAI estimate in the field. Data were stored and processed using the Li-Cor FV2200 software.

Destructive Sampling-Foliage Mass

In addition to the indirect measures of LAI from leaf area:sapwood area ratio and light attenuation, LAI was measured directly by sampling branches from the same 22 destructively sampled trees described above for measuring sapwood area. Destructive sampling provided calibration necessary for evaluation of the two indirect measures of

LAI. Basal diameter (cm) and height (cm) were recorded for every live branch on the 22 felled trees. The crown of the felled tree was then split into thirds by live crown length. Three branches were randomly selected from the top and middle thirds and two branches were randomly selected from the bottom third, totaling 176 sample branches. Each sample branch was returned to the lab and oven dried; foliage was separated from woody material, re-dried, and weighed to get the branch-level estimates of foliage mass.

Statistical Analysis

Sapwood Area

Sapwood area at breast height (m^2) was estimated for each cored sample tree from sapwood thickness (cm) and DBH assuming a circular cross-section of heartwood, inside-bark stemwood, and outside-bark stemwood + bark. The following weighted, nonlinear model was fitted to the resulting data to facilitate estimation of sapwood area at breast height for all plot trees as a function of their basal area at breast height:

[1] $$SA_i = \beta_{10} BA_i^{\beta_{11}} + \varepsilon_{1i}$$

where *SA* is sapwood area at breast height (m^2) on the *i*th tree, *BA* is basal area at breast height on the *i*th tree (m^2), the β_{1k}s are parameters to be estimated from the data, and ε_{1i} is the error term with ε_{1i} ~N(0, $BA^m\sigma_1^2$). To homogenize variance of the residuals, weights of BA_i^{-m} with m=0, 1, 2, and 3 were tested in equation [1]. A weight of BA_i^{-1} proved to be the most appropriate weight as confirmed through visual assessment of weighted residuals plotted on predicted values of SA. This model was fitted separately for each plot and resulting parameter estimates (Table 2-2) were applied to estimate missing *SA*s on Douglas-fir trees on each plot with *BA* computed from DBH measured during the 2012 tree inventory. Sapwood area at crown base (SACB) was also estimated on these trees from sapwood area at breast height by applying an equation developed for this purpose (Hann and Maguire 2013).

Foliage Mass

Foliage mass (g) at the branch level was modeled with the following log transformed linear regression model:

[2] $$\ln(FM_i) = \beta_{2o} + \beta_{21}\ln(BRD_i) + \beta_{22}\ln(RH_i) + \varepsilon_{2i}$$

where *FMi* is foliage mass (g) of the *i*th branch, BRD_i is the basal diameter (cm) of the *i*th branch, RH_i is relative height of the *i*th branch (proportion), the β_{2k}s are parameters to be estimated from the data, and ε_{2j} is the error term with $\varepsilon_{2j} \sim N(0, \sigma_2^2)$. This equation was applied to all the live branches on each felled sample tree to estimate total tree foliage biomass, with log bias corrected by multiplying estimated foliage biomass by $e^{MSE/2}$, where MSE is the mean squared error from the regression model (Flewelling and Pienaar, 1981). The use of a log linear equation form and acceptance of the assumption of constant variance were both graphically supported by a plot of model fitted vs. residual values (Appendix, Figure 1).

An equation for estimating foliage mass at the tree-level was developed in the form of the following nonlinear regression:

[3] $$FM_i = \beta_{30} DBH_i^{\beta_{31}} CL_i^{\beta_{32}} + \varepsilon_{3i}$$

where FM_i is foliage mass (g) of the i^{th} tree, DBH_i is diameter at breast height (cm) of the i^{th} tree, CL_i is crown length (cm) of the i^{h} tree, the β_{3k}s are parameters to be estimated from the data, and ε_{3i} is the error term with $\varepsilon_{3i} \sim N(0,\sigma_3^2)$. Tree level foliage mass was then predicted for each plot tree from the 2012 tree inventory. Foliage mass was converted to leaf area by multiplying by an average specific leaf area of 53.3 (cm/g) and expanding to m^2. Total plot leaf area (m^2) was converted to LAI by dividing by the plot area expressed in the same units (804 m^2).

Sapwood Area Conversion Value

Leaf areas of the Panther Creek sample trees were regressed on sapwood area to develop a predictive model specific to the Panther Creek watershed, resulting in the following linear regression model:

[4] $$LA_{SWi} = \beta_{40} + \beta_{41} SACB_i + \varepsilon_{4i}$$

where LA_{SWi} represents the estimated leaf area of the i^{th} destructively sampled tree (m^2), $SACB_i$ is sapwood area at crown base of the i^{th} destructively sampled tree (cm^2), β_{4k}s are parameters estimated from the data, and ε_{4i} is the error term with ε_{4i} ~N(0, σ_4^2). The assumption of constant variance was supported by a plot of model fitted values vs. residuals values.

Leaf area of Panther Creek sample trees was also estimated assuming the following non-linear form:

[5] $$LA_{SWi} = \beta_{51} SACB_i^{\beta_{52}} + \varepsilon_{5i}$$

where LA_{SWi} and $SACB_i$ are defined above, β_{5k}s are parameters estimated from the data, and ε_{5i} is the error term with ε_{5i} ~N(0,σ_5^2). The assumption of constant variance was visually verified with a plot of model fitted vs. residual values.

Leaf Area Estimation from Sapwood Area

Sapwood area was first converted to tree leaf area assuming that the tree held 0.54 m^2 of leaf area for each cm^2 of sapwood area at crown base (Waring et al. 1982). A second estimate was made interpreting the slope parameter from equation [4] as the average LA/SA for Panther Creek, given that the intercept term from equation [4] was not significantly different from 0 at α=0.05. Third and fourth estimates of leaf area were made by applying fitted equations [4] and [5] to estimates of SACB on all trees. Total plot leaf area estimated by each approach was then determined by summing leaf

area of all Douglas-fir trees on the plot. Total plot leaf area (m^2) was converted to LAI by dividing by the plot area expressed in the same units (804 m^2).

Existing Allometric Equations

Foliage biomass was also estimated for the Panther Creek trees and plots from previously existing allometric equations. The following equations were available for Douglas-fir or for conifer species in general:

Gholz et al. (1979)

[6a] $ln(FM_i) = -2.8462 + 1.7009 \cdot ln(DBH)$

Jenkins et al. (2003)

[6b] $FM_i = exp(-2.2304 + 2.4435 \cdot \ln(DBH)) \cdot exp(-2.9584 + 4.4766/DBH)$

Snell and Anholt (1981)

[6c] $FM_i = (1/2.2046) \cdot \exp(-0.6916 - 0.0546 \cdot \left({DBH}/{2.54}\right)^{0.6842})/(1 + \exp(-0.6916 - 0.0546 \cdot \left({DBH}/{2.54}\right)^{0.6842})) \cdot \exp(-0.7224 + 1.888 \cdot ln\left({HT}/{0.3048}\right) - 0.3873 \cdot ({HT}/{0.3048})/\left({DBH}/{2.54}\right))$

[6d] $FM_i = (1/2.2046) \cdot exp(-0.6916 - 0.0546 \cdot \left({DBH}/{2.54}\right)^{0.6842}) \cdot exp(-0.7224 + 1.888 \cdot ln({HT}/{0.3048}) - 0.3873 * (({HT}/{0.3048})/\left({DBH}/{2.54}\right))$

where *HT* is total height of the tree (m) and FM_i and *DBH* are defined above. Estimates of foliage mass from each equation were converted to grams and plotted with estimates from the Panther Creek foliage mass equations to facilitate graphical comparison.

Method Comparisons

After plot-level LAI was estimated for each of the 22 plots, a comparison was made between indirect estimates of LAI and the direct measurement of LAI from branch

sampling. The correlations between the direct estimate and those from the Li-Cor and LA/SA method were computed to measure the degree of consistency between the alternative approaches. Additionally, mean difference, mean square difference, mean absolute difference, and mean relative difference were calculated to compare each alternative method for calculating LAI to LAI estimated from foliage.

Results

Foliage Mass Equations

Parameter estimates for estimating sapwood area at breast height (Equation [1]) varied by age of the plot and the average size of the trees (Table 2-2). The branch-level equation for estimating foliage mass (Equation [2]) indicated positive effect of both branch diameter and relative height in the crown (Table 2-3). Tree-level foliage mass (Equation [3]) was an increasing function of DBH and CL (Table 2-3). Estimates of foliage mass (FM) from Jenkins et al (2003) were similar to FM from Panther Creek when DBH was less than five centimeters (Fig 2-3). When DBH was above five cm, estimates from Jenkins et al. (2003) increased rapidly and were substantially higher than other estimates of FM. Both equations from Snell and Anholt (1981) produced estimates of FM that were very similar to the direct measurements at Panther Creek.

A 3-D graph of foliage mass as a function of branch diameter (cm) and relative height above ground showed an increase in foliage mass with explanatory variables (Figure 2-4).

Leaf Area Index

Estimates of LAI from Li-Cor (LAI_L) were approximately 35% lower than those from direct measurement of sample branches (LAI_{FM}) on all plots, with the exception of three plots on which Li-Cor predicted higher LAI (Figure 2-4). The correlation between LAI_L and LAI_{FM} was low (-0.06) (Table 2-4). LAI_L ranged from 1.6 to 5.9; LAI_{FM} ranged from 2.65 to 11.47 (Table 2-5). Calculated mean difference was 2.70,

mean square difference was 14.59, mean absolute difference was 3.01, and mean relative difference was 2.11 (Table 2-6).

Estimates of LAI from sapwood allometrics varied between methods of prediction (Figure 2-5). Estimates of LAI from the full form of equation [4] were consistently the lower than all the other allometric equations ([[5] and [6a-d]). LAI estimates increased when the non-linear model form [5] was used. The highest estimates of LAI were generated by applying the Panther Creek average ratio of leaf area to sapwood area (0.66), followed by the average ratio of 0.54 previously suggested for Douglas-fir in general (Waring et al. 1982).

On average, LAI estimates assuming a leaf area to sapwood area ratio of 0.54 m^2/cm^2 (LAI_{SW}) were approximately 27% lower than LAI_{FM}. Estimates of LAI_{SW} using this ratio were between 2.4584 and 5.1962, and its correlation with LAI_{FM} was low and negative (-0.20298).

Estimates applying the average leaf area:sapwood area ratio of 0.66 for Panther Creek (LAI_{SP}) were on average approximately 6% lower than LAI_{FM}. Estimates of LAI_{SP} ranged from 3.0048 to 6.3509, and the correlation between LAI_{SP} and LAI_{FM} was again low and negative (-0.20298). The mean difference between LAI_{SP} and LAI_{FM} was 1.17, the mean squared difference was 9.11 the mean absolute difference was 2.34, and the mean relative difference was 3.82 (Table 2-6).

A trend existed between LAI_{FM} and stand age, DBH (cm), and basal area (m^2) (Table 2-5). In general, LAI_{FM} increased as average DBH, basal area, and average age increased.

Of all the methods for indirectly estimating LAI, estimates based on leaf area:sapwood area ratios (LAI_{SW} and LAI_{SP}) were closer to LAI_{FM} than were those based on LAI_L. However, the ability of LAI_{SP} for estimating LAI_{FM} decreased when LAI_{FM} was eight or greater (Figure 2-4).

Discussion

Range in LAI

Estimates of LAI from foliage mass were determined to be the most appropriate as they fell with the range of LAI for Douglas-fir observed in other studies (Table 2-7). Smith measured LAI ranges between 3.2 and 8.9 for sites with basal areas between 10.5 (m^2/ha) and 97.8 (m^2/ha) (1993). Turner et al. estimated LAI of Douglas-fir to be as high as 16 in old growth stands with an average basal area of 84.1 (m^2/ha) (2000). Marshall and Waring estimated LAI values between 12 and 7.3 for old growth Douglas-fir (1986) (Table 2-7).

Li-Cor

Underestimation of LAI from light attenuation measured by the Li-Cor instrument, relative to direct estimates from sampling felled trees, was consistent with findings in several other studies (Chen et al., 1991; Smith et al., 1993). Underestimation could be due to clumping of foliage which violates the Beer-Lambert assumption that all foliage is randomly distributed, an assumption that is built into the Li-Cor estimates. This assessment is in line with another study that that concluded that underestimates of LAI from the Li-Cor instrument when LAI values were high was due to severe clumping of foliage (Cherry et al. 1998).

Additional bias in estimating LAI from the Li-Cor instrument probably accrues from light intercepted by non-photosynthetic tissues. In this regard, estimates from the Li-Cor could be more appropriately considered Plant Area Indices. Li-Cor is sensitive to any objects that block intercepted light, including shrubs taller than breast height, tree branches, and tree boles. Cherry et al. (1998) also attributed overestimation of LAI by the Li-Cor, particularly when LAI was low, to shading of the device by non-photosynthetic tissues. Similarly, some Li-Cor overestimates probably resulted from light absorption by the heavy vine maple (*Acer circinatum*) on several of the study plots.

To combat inaccurate estimates of LAI_L, other studies have developed calibration values that range from simple to complex and applied them with varying degrees of success (Cherry et al., 1998; Gower and Norman, 1991). However, each calibration method requires the use of destructive sampling and the calibration is probably specific to a given stand structure, offsetting the value of the Li-Cor instrument as a reliable non-destructive approach to estimating LAI.

Sapwood

The closer match between LAI_{FM} or LAI_{SW} and LAI_{SP} for smaller values of LAI than with large values of LAI was consistent with previous studies (Turner et al., 1999). Trees with a higher LAI_{FM} were older and larger with very different stand structure from stands with younger trees. Plots with high LAI_{FM} had visibly larger crowns than plots with low $LAI_{FM.}$ Additionally, the higher basal area and higher DBH in plots with high LAI_{FM} suggest that the ratio of leaf area to sapwood area may be different or more variable among older trees and may require information about sapwood conductivity (e.g., Whitehead et al. 1984) or structural effects on water potential or other physiological parameters to accurately estimate leaf area for each tree and the resulting aggregate LAI.

Foliage Mass

Estimates of foliage mass provide theoretically the most unbiased values of foliage amount on the Panther Creek trees. However, sampling error in estimating total foliage mass of a sample tree can arise from numerous sources. As is typical of biomass studies, sample trees on which foliage mass was measured were not selected randomly from a clearly identified population or stratified by diameter class; therefore, the scope of inference is not clearly defined and biases are possible across tree diameter classes. The crown stratification and random branch sampling approach, however, should have provided an unbiased estimate of foliage mass on a given sample tree.

Because the objective in this study was to estimate projected leaf area, a potential source of error in estimating LAI from foliage mass estimates is the value of specific leaf area (SLA) used to convert from foliage mass to leaf area. The selected value 53.3 cm^2/g was based on knowledge of the area and an understanding of the range in values of SLA for intensively managed Douglas-fir (e.g, Maguire and Bennett 1996). However, SLA is known to vary across a number of environmental gradients. The range of SLA for a given species is genetically pre-determined, but within a species SLA varies systematically with incident light intensity and hence position in the crown and overlying crown structure (Weiskittel et al., 2007; Marshall and Monserud, 2003; Borghetti et al, 1986). Borgehetti et al found variability in SLA between age classes and branch position in the crown, with values in between 85.357 (cm^2/g) for current years foliage in the bottom layer of the tree's crown down to a SLA of 50. 648 (cm^2/g) in the second year age class of foliage at the top of the tree (1986). Weiskittle el al found similar ranges in SLA for Douglas-fir. Current year's foliage had an average SLA of 74.62 ± 19.07 (cm^2/g), foliage in the fourth year age class had an average SLA for 57.81 ± 13.73 (cm^2/g) (Weiskittel et al., 2007). The population average SLA for Douglas-fir trees at Panther Creek was not measured so is not known with any degree of certainty.

Creation of foliage mass equations specific to the Panther Creek watershed does provide an advantage over application of the regional equations previously available (e.g. Gholz et al. 1979). Several sources of potential error must be kept in mind when applying regional equations. First, they were developed for sites outside of the Oregon Coast Ranges, so parameter estimates may be biased for Panther Creek. Additionally, sample sizes used for these biomass equations were typically small relative to the population for which they are estimating, and the target population itself is usually poorly defined; hence, variances may be large and the risk of potential bias by choosing a sample that is not entirely representative of the population must be considered. Equations by Snell and Anholt (1981) were created for dominant and co-dominant trees, but applied to trees that ranged from suppressed to dominate at

Panther Creek. Equations by Gholz et al (1979) and Jenkins et al. (2003) only used DBH to predict FM, primarily because the former were being applied in unmanaged stands in which stand density varied little and in which the correlation between DBH and crown length remained strong. The equation developed from Panther Creek data takes into account the effects of stand density on crown length for a for a given DBH; i.e., stands managed at lower densities would produce trees with longer crowns and great foliage mass for a given DBH. The equation developed by sampling trees at Panther Creek can also account for local differences in attributes such as foliage density that typically cannot be accounted for by combinations of only DBH, total height, and crown length.

Conclusions

An accurate estimate of stand LAI is important for simulating key physiological process such as forest evapotranspiration and photosynthesis. LAI is a dynamic parameter which can vary across an array of stand structural attributes. Three methods were explored to determine the most appropriate estimate of LAI for subsequent application in Penman-Monteith equations for evapotranspiration. Application of previously-developed allometric equations for estimating foliage mass and/or area lead to underestimates of large LAIs, and estimates from the Li-Cor instrument based on light attenuation require calibration to provide reasonable values. Until progress is made on current indirect estimates, the most reliable means to estimate LAI at the accuracy required for simulating physiological process is through direct and destructive sampling of the target population. With efficient sampling designs, e.g., randomized branch sampling (Gregoire and Valentine 2008), this approach may be the best approach for achieving the required accuracy in estimating LAI.

Literature Cited

Barclay, H . & Trofymow, J., 2000. Relationship of readings from the LI-COR canopy analyzer to total one-sided leaf area index and stand structure in immature Douglas-fir. *Forest Ecology and Management* 132, 121–126

Bartelink, H.H. 1996. Allometric relationships of biomass on needle area of Douglas-fir. *Forest Ecology and Management* 86, 193-203

Bolstad, P. V. & Gower, S. T., 1990. Estimation of leaf area index in fourteen southern Wisconsin forest stands using a portable radiometer. *Tree physiology* **7,** 115–124

Borghetti, M., Vendramin, G. G. & Giannini, R., 1986.Specific leaf area and leaf area index distribution in a young Douglas-fir plantation. *Can. J. For. Res.* 16, 1283–1288

Bréda, N. J. J, 2003. Ground-based measurements of leaf area index: a review of methods, instruments and current controversies. *J. Exp. Bot.* 54, 2403–2417

Chen, J. M., Plummer, P. S., Rich, M., Gower, S. T. & Norman, J. M.,1997. Leaf area index measurements. *Journal of Geophysical Research* 102, 29–429

Cherry, M., Hingston, A., Battaglia, M. & Beadle, C., 1998. Calibrating the LI-COR LAI-2000 for estimating leaf area index in eucalypt plantations. *TASFORESTS-HOBART*- 10, 75–82

Dewey, J. C., Roberts, S. D. & Hartley, I., 2006. A comparison of tools for remotely estimating leaf area index in loblolly pine plantations. *Proceedings of the 13th biennial southern silvicultural research conferenceGen. Tech. Rep. SRS* 92, 71–75

Flewelling, J. W. & Pienaar, L. V., 1981. Multiplicative Regression with Lognormal Errors.

Gazarini, L. C., Araujo, M. C. C., Borralho, N. & Pereira, J. S., 1990. Plant area index in Eucalyptus globulus plantations determined indirectly by a light interception method. *Tree physiology* 7, 107–113

Gholz, H. L., 1982. Environmental limits on aboveground net primary production, leaf area, and biomass in vegetation zones of the Pacific Northwest. *Ecology* 63, 469–481

Gower, S. T. & Norman, J. M., 1991. Rapid estimation of leaf area index in conifer and broad-leaf plantations. *Ecology* 72, 1896–1900

Gregoire, T.G. and H.T. Valentine. 2008. Sampling strategies for natural resources and the environment. Chapman & Hall, Boca Raton, LA, USA.474 p.

Grier, C. G. & Running, S. W., 1977. Leaf Area of Mature Northwestern Coniferous Forests: Relation to Site Water Balance. *Ecology* 58, 893–899

Hann, D.W. and D.A. Maguire. 2013. Predicting sapwood area at crown base of Douglas-fir trees. College of Forestry, Oregon State University, Corvallis, OR. Forest Biometrics Research Paper 8. 13 p.

Jenkins, J.C., D.C, C., L.S, H. & R.A, B., 2003. National-Scale Biomass Estimators for United States Tree Species.

Jonckheere, I. *et al.,* 2004. Review of methods for in situ leaf area index determination: Part I. Theories, sensors and hemispherical photography. *Agricultural and Forest Meteorology* 121, 19–35

Lefsky, M. A. *et al.,* 1999. Lidar remote sensing of the canopy structure and biophysical properties of Douglas-fir western hemlock forests. *Remote Sensing of Environment* 70, 339–361

Maguire, D.A. and Bennett. W.S., 1996. Patterns in vertical distribution of foliage on coastal Douglas-fir. Canadian Journal of Forest Research 26:1991-2005.

Maguire, D. A., Brissette, J. C. & Gu, L., 1998. Crown structure and growth efficiency of red spruce in uneven-aged, mixed-species stands in Maine. *Canadian Journal of Forest Research* 28, 1233–1240

Marshall, J. D. & Monserud, R. A, 2003. Foliage height influences specific leaf area of three conifer species. *Can. J. For. Res.* 33, 164–170

Marshall, J.D. & Waring, R.H., 1986. Methods of Estimating LAI in Old-growth Douglas-fir. *Ecology*. 67, 975-979

Means, J. E. *et al.* 2000. Predicting forest stand characteristics with airborne scanning lidar., *PE & RS- Photogrammetric Engineering & Remote Sensing* 66, 1367–1371

Medhurst, J. L. & Beadle, C. L., 2001. Crown structure and leaf area index development in thinned and unthinned Eucalyptus nitens plantations. *Tree Physiol* 21, 989–999

Richardson, J. J., Moskal, L. M. & Kim, S.-H., 2009. Modeling approaches to estimate effective leaf area index from aerial discrete-return LIDAR. *Agricultural and Forest Meteorology* 149, 1152–1160

Smith, F. W., Sampson, D. A. & Long, J. N., 1991. Notes: Comparison of Leaf Area Index Estimates from Tree Allometrics and Measured Light Interception. *Forest Science* 37, 1682–1688

Smith, N. J., Chen, J. M. & Black, T. A. Effects of clumping on estimates of stand leaf area index using the LI-COR LAI-2000. *Can. J. For. Res.* 23, 1940–1943 (1993).

Snell, J.A. and B.F. Anholt. 1981. Predicting crown weight of coast Douglas-fir and western hemlock. USDA-FS Res. Pap. PNW-281.

Standish, J.T., G.H. Manning, and J.P. Demaerschalk. 1985. Development of biomass equations for British Columbia tree species. Pacific Forestry Research Centre, Victoria, BC. Can. For. Serv. Inf. Rep. BC-X-264.

Thomas, S.C. and Winner, W.E. 2000. Leaf area index of old-growth Douglas-fir forests estimated from direct structural measurements in the canopy. *Canadian Journal of Forest Resources* 30, 1922-1930

Turner, D. P., Acker, S. A., Means, J. E. & Garman, S. L., 2000. Assessing alternative allometric algorithms for estimating leaf area of Douglas-fir trees and stands. *Forest Ecology and Management* 126, 61–76

Waring, R. H., Emmingham, W. H., Gholz, H. L. & Grier, C. C., 1978. Variation in Maximum Leaf Area of Coniferous Forests in Oregon and Its Ecological Significance

Waring, R.H., Schroeder, P.E., Oren, R., 1982. Application of the pipe model theory to predict canopy leaf area. *Journal of Forest Science* 12, 556-560

Waring, R. H., Thies, W. G. & Muscato, D., 1980. Stem growth per unit of leaf area: a measure of tree vigor. *Forest Science* 26, 112–117

Weiskittel, A. R., Temesgen, H., Wilson, D. S. & Maguire, D. A., 2008. Sources of within-and between-stand variability in specific leaf area of three ecologically distinct conifer species. *Annals of forest science* 65, 103–103

Whitehead, D., Grace, J. C. & Godfrey, M. J. S., 1990. Architectural distribution of foliage in individual Pinus radiata D. Don crowns and the effects of clumping on radiation interception. *Tree Physiology* 7, 135–155

Table 2-1. Attributes of 22 plots sampled in association with soil pits on the Panther Creek Watershed.

Plot	Number of Trees		DBH (cm)		Height (m)		Douglas-fir Basal Area (m^2) per HA
	> 10cm	≤ 10cm	Mean	Range	Mean	Range	
200101	40	22	34.21	2.60 - 108.60	26.00	3.90 - 63.10	97.0571
200102	26	1	51.36	8.7 - 131.10	35.90	4.30 - 57.20	86.7927
200105	57	0	25.98	12.10 - 45.70	26.18	13.10 - 33.70	41.4637
200106	26	0	27.42	9.20 - 53.00	22.44	3.80 - 38.10	40.2291
200108	30	0	44.54	23.50 - 74.6	37.15	27.70 - 46.10	62.5913
200109	17	2	64.30	5.50 - 118.90	45.28	5.40 - 60.90	87.9122
200110	18	0	68.61	52.30 - 83.40	50.38	47.5 - 53.60	84.2527
200111	31	0	42.35	13.50 - 74.30	32.20	14.60 - 43.60	63.4817
200201	101	2	27.72	6.80 - 72.20	27.02	7.70 - 43.70	89.0111
200204	33	0	35.67	20.70 - 56.20	31.37	18.00 - 37.20	43.3455
200205	48	0	30.28	10.30 - 54.00	28.09	7.90 - 35.90	46.8178
200206	56	1	34.13	7.80 - 52.30	26.94	6.90 - 35.90	69.3837
200207	21	1	41.94	3.10 - 65.40	32.26	2.40 - 42.4	40.5433
200208	37	0	39.70	10.30 - 71.50	30.88	6.70 - 44.90	66.9142
200209	29	5	33.88	2.50 - 90.90	27.84	3.20 - 53.40	47.6550
200210	41	1	33.12	9.80 - 144.90	29.00	9.20 - 35.60	60.6578
200211	23	0	47.48	22.90 - 69.70	42.64	26.60 - 55.00	54.1473
200302	52	0	26.78	14.00 - 41.40	25.12	14.80 - 31.50	38.3006
200303	18	0	70.81	23.30 - 113.00	42.93	14.30 - 57.10	104.7081
200306	46	0	33.42	21.20 - 47.50	31.82	26.70 - 36.70	51.7638
200310	56	6	21.93	6.50 - 46.50	15.48	1.60 - 21.90	31.0110
200313	32	2	27.60	3.70 - 42.50	21.83	4.50 - 27.70	25.9131

Table 2-2. Plot-level parameter estimates and standard errors for estimating sapwood area at breast height from DBH (Equation 1).

Plot	β_{10}	β_{11}	Stand Error β_{10}	Stand Error β_{11}
200101	0.2111	1.1277	0.0189	0.1230
200102	0.1887	0.8943	0.0197	0.0849
200105	0.4736	1.1095	0.0694	0.0567
200106	0.3732	0.9794	0.0685	0.0877
200108	0.2036	0.9298	0.0263	0.0774
200109	0.1757	1.0498	0.0091	0.0680
200110	0.1949	1.0848	0.0309	0.1691
200111	0.2140	0.9173	0.0569	0.1625
200201	0.2230	0.9825	0.0332	0.0741
200204	0.2128	0.7489	0.0489	0.0989
200205	0.2991	0.9011	0.0782	0.1051
200206	0.3322	1.1367	0.0693	0.0996
200207	0.1956	0.8844	0.0336	0.1001
200208	0.2166	0.9581	0.0364	0.0954
200209	0.2209	0.8062	0.0271	0.0605
200210	0.1417	0.6186	0.0214	0.0618
200211	0.5066	1.4985	0.0707	0.0981
200302	0.2948	0.8558	0.0645	0.0797
200303	0.1726	1.0350	0.0102	0.0839
200304	0.2517	0.8433	0.0832	0.1440
200305	0.3135	1.0663	0.0546	0.0797
200306	0.4779	1.0987	0.1287	0.1170
200309	0.2548	0.8661	0.0353	0.0705
200310	0.3530	0.8994	0.0496	0.0513
200311	0.2260	0.9563	0.0294	0.0750
200312	0.2365	0.8627	0.0491	0.0924
200313	0.2582	0.7682	0.0892	0.1349

Table 2-3. Parameter estimates, standard errors and associated p-values for estimating branch-level foliage biomass (Equations [2]), tree-level foliage biomass (Equation [3]), and tree-level foliage area from sapwood area at crown base (Equation [4]).

Parameter	Estimate	Standard Error	P-Value
β20	-0.9171	0.2203	< 0.0001
β21	2.0396	0.0776	< 0.0001
β22	0.5535	0.0792	< 0.0001
β30	1.2615	0.9867	0.2173
β31	1.9255	0.1124	< 0.0001
β32	0.3858	0.1083	0.0022
β40	-34.2883	16.758	0.0548
β41	0.66009	0.04182	< 0.0001
β51	0.16499	0.08805	0.0764
β52	1.20179	0.08661	<0.0001

Table 2-4. Correlations between LAI estimated derived from light attenuation measured by the Li-Cor instrument, sapwood allometrics, and estimates of foliage mass on destructively sampled trees.

Methods	Correlation
$LAI_{FolMass}$ LAI_{Licor}	-0.0611
LAI_{FM} $LAI_{SapWaring}$	-0.2029
LAI_{FM} $LAI_{SapwoodPC}$	-0.2029
LAI_{FM} LAI_{SapLM}	0.0335
LAI_{FM} LAI_{SapNLM}	0.0858

Table 2-5. Range in LAI estimates based on light attenuation measured by the Li-Cor Tall Plant Canopy Analyzer, by destructive sampling of felled trees for foliage mass, and by two alternative leaf area:sapwood area ratios.

Plot	LAI: Li-Cor	LAI: Foliage Mass	LAI: Sapwood Allometrics Ratio = 0.66	LAI: Sapwood Allometrics Ratio = 0.54	Plot Basal Area (m^2)	Average DBH (cm)	Age (years)
200101	3.45	11.1524	4.7615	3.8958	8.56	34.21	113.89
200102	3.82	8.3845	4.8125	3.9375	7.44	51.36	91.50
200105	1.64	3.5400	4.5625	3.7330	4.06	25.98	44.44
200106	2.09	4.3158	5.0082	4.0976	3.65	27.42	44.13
200108	3.91	5.9102	4.2250	3.4569	5.50	44.54	63.56
200109	2.57	10.3277	3.9892	3.2639	7.23	64.30	110.25
200110	3.95	8.4264	3.8577	3.1563	7.83	68.61	118.63
200111	4.09	6.7745	4.8548	3.9721	5.25	42.35	87.75
200201	2.75	6.9854	6.3509	5.1962	7.71	27.72	62.78
200204	4.69	4.5666	5.5214	4.5175	3.50	35.67	34.78
200205	4.37	4.6953	5.9523	4.8700	3.86	30.28	34.78
200206	3.87	6.1958	5.2044	4.2582	5.98	34.13	63.44
200207	2.42	4.0340	3.0048	2.4584	3.99	41.94	62.43
200208	1.99	6.6031	4.7230	3.8642	5.73	39.70	62.00
200209	4.53	5.5635	4.7845	3.9146	3.86	33.88	53.63
200210	2.08	5.1733	5.8252	4.7660	5.16	33.12	34.57
200211	2.63	5.2086	3.0220	2.4725	4.94	47.48	59.00
200302	3.08	3.6228	5.8906	4.8196	3.23	26.78	25.67
200303	3.13	11.4702	4.7456	3.8828	8.47	70.81	113.50
200306	4	4.8066	5.9191	4.8429	4.19	33.42	34.33
200310	5.29	3.1586	5.8967	4.8246	2.23	21.93	22.44
200313	3.73	2.6486	4.7214	3.8630	2.31	27.60	25.22

Table 2-6. Mean difference statistics for comparing methods of estimation of LAI.

Method of Estimation	Statistic	Value
Sapwood Ratio: Panther Creek	Mean Difference	1.1787
	Mean Squared Difference	9.1082
	Mean Absolute Difference	2.3396
	Mean Relative Difference	3.8187
Sapwood Ratio: Waring	Mean Difference	2.0682
	Mean Squared Difference	11.5754
	Mean Absolute Difference	2.4756
	Mean Relative Difference	2.8352
LiCor	Mean Difference	2.7038
	Mean Squared Difference	14.5914
	Mean Absolute Difference	3.0071
	Mean Relative Difference	2.1089

Table 2-7. Ranges in LAI from the literature derived through multiple methodologies

	Min	Max	Method	Source
	5.3	16	Allometric Relationships	Turner et al (2000)
BA (m^2/ha)	23.8	84.1		
	3.2	8.9	Destructive Sampling	Smith (1993)
BA (m^2/ha)	10.5	97.8		
	4.9	7.4	Allometric Relationships	Bartelink (1996)
BA (m^2/ha)	27.2	21.6		
	7.3	12	Allometric Relationships	Marshall and Waring (1986)
BA (m^2/ha)	63	52		
	8.2 ± 1.8	9.3 ± 2.1	Vertical Sampling	Thomas and Winner (2000)
BA (m^2/ha)	NA	NA		

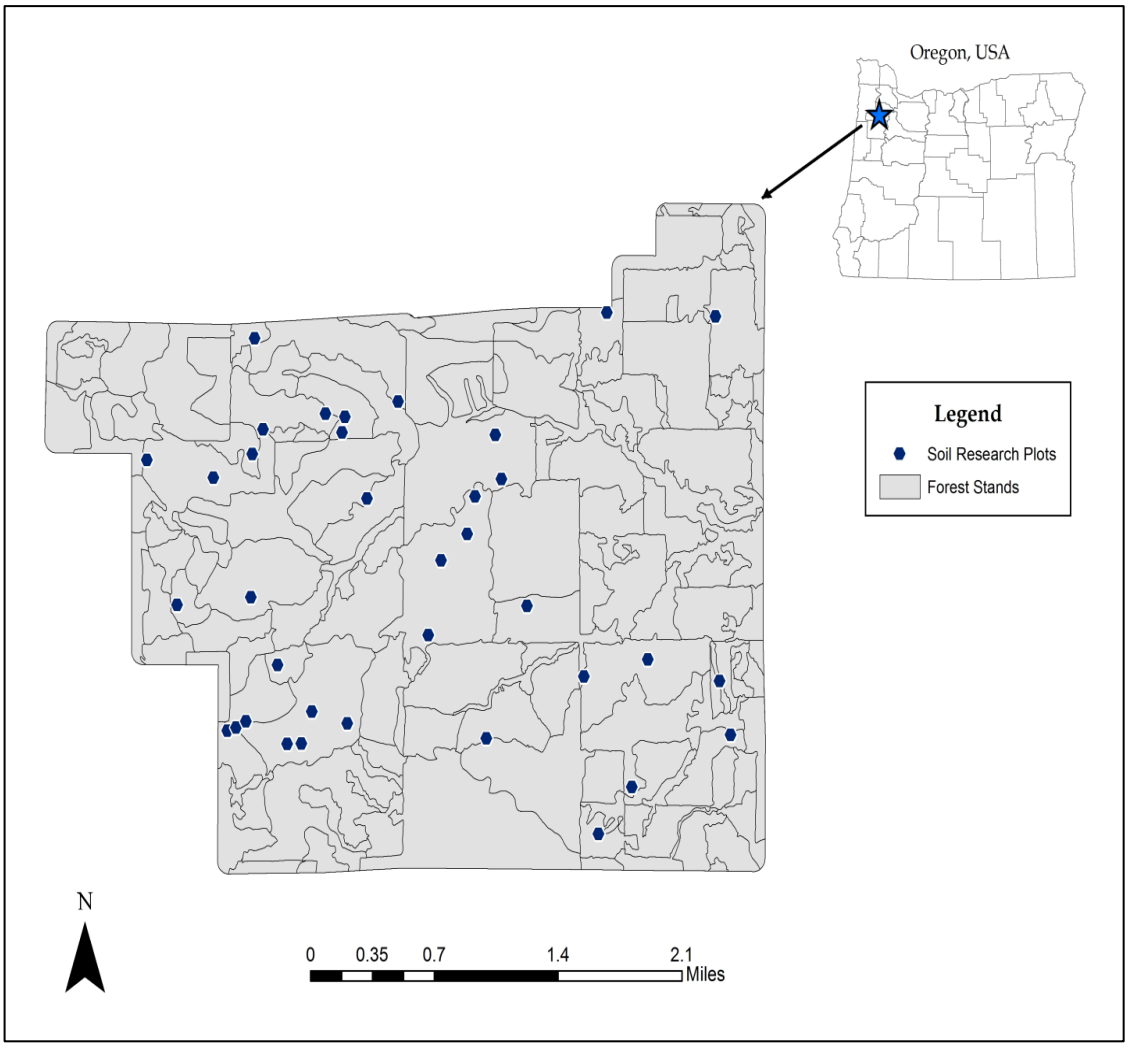

Figure 2-1: Map of the Panther Creek Watershed with location of soil research plots and delimitation of individual forest stands

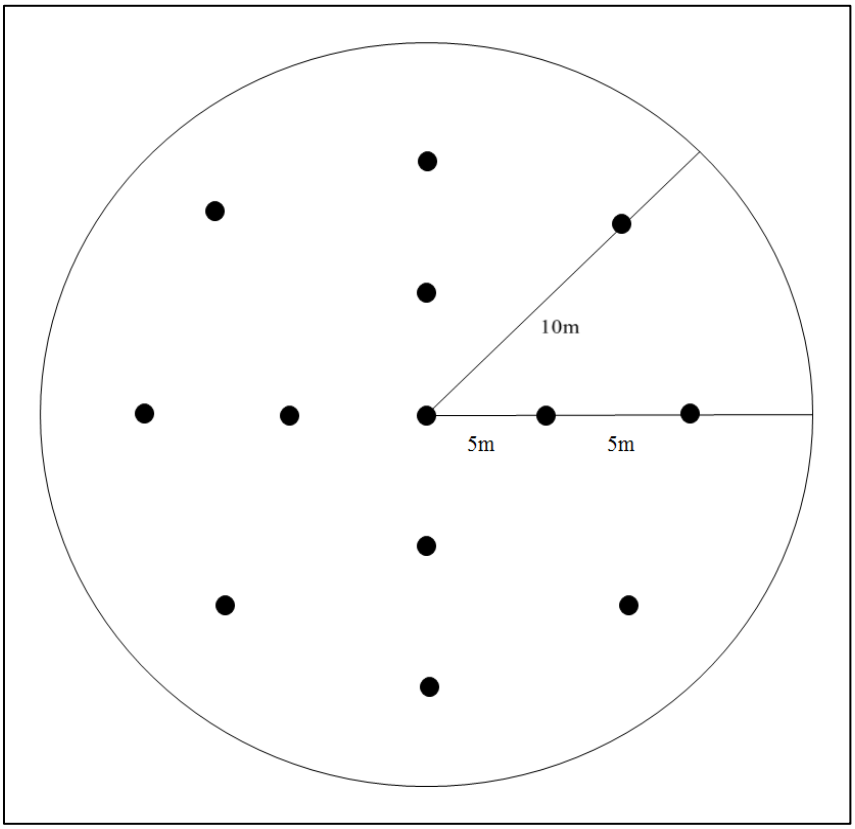

Figure 2-2: Distribution of sample points for Li-Cor measurement of light attenuation.

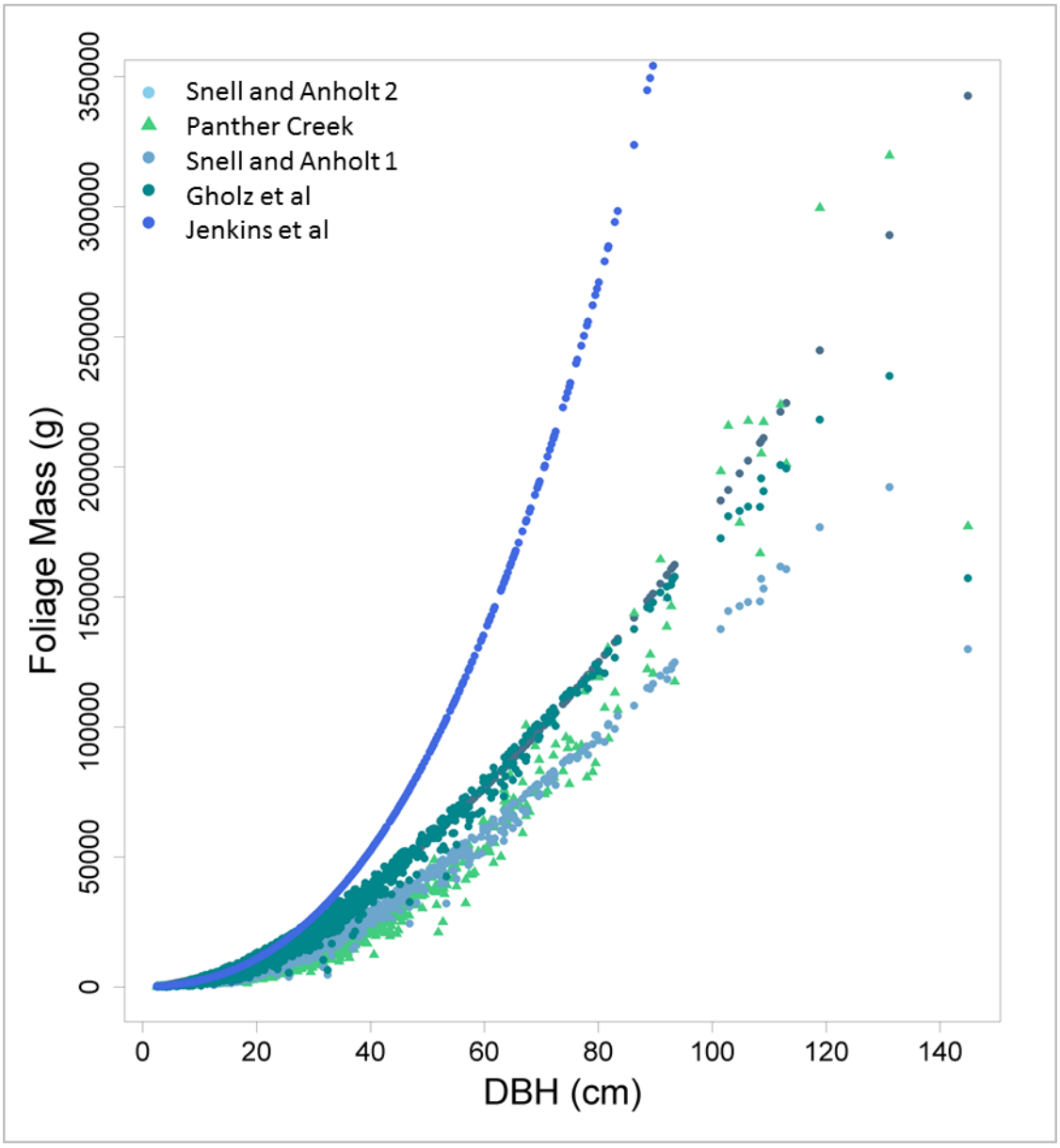

Figure 2-3. Douglas-fir foliage mass for trees of varying DBH estimated from equations in the literature and from the equation developed from trees sampled at Panther Creek. Jenkins et al. (2003) and Gholz et al. (1979) use only DBH as a predictor, Snell and Anholdt (1981) use both DBH and total tree height, and the Panther Creek equation uses both DBH and crown length.

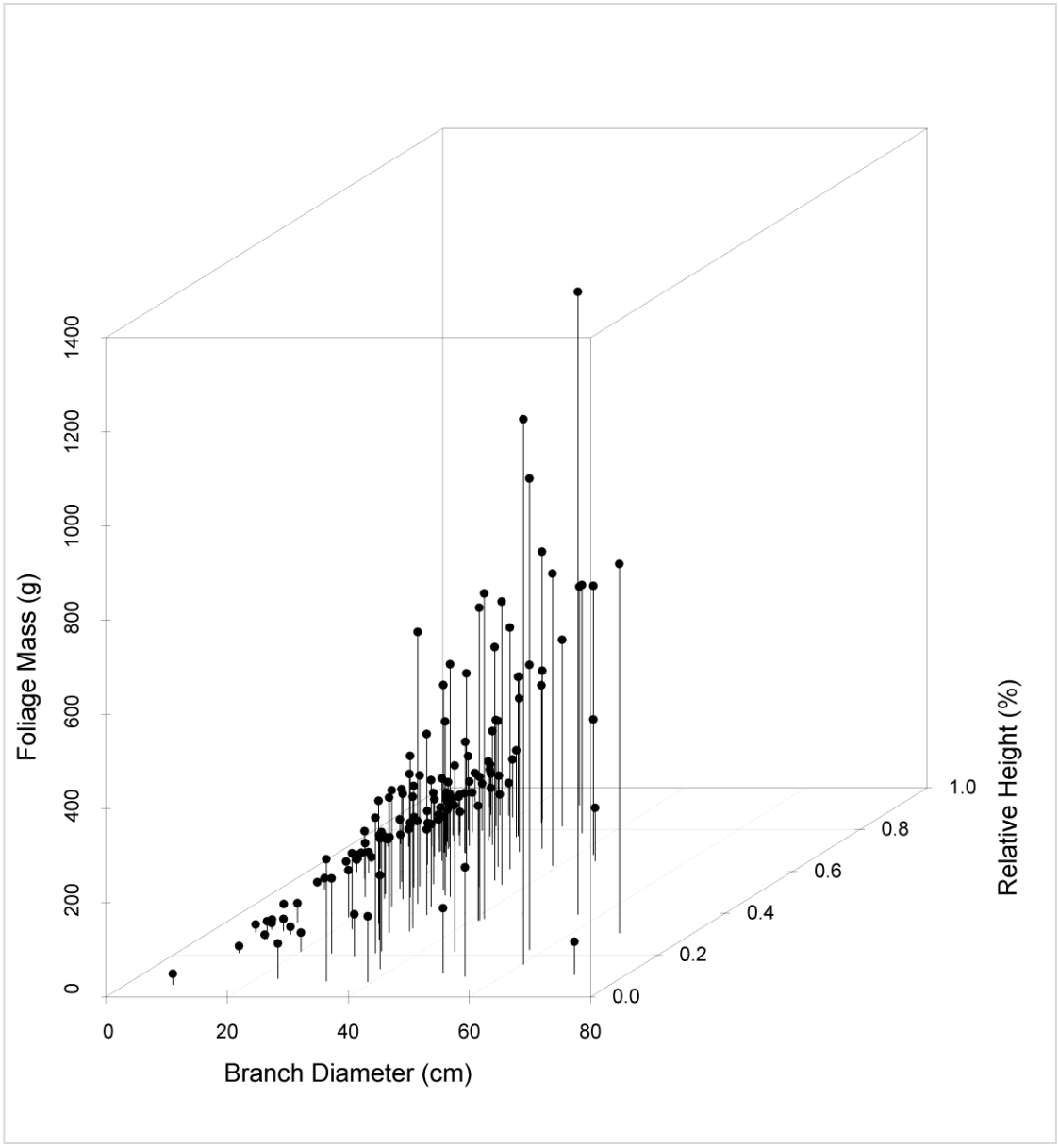

Figure 2-4. Foliage mass (g) against branch diameter (cm) and relative height (%).

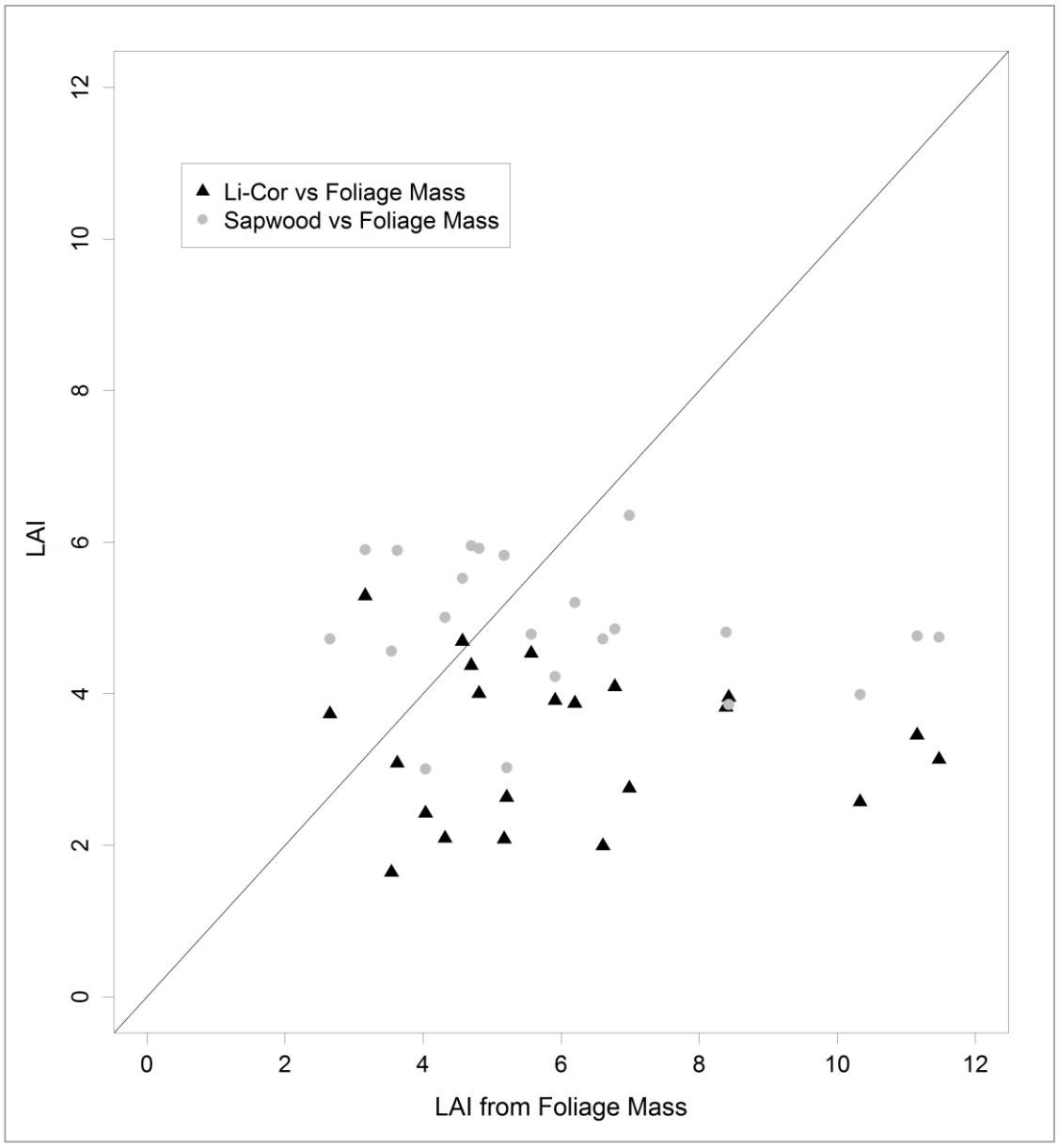

Figure 2-5. LAI estimated from Li-Cor measurements of light attenuation and from leaf area:sapwood ratios evaluated against LAI estimated by felling sample trees and measuring sample branches. Perfect correspondence between indirect methods and felled tree sampling would be indicated by points on the 1:1 line.

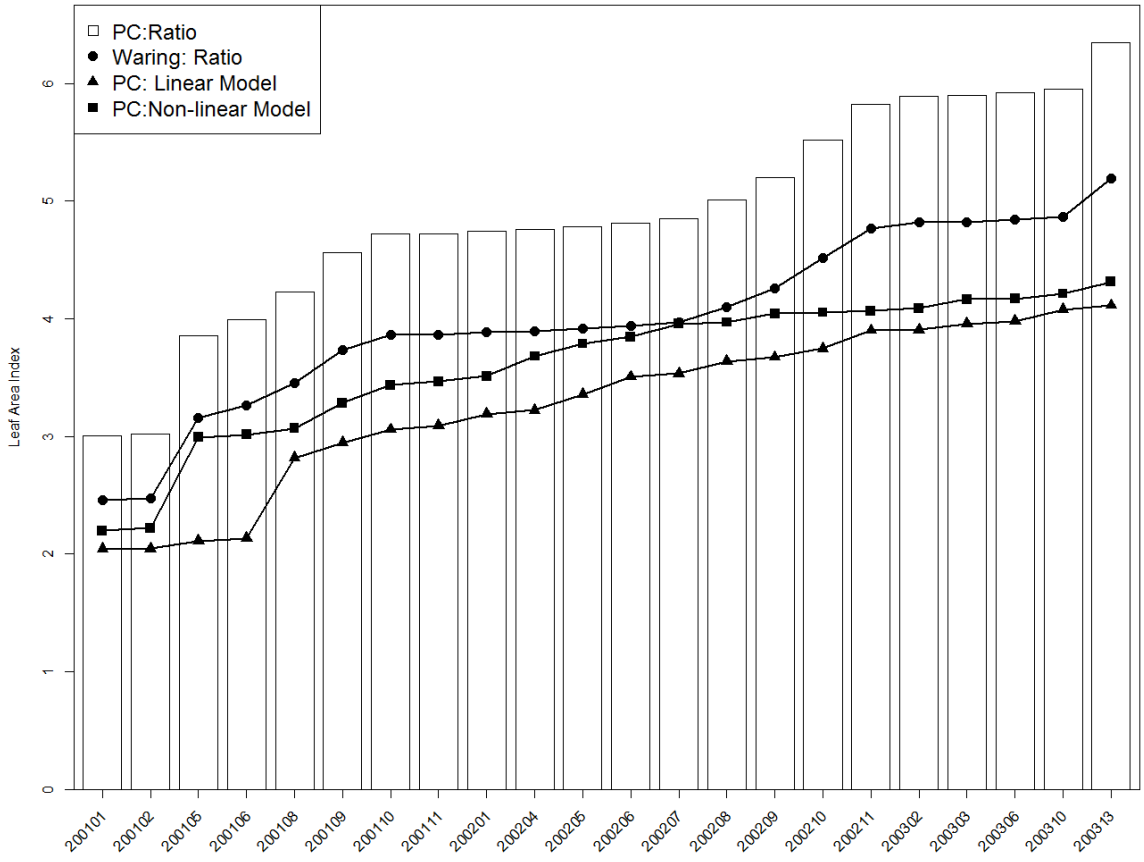

Figure 2-6. Comparison between estimates of LAI from varying sapwood area allometrics.

CHAPTER 3: CHARACTERIZATION OF SOIL MOISTURE DRAWDOWN IN INTENSIVELY MANAGED DOUGLAS-FIR STANDS

Nicole Rogers, Douglas Maguire, Douglas Mainwaring

Department of Forest Engineering, Resources, and Management, College of Forestry, Oregon State University, Corvallis, OR, 97330

Abstract

Understanding the forest water balance as it relates to soils is an important component of understanding overall forest productivity. Twenty soil pits located in the Oregon Coast Ranges were utilized to explore changes in daily and cumulative soil water loss over the summer growing season of 2012. Additionally, the relationship between soil texture and field capacity was examined and multiple linear regressions were developed to predict soil water loss at varying temporal scales from climatic factors and site-specific characteristics. Growing season water loss from soil varied from 0.063 to 0.271 m^3/m^3 among plots. Mean field capacity did not differ significantly among soil textural classes at a depth of 5 cm or 50 cm. Multiple linear regressions at daily and seasonal scales predicted a relatively small proportion of the variation in soil water loss with the explanatory variables tested.

Introduction

Spatial and temporal dynamics of soil water in forested watersheds are important components for modeling forest productivity. In drought prone forests of the Pacific Northwest, fluctuations in soil moisture have direct ties to key physiological processes such as evapotranspiration (ET), total gas exchange, and photosynthetic activity (Emmingham and Waring, 1976; Bond and Kavanagh, 1996; Oren et al, 1998).

To incorporate important soil water properties into forest growth models, assumptions or inferences must be made about soil attributes that influence water holding capacity and plant available water (Granier et al., 1999; Wilson et al., 2000). Possible sources of this soils information include coarse scale soil maps such as those provided by the USDA Natural Resources Conservation Service. However, the widely recognized finer-scale variability in soil attributes creates difficulties in extracting information from coarse soil maps for accurately estimating average soil water holding capacity for individual stands (Lathrop et al., 1995), and for characterizing the dynamics of water potentially available to plants throughout the growing season.

A tremendous amount of work has been done on modeling the hydrological dynamics of forested ecosystems from a number of perspectives. A capacity for predicting water yields on the level of small and large watersheds is important to forest managers who are responsible for maintaining water quality and quantity both for human consumption and for support of aquatic/riparian systems and organisms (e.g., salmon in the Pacific Northwest). Many hydrological models have been developed for simulating surface and sub-surface water flow in forested ecosystems, including those developed for enhancing our fundamental understanding of hydrological processes (Granier et al., 1999; Clapp and Hornberger, 1978) and those developed for predicting the ramifications of forest management alternatives on water quantity and quality (Rothacher, 1970; Siebert and McDonnell, 2010). These models have been constructed under a very different objective than understanding water limitations on forest productivity, but many components of these models are relevant to predicting the amount of plant available water throughout the growing season. Models built for the primary purpose of simulating net primary production as a function of resource availability and basic ecophysiological processes contain constructs of widely varying complexity to represent basic soil attributes such as water holding capacity and plant available water at a daily or hourly resolution (Landsberg and Waring 1997).

In the growth model 3PG, the soil moisture sub-model interacts with vapor pressure deficits through the stomatal conductance term to drive productivity, requiring a measure of soil salinity to run properly (Morris and Collopy, 2001). The biome scale model Biome BGC requires input of climate data on a daily resolution, soil moisture at field capacity, critical water potential, and initial soil water (Running and Hunt, 1993).

If these models are validated, the validation is typically done on the basis of NPP, in part because the data for validating soil water content on a daily, weekly, or even monthly resolution requires a significant investment in installation and calibration of instruments, as well as in management, editing, and analysis of complex datasets.

Only in some relatively unusual cases has the accuracy of the soil water sub-model been validated (Weiskittel et al. 2010).

Techniques for monitoring soil water content have varied among studies and over time, the latter due to both advances in the technology for continuous monitoring and reductions in the costs of the required instruments.

One instrument for soil moisture monitoring encountered in forestry is the a neutron probe, an instrument that provides data that can be converted to volumetric water content with calibration curves (Dahms, 1971). Additionally, soil moisture can be measured almost continuously by monitoring electrical resistance with probes placed into the soil at desired depths (Czarnomski et al., 2005; Dinger and Rose, 2009).

The general objective of this study was to characterize water holding capacity and soil moisture draw down over the summer growing season on plots dominated by Douglas-fir on the eastern edge of the Oregon Coast Ranges. Achieving this general objective involved pursuit of the following specific objectives of the analysis: 1) determine the daily volumetric water content of the top 50 cm of the soil at a set of 20 sample plots; 2) determine the field capacity of the top 50 cm of the soil at the same set of sample plots 3) develop regression models that predict daily soil water loss as a function of daily climatic variables, stand structural characteristics, and soil attributes specific to each plot; 4) develop regression models that predict seasonal soil water loss as a function of physical site characteristics.

Material and Methods

Study Site

Data utilized for this project were collected during the summer of 2012 at the Panther Creek Watershed. The watershed is located in the northern portion of the Oregon Coast Ranges within Yamhill County (Figure 3-1). Panther Creek covers an area of 2580 hectares and includes public and private ownership. Elevation across the

watershed ranges between approximately 170 and 700m. Dominant vegetation includes Douglas fir (*Pseudotsuga menziesii*), western hemlock (*Tsuga heterophylla*), western red cedar (*Thuja plicata*), big leaf maple (*Acer macrophyllum*), and red alder (*Alnus rubra*) in stands that, in general, are under active management for timber production.

Soils in the Coast Ranges are strongly related to their geomorphic surfaces and are volcanic or sedimentary in origin (Balster and Parsons, 1966). In areas of volcanic parent material, the underlying basalt layer is commonly overlaid with soil textures in the lower third of the soil texture triangle (Natural Resources Conservation Service). In areas of sedimentary origin, sandstones and shales are typically overlaid with soil textures in the lower left corner of the soil texture triangle.

Climate within the study area can be characterized as having cool, wet winters and hot, dry summers. Periodic drought is common during summer months. Total precipitation is 1600 mm annually with average minimum January temperatures ranging from -2 to 2^{o} C and average maximum July temperatures from 20 to 25^{o}C (ClimateWNA).

Research plots across the watershed were established in two phases, Phase I for LiDAR ground-truthing and Phase II for soil research. Plots were circular with a 16m radius. For this project research was confined to 27 Phase II plots with Douglas-fir comprising $\geq$ 80% of total plot basal area. This compositional threshold was established to focus on plots as close to pure Douglas-fir as possible. Leaf area index had been previously been determined on these plots, see Chapter 2 of this thesis, to facilitate concurrent simulation of ET and soil moisture characteristics.

Douglas-fir age on individual plots ranged between 21- and 139-years-old at breast height. Plot basal area and tree density ranged from 25.9 to 104.7 m^2/ha and 223 to 1255 trees/ha, respectively (Table 3-1). Twenty-four of the 27 plots were naturally regenerated after clearcut harvesting, and the three remaining plots were planted.

Field Measurements

Available Data

Detailed soil data were collected to NRCS specifications at 26 of the 27 sampled soil research plots. A mini-meteorological station was established at each soil research plot and was equipped to record soil volumetric water content (m^3/m^3) and temperature at two-hour intervals throughout the day (Figure 3-2). Decagon EC-5 soil moisture sensors at each mini-met station were installed at depths of 5 cm and 50 cm from the top of mineral soil and data from the sensors were stored on a Decagon EM-50 Analog Data Logger and manually downloaded on a three-month cycle. Downloaded data were returned to the lab and graphically assessed for errors and missing observations (Figure 3-3). Volumetric water content was converted to an average daily value using the arithmetic mean.

At seven soil research plots sensors had missing data at 5 cm, 50 cm, or both depths and were therefore not used in this analysis, leaving a total of 20 plots.

In addition to each mini-meteorological station, a complete weather station was established at Panther Creek (Figure 3-4). Climate data were recorded on an hourly resolution. Measured climate data used in the current analysis included total precipitation (mm), temperature (^oC), vapor pressure deficit (kPa), relative humidity (%), and photosynthetically active radiation (uE). Data were collected from the weather station every three months and returned to the lab for quality control. Average daily values were computed from the hourly climate data as the arithmetic mean.

Data for this analysis were limited to the summer growing season between July 1st and September 30th. A start date July 1st was selected to focus on the period of water use during which soil received little to no recharge from precipitation (Figure 3-5).

Statistical Analysis

Average Volumetric Water Content

The predicted volumetric water content (VWC) at 25cm for each day was assumed to represent average VWC for the top 50 cm of soil on each plot and was linearly interpolated as:

$$[1] \qquad AVWC_j = VWC_{5\ cm} + \frac{(25-5)}{(50-5)}(VWC_{50\ cm} - VWC_{5\ cm})$$

where $AVWC_j$ is average volumetric water content (m^3/m^3) at 25-cm depth on the *j*th day and VWC_{5cm} and VWC_{50cm} are the volumetric water contents at depth into mineral soil of 5 cm and 50 cm, respectively, for that same *j*th day (Figure 3-6).

Change in Volumetric Water Content

Daily change in average volumetric water content (m^3/m^3) from each plot was viewed as a simple proxy for water lost to evapotranspiration (ET), recognizing that some water will move in liquid or vapor state vertically and horizontally along water potential gradients in the soil. To determine daily water loss (m^3/m^3), the difference in average VWC at 25 cm between the current day and previous day was calculated. Cumulative water loss (m^3/m^3) was also calculated for each day during the growing season as the total of daily water losses from July 1 to that day. Total water loss for the entire season was the cumulative water loss on September 30.

Field Capacity and Soil Texture

Field capacity of each plot was calculated at 5 cm and 50 cm using measured VWC. Specifically, field capacity was assumed to be the average minimum VWC between January and April of 2012, with values exceeding these minimum assumed to represent water that had infiltrated during winter storms but that had not had time to drain gravitationally to field capacity.

Measured field capacities at 5 cm and 50 cm on each plot were grouped by soil texture and analyzed graphically for trends by texture (Figure 3-7a, b). Significant differences among soil texture classes were tested by one-way ANOVA at $\alpha = 0.05$.

Empirical Prediction of Soil Water Loss

Full regression models were fitted to predict soil water loss on a daily and total growing-season basis from a full set of potential predictor variables. Correlations between each proposed explanatory variable and water loss as the response variable (m^3/m^3) were calculated initially to assess potential predictive power. Final models for both daily and cumulative seasonal water loss were then determined by backward elimination of variables that were not significant at $\alpha=0.10$.

Daily water loss was estimated from two multiple linear regression models. The first computed water loss as a function of climatic variables measured at the watershed resolution from the single weather station. The second model utilized site-specific soil attributes; site-specific stand structural and physical attributes, and Stage's (1976) transformation of slope and aspect to calibrate the watershed climate variables to the physiographic position of each plot.

Total seasonal water loss was estimated as a linear function of stand structural characteristics, soil attributes suspected to influence water holding capacity, and physiographic position as represented by Stage's (1976) transformation of slope and aspect.

Results

Field Capacity and Soil Texture

Field capacity varied within and between textural groups (Table 3-2a,b; Figure 3-7a, b). Plots with a clay or clay loam texture at 5 cm only had one observation each. Of plots with multiple observations, soils with a silty clay loam texture had the highest average field capacity. Soils with a silt loam texture had the lowest average field

capacity and the greatest variance within the textural class. At 50 cm, silt loams had the highest field capacity. Loam textures had the lowest average field capacity and greatest within-class variance. Clay textures, loamy sand textures, and silty clay textures had only one observation each at 50 cm. The ANOVA on those textural classes with >1 observation indicated no significant difference in mean FC at 5 cm and 50 cm depth (p= 0.79 and 0.29, respectively).

Change in Volumetric Water Content

Daily water loss varied tremendously from plot to plot. Initial values of VWC (field capacity) ranged from 0.17 to 0.40 (m^3/m^3) among plots. End of growing season values for VWC fell to between 0.06 and 0.26 (m^3/m^3). The seasonal trend in daily average VWC also varied tremendously among the plots, ranging from nearly straight lines to curves that were approximately reverse-sigmoid in shape (Figure 3-8).

Daily water loss illustrated the implications of the seasonal trends in average daily VWC through the growing season (Figure 3-9). Plots with a reverse-sigmoid shape (Figure 3-8) resulted from a daily pattern that started with relatively high daily water loss (e.g., 5-10 mm) and ended with almost no water lost on specific days near the end of the growing season (Figure 3-9).

Total seasonal water loss was similarly quite variable among plots. The greatest seasonal water loss was on Plot 200207, with 0.27 m^3 of water lost per m^3 of soil. Plot 200211 had the lowest seasonal water loss at 0.06 m^3/m^3, and Plot 200208 experienced a loss near the median value of 0.12 m^3 of water per m^3 of soil over the entire growing season (Table 3-3). Consistent with the curves showing trends in daily VWC over the growing season, the trends in cumulative daily water loss ranged from near linear relationships to curves that started with steep slopes and that gradually became asymptotic to the ending total water loss for the season (Figure 3-10).

Predicted Water Loss

Strength of correlations between water loss and explanatory variables varied from a daily to seasonal resolution (Table 3-4 a, b). Daily water loss was most strongly correlated with PAR (0.2305) and most weakly correlated with the Stage (1976) slope x cosine transformation of aspect (-0.0261). Total seasonal water loss had the strongest correlation with Stage's (1976) slope x sine transformation of aspect (0.3022) and weakest correlation with LAI (-0.1815).

The final model tested for describing daily soil water loss as a function of climate variables only was of the form:

[2] $\log(DWL_i) = \beta_{20} + \beta_{21}VPD_i + \beta_{23}PAR_i + \beta_{23}g_{s_i} + \beta_{24}T_i + \beta_{25}RH_i + \varepsilon_{2i}$

where DWL_i is daily water loss on day i (m^3/m^3), VPD_i is vapor pressure deficit on day i (mb), PAR_i is photosynthetically active radiation received on day i (uE), g_{s_i} is stomatal conductance on day i (cm/s), T_i is air temperature on day i, RH_i is relative humidity on day i (%), β_{2k}s are parameters estimated from the data, and ε_{2i} is the error term with $\varepsilon_{2i} \sim N(0, \sigma_2^2)$. A graph of model fitted values vs. residual values supported the assumption of constant variance (Appendix, Figure 2). The model yielded an adjusted R^2 of 0.2216, parameter estimates were all significantly different from zero (Table 3-5), and the predictors exhibited a range in values (Table 3-6).

The final model for describing daily soil water loss as a function of weather, physiographic, and stand structural variables took the following form:

[3] $\log(DWL_i) = \beta_{30} + \beta_{31}VPD_i + \beta_{32}PAR_i + \beta_{33}g_{si} + \beta_{34}T_i + \beta_{35}RH_i + \beta_{36}LAI + \beta_{37}FC + \beta_{38}s \cdot \cos(A) + \beta_{39}S \cdot sin(A) + \epsilon_{3i}$

where DWL_i is soil water loss on day i (m^3/m^3), VPD_i is vapor pressure deficit on day i (mb), PAR_i is photosynthetically active radiation received on day i (uE), g_{s_i} is stomatal conductance on day i (cm/s), T_i is air temperature on day i, RH_i is relative

humidity on day *i* (%), LAI is leaf area index, *FC* is field capacity at 5 cm, *S* is slope (%) / 100, *A* is plot azimuth, β_{3k}s are parameters estimated from the data, and ϵ_{3i} is the error term with ϵ_{3i} ~N (0, σ_3^2). A graph of model fitted vs. residual values supported the assumption of constant variance (Appendix, Figure 3). The model yielded an adjusted R^2 of 0.2778, parameter estimates were all significantly different from zero (Table 3-5), and the predictors exhibited a range in values (Table 3-6).

The final model for describing total growing season water loss took the following form:

[4] $$WL_i = \beta_{40} + \beta_{41} LAI_i + \beta_{42} BA_i + \beta_{43} S_i \cdot \cos(A_i) + \epsilon_{4j}$$

where WL_i is total soil water loss during the growing season on plot *i* (m^3/m^3), LAI_i is leaf area index for plot *i*, BA_i is initial basal area (m^2) for plot *i*, S_i is slope (%) / 100 for plot *i*, A_i is plot azimuth from north for plot *i*, β_{4k}s are parameter estimated from the data, and ϵ_{4i} is the error term with ϵ_{4i} ~N (0, σ_4^2). The assumption of constant variance was supported by a graph of model fitted vs. residual values (Appendix, Figure 4). The model generated an adjusted R^2 of 0.1984, parameter estimates were all significantly different from zero (Table 3-5), and the predictors exhibited a range in values (Table 3-6).

Discussion

Evapotranspiration from Volumetric Water Content

The variability in soil water loss between plots can be attributed to inherent spatial heterogeneity of soils and difference in microclimate and hence evaporative demand between stands (Lathrop, 1995; Sharma, 1979). Stand structural (e.g., LAI), physiological, and site specific characteristics affecting water loss are important to consider. A study by Brooks et al. (2002) highlighted the importance of hydraulic redistribution of water by the roots on the soil water balance. During August, they found that up to 28% of water removed daily from the top 2 m of soil in a 20 year old

Douglas-fir stand was replaced each night by hydraulic redistribution. In this study, any water that may have been added by hydraulic lift was ignored, with water use assumed equal to only differences in daily VWC. This study also assumed that water was absorbed from only the top 0.5 m of mineral soil, where the vast majority of fine roots are located (Eis, 1987; McGinn, 1963). If a significant amount of water was pulled from lower rooting depths then total water use was underestimated.

The cover of competing ground vegetation and additional tree species at each plot was not factored into this study, but could be an important part in modeling water loss. Plots used in this study were constrained to those with a Douglas-fir basal area of 80% or greater, leaving up to 20% basal area in other species which would also be drawing water from the soil. Presence of competing vegetation in the understory can have a significant effect on soil volumetric water content under dry conditions and under LAIs that are below 3, allowing more radiation to reach lower levels (Kelliher and Black, 1986).

A point to consider further is the relationship between volumetric water content and depth within the soil. For this study, a straight line was fit between values of measured volumetric water content at 5cm and 50cm. However, a non-linear model may be more appropriate to predict VWC for a given depth, accounting for variation in water retention and soil texture (Saxton et al., 1986; Clapp and Hornberger, 1978). In this case, the integral of this non-linear function would provide a more accurate estimate of total VWC.

Values of VWC determined in this study were similar to values found in other studies for Douglas-fir in the Pacific Northwest, despite slight differences in depth of soil moisture sensors. Warren et al (2005) found values of VWC at the start of the dry season to be 0.22 (m^3/m^3) for a young stand of Douglas-fir and 0.18 (m^3/m^3) for an older Douglas-fir stand at a depth of 20cm. At the end of the dry season, VWC had dropped to 0.12 (m^3/m^3) for the young stand and 0.10 (m^3/m^3) for the older plot (Warren et al., 2005). The depth at which VWC is monitored may be important for

accurately capturing water loss from the soil to ET. At Panther Creek, no attempt was made to extrapolate lower than the 50 cm moisture probe to eliminate uncertainty in the pattern of VWC change to greater depths. While fine roots located in the top soil layers play an important role in water transport, tracking water utilized by the tree, especially later in to the summer, may require knowledge of VWC at greater depths (Brooks et al., 2000; Dahms, 1971).

Finally, calibration of soil moisture sensors must also be addressed. For this study, raw data from Decagon EC-5 soil moisture sensors were assumed to yield accurate estimates of VWC. Measurements are based on the dielectric constant of the soil which varies with changing texture and salinity of the soil (Kennedy et al., 2003). Czarnomski et al. (2005) found that estimated VWC could differ as much as 11.5% from true VWC calibrated by factory recommendations, but noted precision within 3% of true VWC when calibrated with a simple linear regression equation. The study also noted that calibration was not as effective for extremely dry or moist soils and that values of VWC were slightly temperature dependent (Czarnomski et al., 2005). For other forest soils in the Oregon Coast Ranges, calibration curves have demonstrated that direct readings from the Decagon EC-5 overestimate VWC to varying degrees, and commonly required 4^{th} order polynomials (Andoni Urteaga, personal communication). However, the impact of calibration on estimates of water loss (i.e., differences in successive estimates of VWC) are probably minimal.

Field Capacity

Field capacity is defined as the percentage of water held in the soil after free drainage has subsided (Brady and Weil, 2008). Texture is a key factor in determining the amount of water that is held, with clay soils typically having higher field capacities, followed by silt and sand (Table 3-7). However, additional properties of the soil affect field capacity. Soils with a higher bulk density will have restricted water movement as will soils with blockier structure (Brouwer, et al, 1985). The percentage of organic matter and rock content in the soil also contributes to or detracts from, respectively,

field capacity at each plot (Brady and Weil, 2008). The weak relationship between mean field capacity and soil texture at each plot may be attributable to one or several of these complicating factors. For example, if the amount of organic matter varied among plots, the resulting variability in FC would be expected greatest at 5 cm and least at 50 cm due to the general decline in organic matter content with soil depth. At 50 cm there might also be greater consistency in structure and density among the plots.

Field capacity measured in this study does fall in within the realm of values measured in other studies. A study by Black (1979) found field capacity for two sites with gravelly sandy loam soils on Vancouver Island to be 0.215 (m^3/m^3) and 0.213 (m^3/m^3). Variability from these values seen at Panther Creek can be attributed to the wider spectrum of soils present at the watershed.

Predicted Soil Moisture

Soil water loss proved to be a challenging value to predict at both a daily and seasonal resolution. Inclusion of site specific structural and soil attributes did provide marginal improvement in explained variance of modeled daily water loss in comparison to a model based strictly on climate data. This result highlights the importance of calibrating climate data to the site level or measuring climate data directly on site for improved estimates of soil water loss. At a seasonal resolution, the explained variance decreased again suggesting predictions of water loss are best made at finer scale resolutions.

However, important information about the role of VPD and slope in soil water loss can be gained from the behavior of trigonnometric variables. At the seasonal scale, only *cos(A)* is significant in the model. The peak of this function is on north facing aspects, while the lowest point is along south facing aspects. The behavior of this function suggests that water loss is greatest on north facing slopes, with water loss increasing as slope increases. On south facing slopes, the low water loss is driven by VPD.

Beyond simple measures of soil VWC, actual water potentials at the root, soil, stem, and leaf level may add important information to the model and increase predictive power (Bond and Kavanagh, 1996). In addition, other tree species drew on soil moisture, so estimation of water loss to these trees and other competing vegetation should be added to the model as better information on these species becomes available.

Conclusions

The heterogeneous nature of soil hydraulic processes can make them challenging to characterize. As demonstrated in this research, the variability from site to site in soil attributes requires detailed data on climate and stand structure to begin modeling water loss from forest soils to evapotranspiration. However, further work on modeling forms and consideration of additional variables is needed for accurate predictions of water loss at the stand level. Ultimately, improved simulation of these processes is important for capturing variability in productivity under a wide range of silvicultural regimes in drought prone regions, such as the Pacific Northwest.

Literature Cited

Balster, C. A., Parsons, R. B., 1968.Service, U. S. S. C. & Station, O. S. U. A. E. *Geomorphology and soils, Willamette Valley, Oregon*. (Corvallis, Or. : Agricultural Experiment Station, Oregon State University.

Bond, B. J. & Kavanagh, K. L., 1999. Stomatal behavior of four woody species in relation to leaf-specific hydraulic conductance and threshold water potential. *Tree Physiol* 19, 503–510.

Black, T.A., 1979. Evapotranspiration from Douglas-fir stands exposed to soil water deficits. *Water Resources Research* 15, 164-170.

Brady, N.C. and Weil R.R., 2008. The Nature and properties of soils; Fourteenth Edition. Fourth Edition. Pearson Prentice Hall, Inc., Upper Saddle River, New Jersey, USA. 32-264.

C. Brouwer, C., Goffeau, A., Heibloem, M., 1985. Irrigation Water Management: Training Manual No. 1 - Introduction to Irrigation, *Food and Agriculture Organization of the United Nations*.

Brooks, J. R., Meinzer, F. C., Coulombe, R. & Gregg, J, 2002. Hydraulic redistribution of soil water during summer drought in two contrasting Pacific Northwest coniferous forests. *Tree Physiol* 22, 1107–1117.

Clapp, R. B. & Hornberger, G. M., 1978. Empirical equations for some soil hydraulic properties. *Water Resources Research* 14, 601–604.

Coops, N. ., Waring, R. & Landsberg, J., 1998. Assessing forest productivity in Australia and New Zealand using a physiologically-based model driven with averaged monthly weather data and satellite-derived estimates of canopy photosynthetic capacity. *Forest Ecology and Management* 104, 113–127.

Czarnomski, N. M., Moore, G. W., Pypker, T. G., Licata, J. & Bond, B. J., 2005. Precision and accuracy of three alternative instruments for measuring soil water content in two forest soils of the Pacific Northwest. *Can. J. For. Res.* 35, 1867–1876.

Dahms, W. G., 1971. Growth and soil moisture in thinned lodgepole pine. USDA Forest Service Research Paper, PNW-127: 37 p.

Dinger, E. J. & Rose, R., 2009. Integration of soil moisture, xylem water potential, and fall–spring herbicide treatments to achieve the maximum growth response in newly planted Douglas-fir seedlings. *Can. J. For. Res.* 39, 1401–1414.

Eis, S., 1974. Root System Morphology of Western Hemlock, Western Red Cedar, and Douglas-fir. *Can. J. For. Res.* 4, 28–38.

Emmingham, W.H. and Waring, R.H., 1977. An index of photosynthesis for comparing forest sites in western Oregon. *Canadian Journal of Forest Resources* 7, 165-174.

Granier, A., 1987. Evaluation of transpiration in a Douglas-fir stand by means of sap flow measurements. *Tree physiology* 3, 309–320.

Granier, A., Bréda, N., Biron, P. & Villette, S.,1999. A lumped water balance model to evaluate duration and intensity of drought constraints in forest stands. *Ecological Modelling* 116, 269–283.

Jassal, R. S. *et al.*, 2007. Components of ecosystem respiration and an estimate of net primary productivity of an intermediate-aged Douglas-fir stand. *Agricultural and Forest Meteorology* 144, 44–57.

Kennedy, J.R., Keefer, T.O., Paige, G.B., Barnes, E. 2003. Evaluation of dielectric constant-based soil moisture sensors in a semi-arid rangeland. Proc. 1st Interagency Conf. on Research in the Watersheds, K.G. Renard, S. McElroy, W. Gburek, E. Canfield, and R.L. Scott (eds.), Oct. 27-30, Benson, AZ, pp.503-508.

Landsberg, J. J. and Waring, R. H., 1997. A generalized model of forest productivity using simplified concepts of radiation-use efficiency, carbon balance and partitioning. *Forest Ecology and Management* 95, 209–228.

Lathrop Jr., R. G., Aber, J. D. & Bognar, J. A., 1995. Spatial variability of digital soil maps and its impact on regional ecosystem modeling. *Ecological Modelling* 82, 1–10.

McGin, R.G., 1963. Characteristics of Douglas-fir Root Systems. Canadian Journal of Botany 41, 105-122.

Morris, J.D. and Collopy, J.J. 2001. Validating plantation water used predictions from the 3PG forest growth model. The Australian National University International Congress on Modeling and Simulation Proceedings. 427-442.

Oren, R. *et al.*, 2001. Sensitivity of mean canopy stomatal conductance to vapor pressure deficit in a flooded Taxodium distichum L. forest: hydraulic and non-hydraulic effects. *Oecologia* 126, 21–29.

Oren, R., Phillips, N., Katul, G., Ewers, B. E. & Pataki, D. E., 1998. Scaling xylem sap flux and soil water balance and calculating variance: a method for

partitioning water flux in forests. *Annales des Sciences Forestières* 55, 191–216.

Price, D. T., Black, T. A. & Kelliher, F. M., 1986. Effects of salal understory removal on photosynthetic rate and stomatal conductance of young Douglas-fir trees. *Can. J. For. Res.* 16, 90–97.

Rothacher, J., 1970. Increases in Water Yield Following Clear-Cut Logging in the Pacific Northwest. *Water Resources Research* 6, 653–658.

Running, S.W. and E.R. Hunt, Jr.. 1993. Generalization of a forest ecosystem process model for other biomes, BIOME-BGC, and an application for global-scale models. Pp. 141-158 *In* J.R. Ehleringer and C.B. Field (eds.) Scaling Physiological Processes: Leaf to Globe. Academic Press, Inc. New York.

Saxton, K. E., Rawls, W. J., Romberger, J. S. & Papendick, R. I., 1986. Estimating Generalized Soil-water Characteristics from Texture. *Soil Science Society of America Journal* 50, 1031–1036

Sharma, M. L. & Luxmoore, R. J., 1979. Soil spatial variability and its consequences on simulated water balance. *Water Resources Research* 15, 1567–1573.

Seibert, J. & McDonnell, J. J., 2010. Land-cover impacts on streamflow: a change-detection modelling approach that incorporates parameter uncertainty. *Hydrological Sciences Journal* 55, 316–332

Stage, A. R., 1976. Notes: An Expression for the Effect of Aspect, Slope, and Habitat Type on Tree Growth.

Waring, R. H. & Landsberg, J. J., 2011. Generalizing plant–water relations to landscapes. *J Plant Ecol* 4, 101–113.

Warren, J. M., Meinzer, F. C., Brooks, J. R. & Domec, J. C., 2005. Vertical stratification of soil water storage and release dynamics in Pacific Northwest coniferous forests. *Agricultural and Forest Meteorology* 130, 39–58

Weiskittel, A. R., Maguire, D. A., Monserud, R. A. & Johnson, G. P., 2010. A hybrid model for intensively managed Douglas-fir plantations in the Pacific Northwest, USA. *European Journal of Forest Research* 129, 325–338.

Wilson, K. B., Hanson, P. J., Mulholland, P. J., Baldocchi, D. D. & Wullschleger, S. D., 2001. A comparison of methods for determining forest evapotranspiration and its components: sap-flow, soil water budget, eddy covariance and catchment water balance. *Agricultural and Forest Meteorology* 106, 153–168.

Table 3-1. Attributes of the 20 plots sampled in association with soil pits on the Panther Creek Watershed.

Plot	Number of Trees		DBH (cm)		Height (m)		Douglas-fir Basal Area (m^2) per HA	LAI
	> 10cm	≤ 10cm	Mean	Range	Mean	Range		
200101	40	22	34.21	2.60 - 108.60	26.00	3.90 - 63.10	97.057	11.152
200102	26	1	51.36	8.7 - 131.10	35.90	4.30 - 57.20	86.793	8.385
200105	57	0	25.98	12.10 - 45.70	26.18	13.10 - 33.70	41.464	3.540
200106	26	0	27.42	9.20 - 53.00	22.44	3.80 - 38.10	40.229	4.316
200108	30	0	44.54	23.50 - 74.6	37.15	27.70 - 46.10	62.591	5.910
200109	17	2	64.30	5.50 - 118.90	45.28	5.40 - 60.90	87.912	10.328
200111	31	0	42.35	13.50 - 74.30	32.20	14.60 - 43.60	63.482	6.775
200201	101	2	27.72	6.80 - 72.20	27.02	7.70 - 43.70	89.011	6.985
200206	56	1	34.13	7.80 - 52.30	26.94	6.90 - 35.90	69.384	6.196
200207	21	1	41.94	3.10 - 65.40	32.26	2.40 - 42.4	40.543	4.034
200208	37	0	39.70	10.30 - 71.50	30.88	6.70 - 44.90	66.914	6.603
200209	29	5	33.88	2.50 - 90.90	27.84	3.20 - 53.40	47.655	5.564
200302	52	0	26.78	14.00 - 41.40	25.12	14.80 - 31.50	38.301	3.623
200303	18	0	70.81	23.30 - 113.00	42.93	14.30 - 57.10	104.708	11.470
200304	38	0	31.56	13.70 - 60.80	29.18	12.30 - 39.80	41.176	3.953
200305	54	0	33.91	18.7 - 51.20	34.36	25.50 - 40.20	64.269	5.530
200310	56	6	21.93	6.50 - 46.50	15.48	1.60 - 21.90	31.011	3.159
200311	44	0	38.49	16.9 - 89.90	33.21	16.60 - 43.80	74.791	6.558
200312	40	4	30.62	2.9 - 61.80	25.75	3.40 - 32.80	46.983	4.128
200313	32	2	27.60	3.70 - 42.50	21.83	4.50 - 27.70	25.913	2.649

Table 3-2a. ANOVA for testing differences in field capacity among soil textural classes at 5 cm.

	Df	**SS**	**MS**	**F**	**P-value**
Texture Effect	5	1221	244.1	0.464	0.798
Error	20	10523	526.2		

Table 3-2b. ANOVA for testing differences in field capacity amongsoil textural classes at 50 cm.

	Df	**SS**	**MS**	**F**	**P-value**
Texture Effect	3	156.6	52.2	1.351	0.29
Error	18	695.6	38.65		

Table 3-3. Plot level values of total seasonal water loss over the growing season (m^3/m^3).

Plot	Cumulative Water Use (m^3/m^3)
200101	0.1668
200102	0.0732
200105	0.1038
200106	0.0799
200108	0.1074
200109	0.1771
200111	0.1611
200201	0.0884
200206	0.0973
200207	0.2706
200208	0.1254
200209	0.1319
200302	0.1745
200303	0.1026
200304	0.1040
200305	0.1076
200310	0.1345
200311	0.0635
200312	0.2256
200313	0.1774

Table 3-4a. Correlation between daily soil water loss and proposed explanatory variables (Equation [2] and Equation [3]).

Variables	**Correlation**
Average Daily VPD	-0.0279
Average Daily RH	0.0767
Average Daily Temp	0.0641
Average Daily Precip	-0.0333
Average Daily g_s	0.0316
Average Daily PAR	0.2304
LAI	-0.0879
Basal Area	-0.1395
Stage Cosine Transformation	0.0261
Stage Sine Transformation	0.0826
Field Capacity 5 cm	0.1338
Field Capacity 50 cm	-0.0365

Table 3-4b. Correlation between cumulative seasonal water loss and proposed explanatory variables (Equation [4]).

Variables	**Corrleation**
LAI	-0.1815
Basal Area	-0.2813
Stage Cosine Transformation	0.2955
Stage Sine Transformation	0.3022
Field Capacity 5 cm	0.2322
Field Capacity 50 cm	-0.2482

Table 3-5. Parameter estimates, standard errors and associated p-values for estimating soil water loss (m^3/m^3) (Equations [2], Equation [3], and Equation [4])

Response	Parameter	Estimate	Standard Error	P-Value
DWL	β20	20.2200	5.6350	< 0.0001
DWL	β21	-0.8355	0.1570	< 0.0001
DWL	β22	0.0048	0.0003	< 0.0001
DWL	β23	-63.1800	10.9300	< 0.0001
DWL	β24	0.1858	0.0402	< 0.0001
DWL	β25	-0.0325	0.0152	0.0331
DWL	β30	19.5325	5.4281	< 0.0001
DWL	β31	-0.8369	0.1513	< 0.0001
DWL	β32	0.0048	0.0003	< 0.0001
DWL	β33	-63.1545	10.5251	< 0.0001
DWL	β34	0.1857	0.0387	< 0.0001
DWL	β35	-0.0216	0.0097	0.0257
DWL	β36	2.8134	0.3474	< 0.0001
DWL	β37	1.3757	0.1776	< 0.0001
DWL	β38	-0.0332	0.0147	0.0237
WL	β40	0.1193	0.0437	0.0183
WL	β41	0.0258	0.0130	0.0717
WL	β42	-0.0304	0.0158	0.0784
WL	β43	0.1319	0.0677	0.0749

Table 3-6 Range in predictor variables associated with estimating soil water loss (m^3/m^3) (Equations [2], Equation [3], and Equation [4])

Equation	Variable	Mean	Min	Max
2, 3	VPD (mb)	8.292647	0.86125	23.81583
2, 3	PAR (uE)	480.3822	89.59142	694.0265
2, 3	gs (cm/s)	0.375291	0.21558	0.426421
2, 3	Temp ^oC	16.9447	11.41542	25.595
2, 3	RH (%)	64.22174	25.53542	93.69167
3	LAI (m^2/m^2)	6.042841	2.648551	11.47017
3	FC (m^3/m^3)	0.272716	0.161705	0.393453
3	S	0.322406	0.1	0.65
3	sin(A)	0.083113	-0.14943	0.353553
3	cos(A)	0.172349	-0.33807	0.65
4	LAI (m^2/m^2)	6.042841	2.648551	11.47017
4	BA (m^2/ha)	0.262013	1.390366	0.000616
4	S	0.322406	0.1	0.65
4	cos(A)	0.132292	0.65	-0.33807

Table 3-7. Plot soil textures and estimated field capacity at 5cm and 50cm and (m^3/m^3).

Plot	Texture 5cm	Texture 50 cm	Field Capacity 5cm (m^3/m^3)	Field Capacity 50cm (m^3/m^3)
200101	Clay loam	Silty clay loam	0.3935	0.4217
200102	Clay	Clay	0.1658	0.5106
200105	Silt loam	Clay loam	0.1617	0.4411
200106	Silty clay loam	Silty clay	0.3839	0.4323
200108	Silt loam	Silt loam	0.3038	0.3534
200109	Silty clay loam	Silt loam	0.3551	0.4515
200111	Silty clay loam	Silty clay loam	0.2883	0.3185
200201	Sandy loam	Silt loam	0.4076	0.4064
200206	Loam	Loam	0.2174	0.2934
200207	Loam	Loamy sand	0.3274	0.2606
200208	Sandy loam	Loam	0.3252	0.2273
200209	Sandy loam	Silt loam	0.3892	0.4643
200211	Loam	Silty clay loam	0.2887	0.4034
200302	Silt loam	Loam	0.2273	0.3937
200303	Loam	Clay loam	0.2482	0.4246
200304	Silt loam	Silty clay loam	0.1752	0.2259
200305	Silt loam	Silty clay loam	0.2534	0.4039
200310	Loam	Silty clay loam	0.3671	0.4398
200311	Silt loam	Silty clay loam	0.2433	0.4090
200312	Silt loam	Silty clay loam	0.2504	0.3478
200313	Sandy loam	Loam	0.3264	0.4649

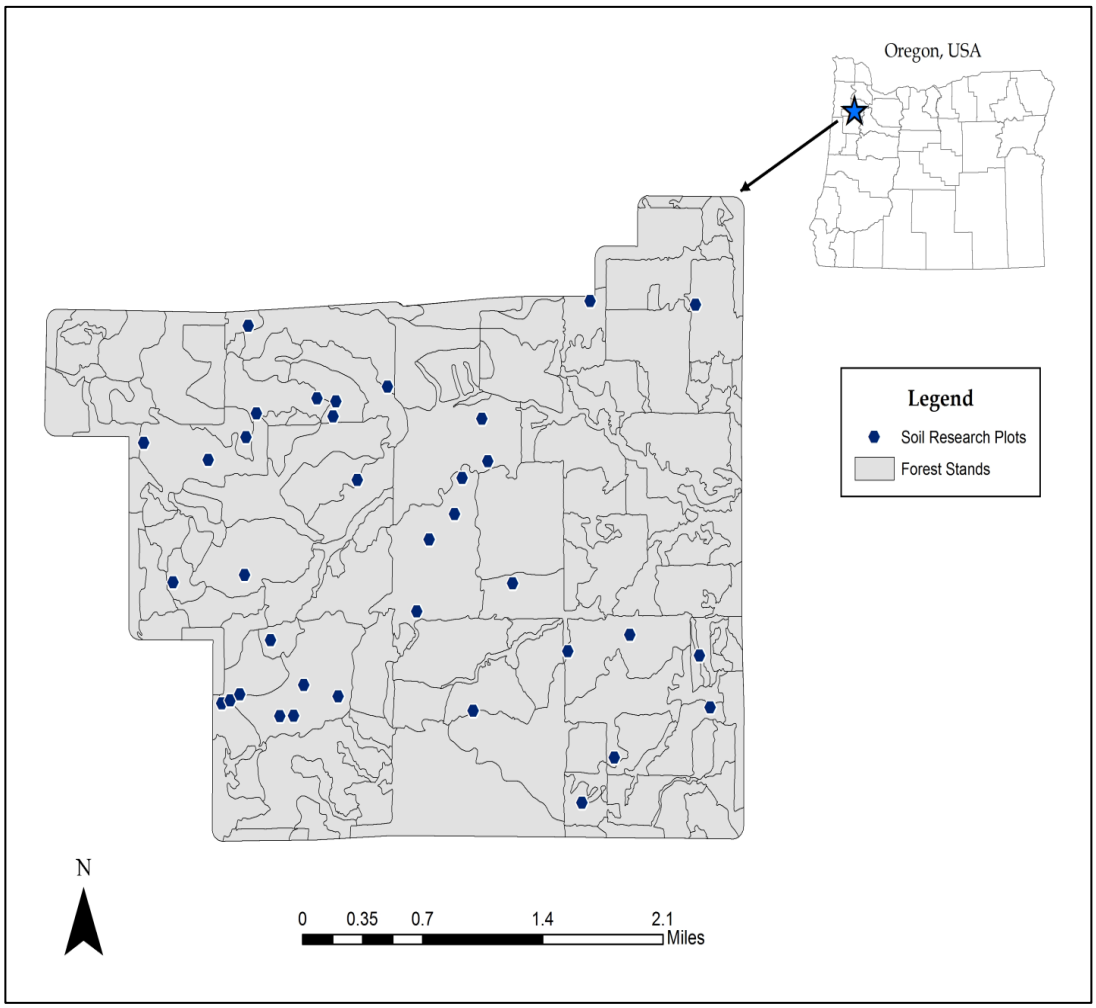

Figure 3-1: Map of the Panther Creek Watershed with location of soil research plots

Figure 3-2: Mini-meteorological station established for monitoring soil volumetric water content (m^3/m^3) at two-hour intervals.

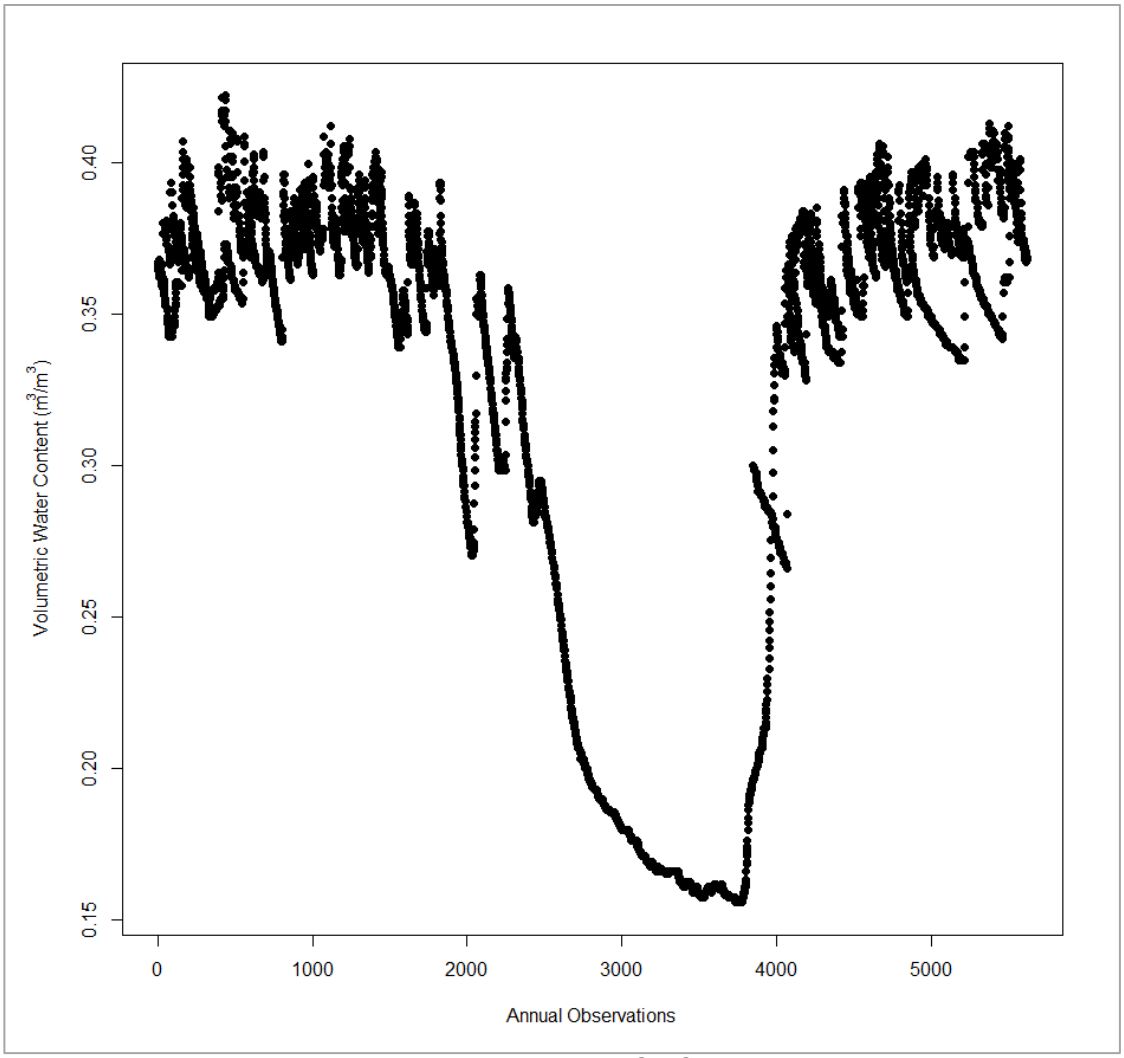

Figure 3-3: Raw soil volumetric water content (m^3/m^3) at two-hour interval collected from one mini-meteorological station for 2012.

Figure 3-4. Mega-meteorological station at Panther Creek, collecting detailed climate data.

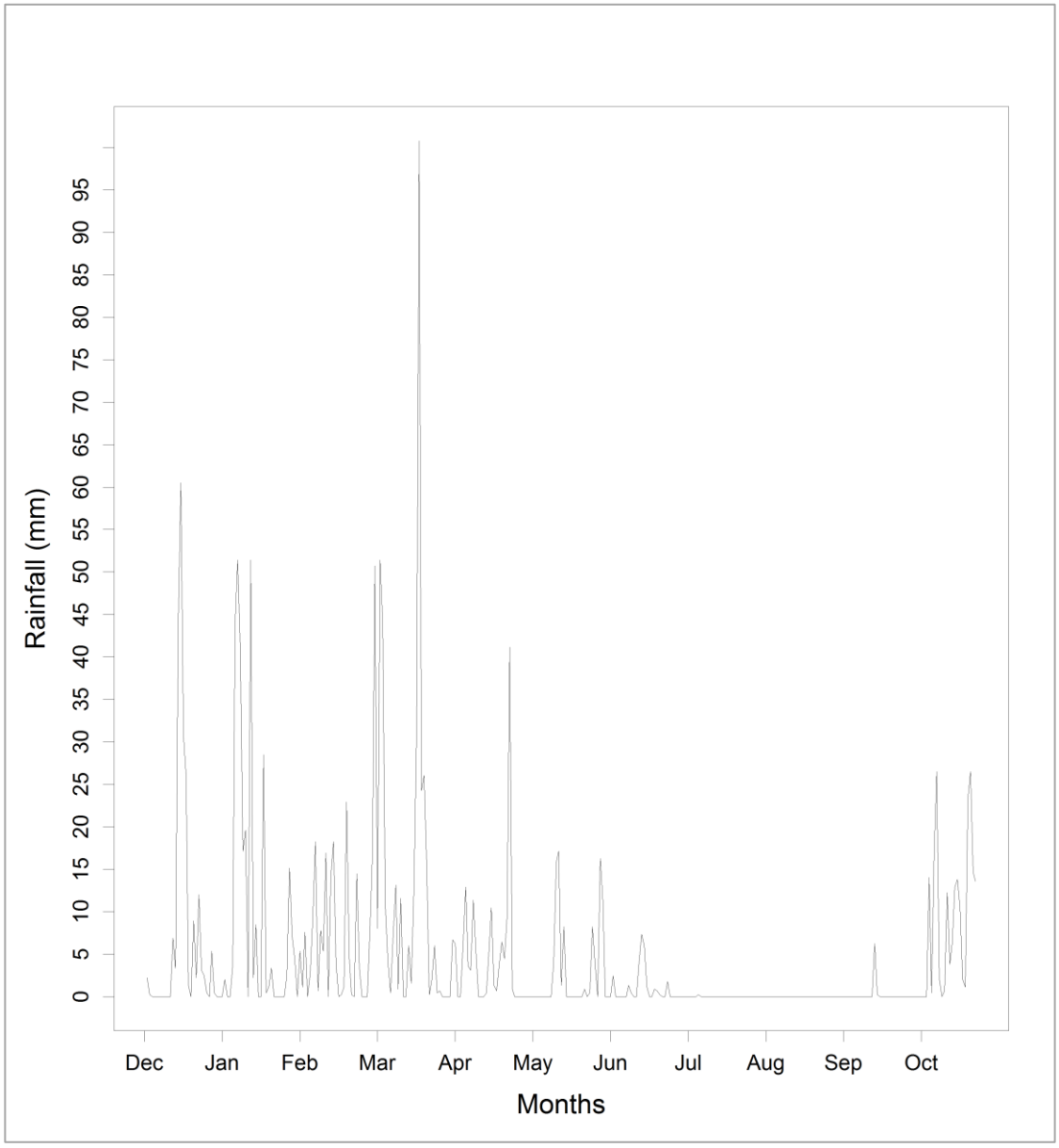

Figure 3-5. Daily total precipitation measured at the Panther Creek mega-meteorological weather station between December 2011 and October 2012.

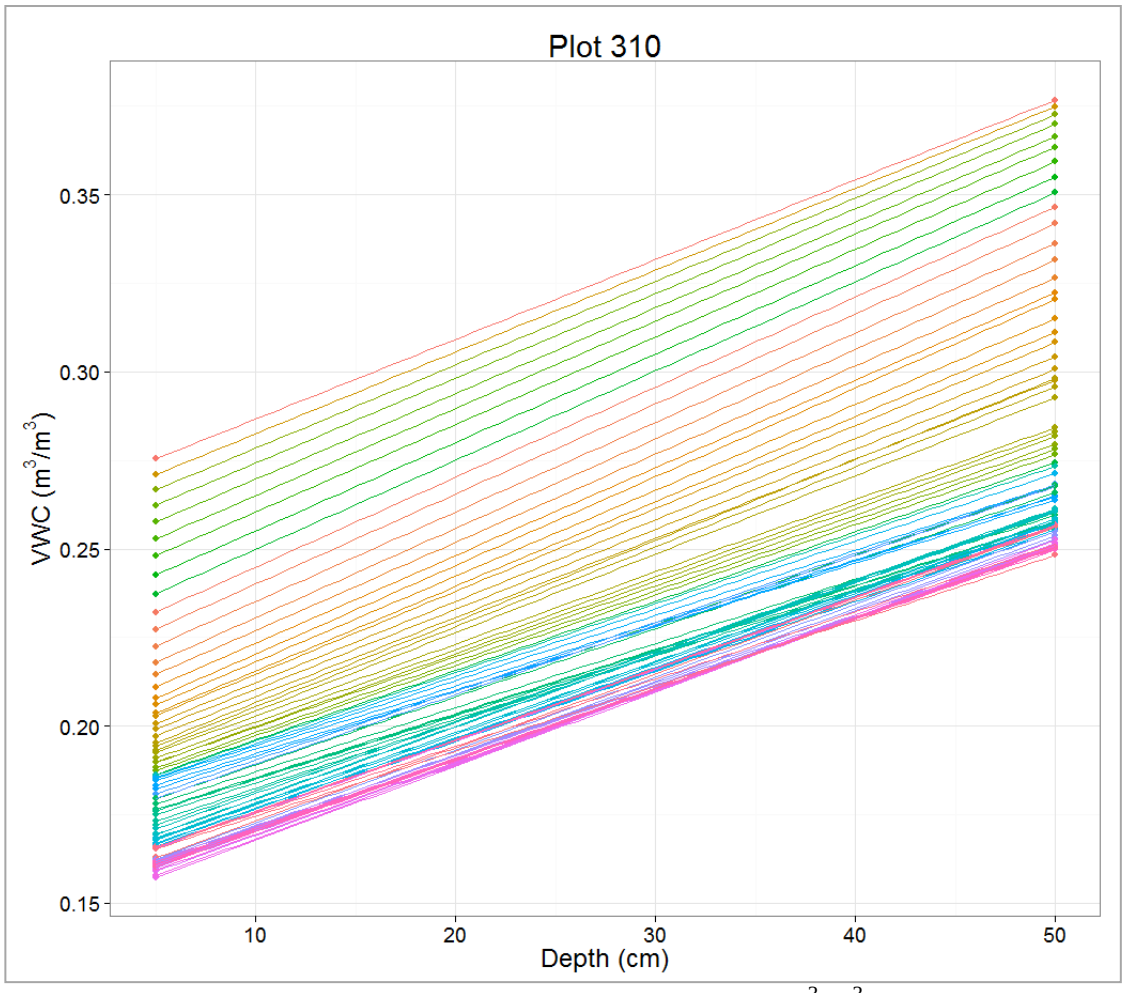

Figure 3-6: Trend of daily VWC by depth into mineral soil (m^3/m^3).

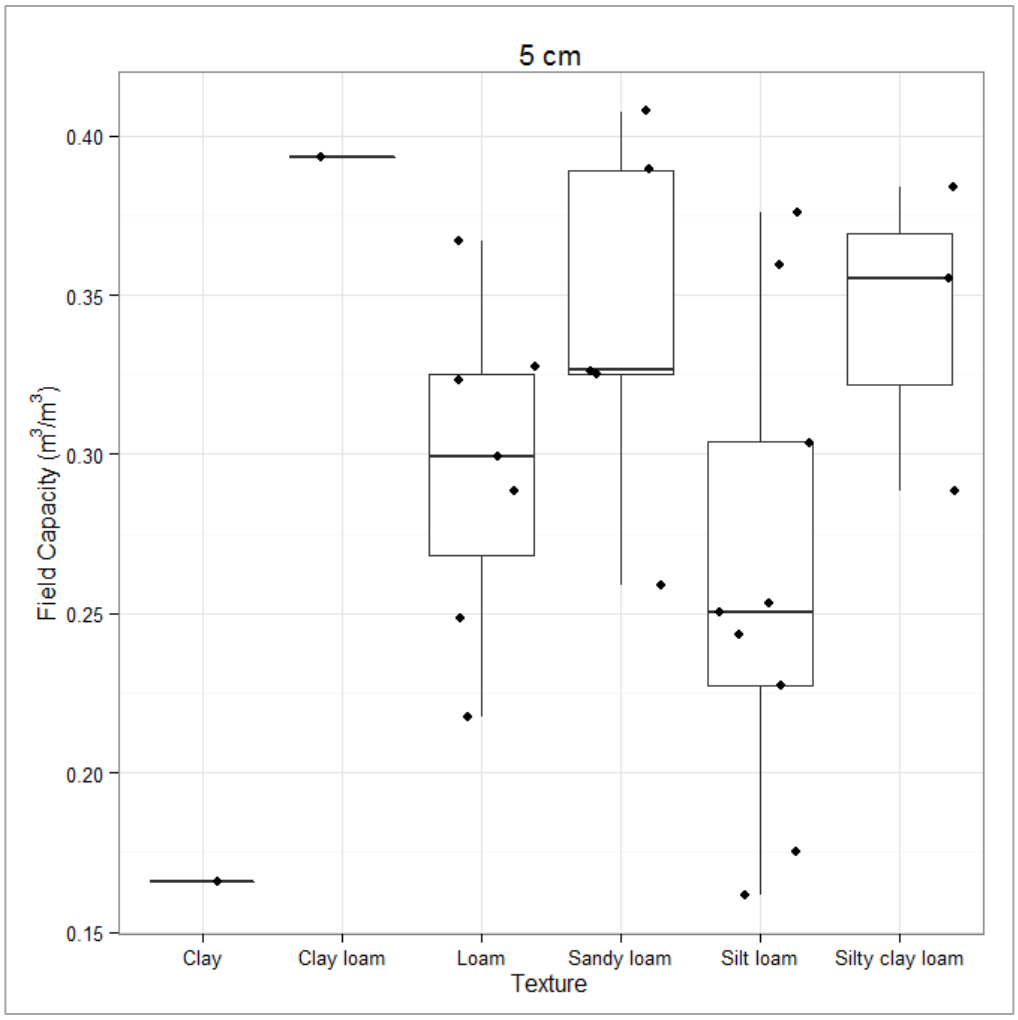

Figure 3-7a: Plot field capacity by texture at 5cm depth from top of mineral soil

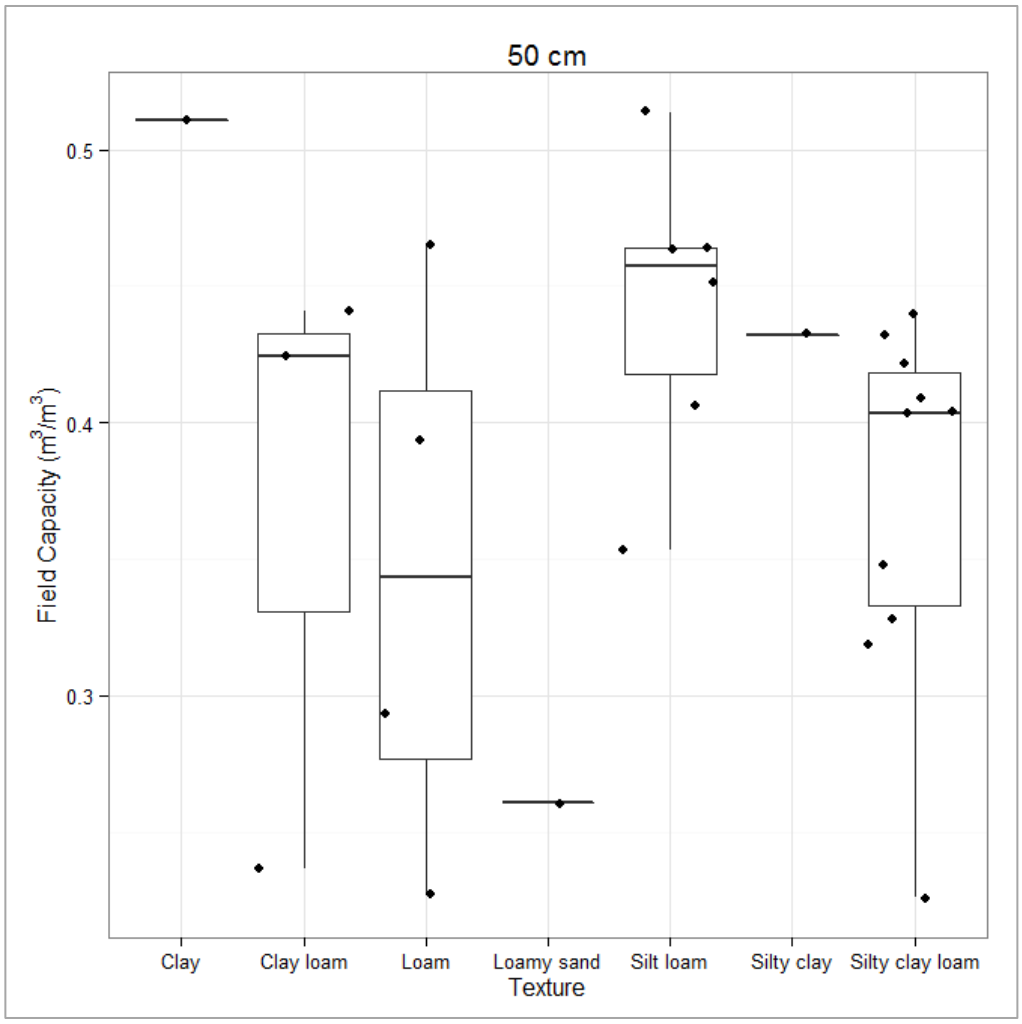

Figure 3-7b: Plot field capacity by texture at 50cm depth from top of mineral soil.

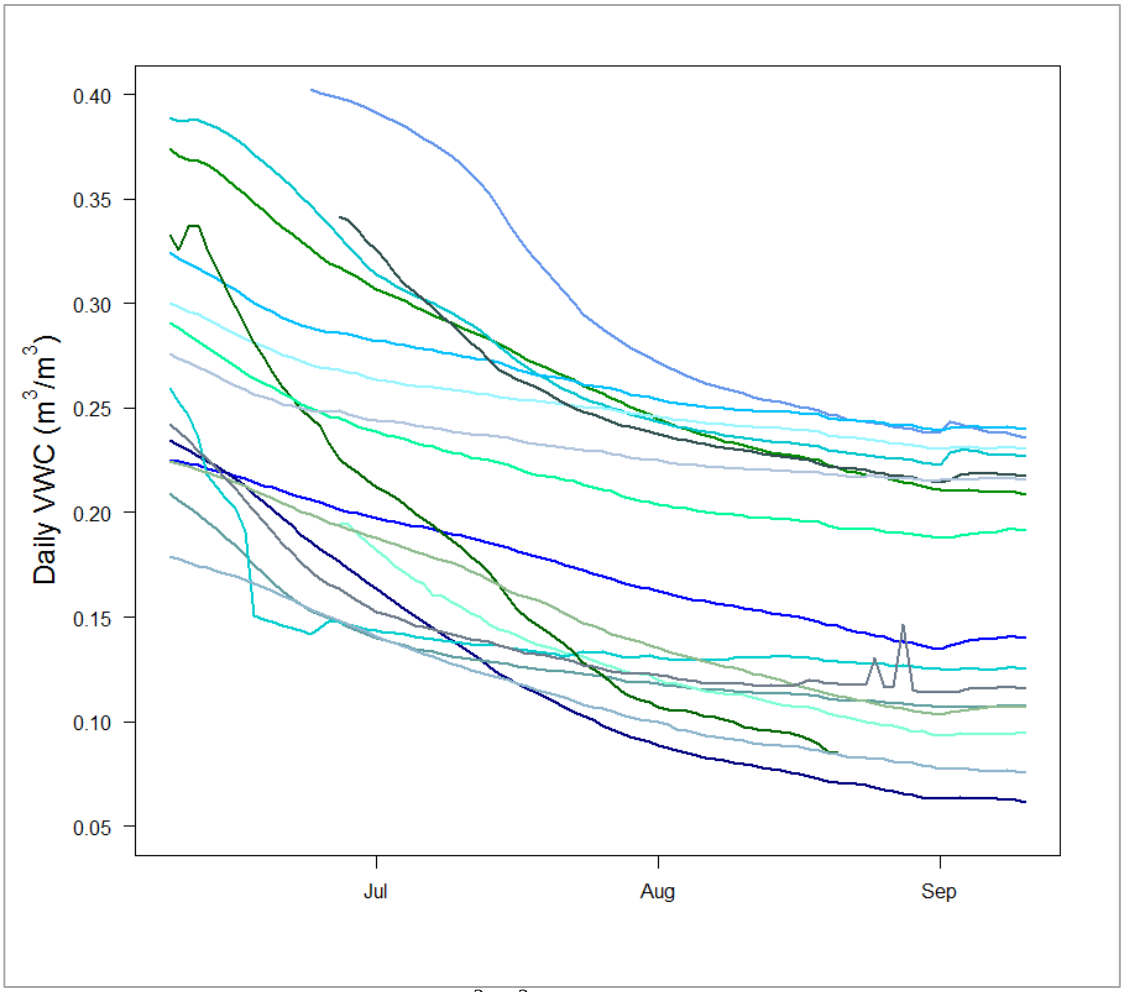

Figure 3-8. Average Daily VWC (m^3/m^3) estimated for the top 50cm of soil on each soil research plot.

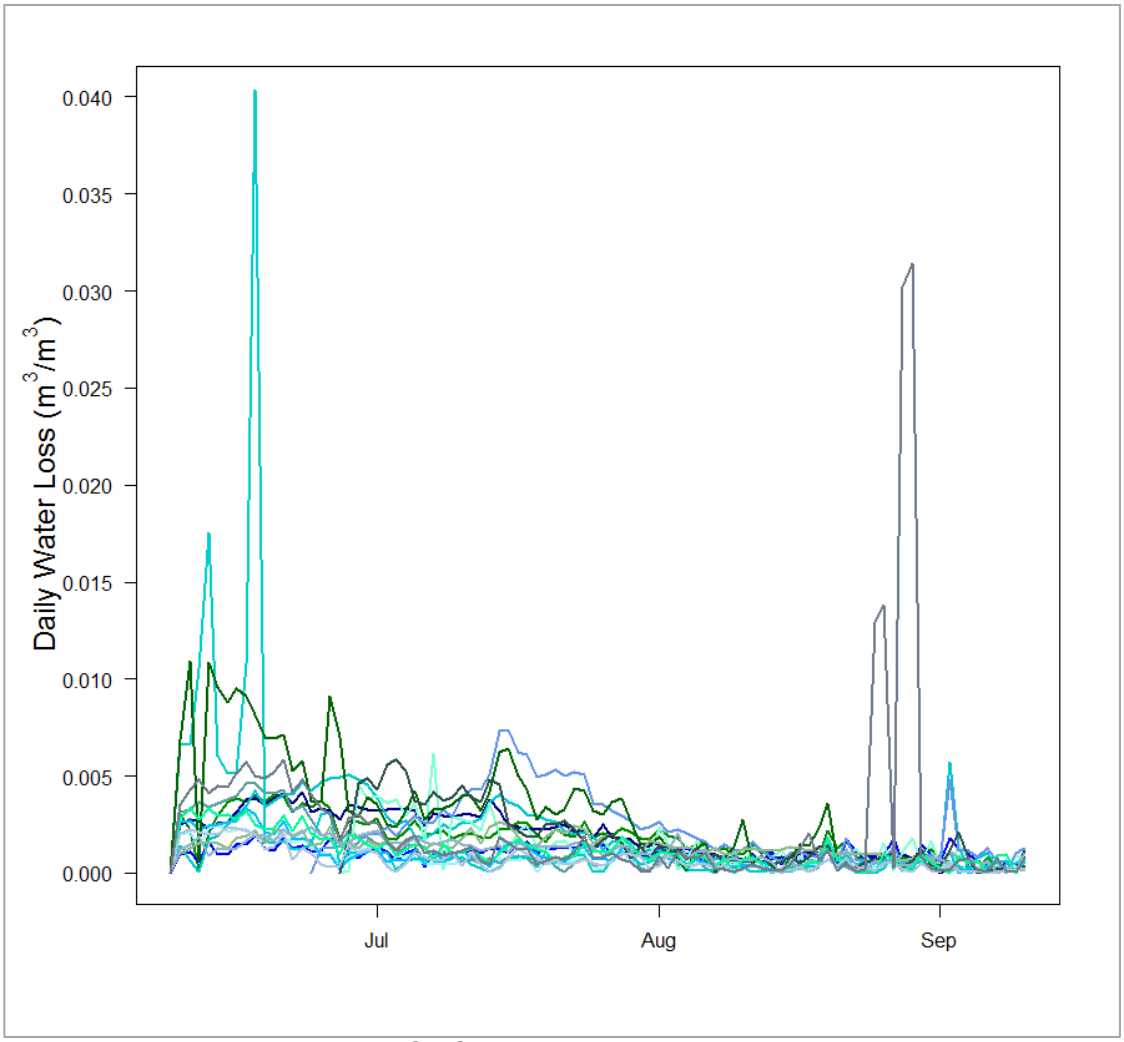

Figure 3-9. Daily water loss (m^3/m^3) estimated for the top 50cm of soil on each soil research plot.

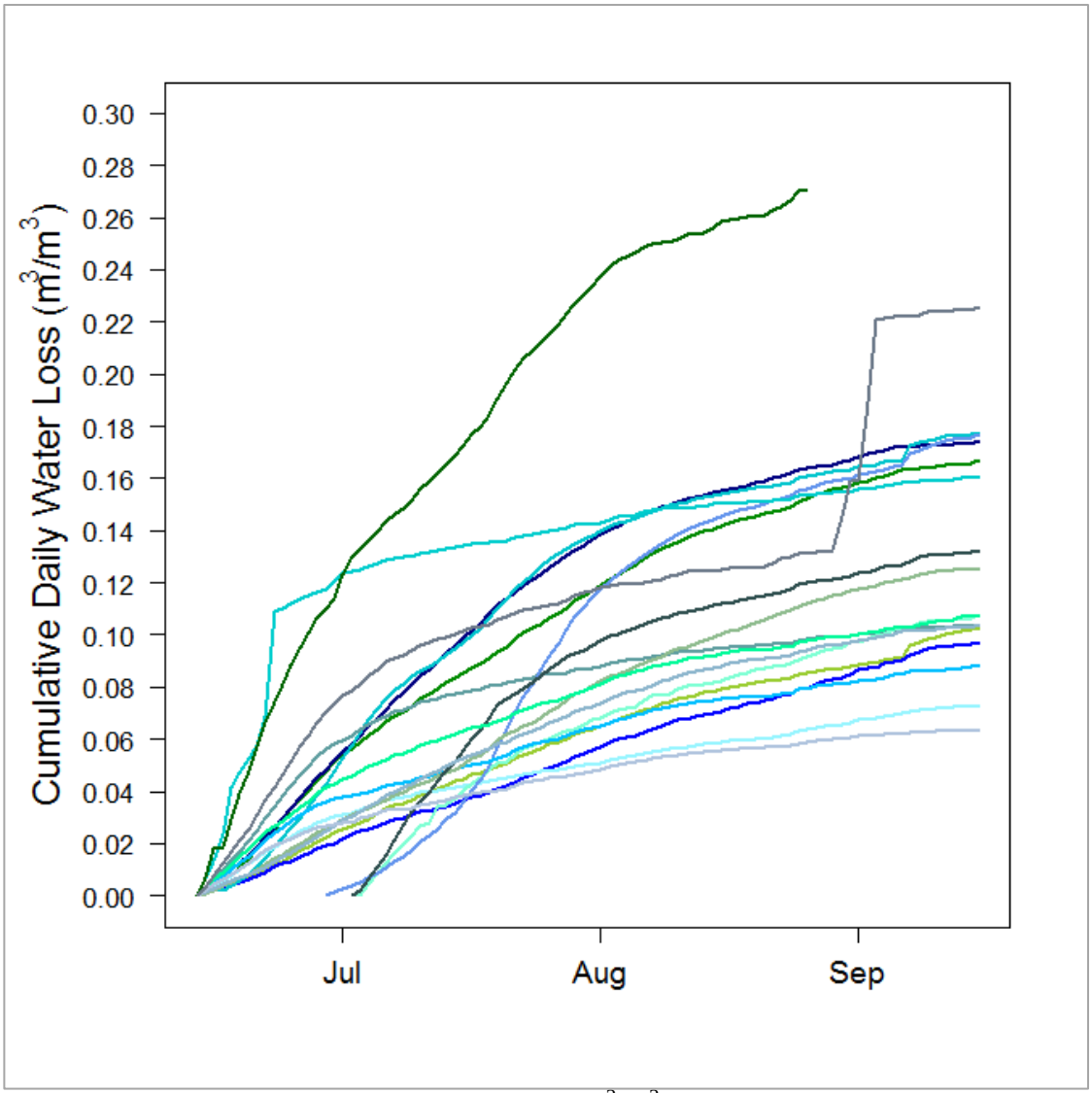

Figure 3-10. Cumulative daily soil water loss (m^3/m^3) estimated for the top 50cm of soil on each soil research plot.

CHAPTER 4: SIMULATION AND VALIDATION OF EVAPOTRANSPIRATION FROM INTENSIVELY MANAGED DOUGLAS-FIR FORESTS

Nicole Rogers, Douglas Maguire, Douglas Mainwaring

Department of Forest Engineering, Resources, and Management, College of Forestry, Oregon State University, Corvallis, OR, 97330

Abstract

Evapotranspiration links photosynthesis to water loss during the process of net gas exchange. This gas exchange occurs through stomata on the surface of conifer needles. A common methodology for estimating evapotranspiration from climatic and physiological variables is application of the Penman-Monteith equation that takes into account stomatal conductance or its inverse, stomatal resistance. However, obtaining this and other appropriate physiological parameters of the model and the climate data for driving the implied processes are difficult to attain at the resolution needed to differentiate the rate of ET among Douglas-fir stands managed under differing silvicultural regimes. In this study, predictions from Penman-Monteith equations are compared against measurements of daily water loss from soils underlying a wide variety of managed stand structures. Cumulative soil water loss over the growing season ranged between 0.06 and 0.27 (m^3/m^3), cumulative ET was between 0.23 and 0.99 (m^3/m^3). Variability in ET estimated from the Penman-Monteith equation and soil water loss suggests that further adjustments must be made in both to improve the credibility of validation.

Introduction

Understanding the tradeoff between water use and productivity is critical for modeling growth of intensively managed Douglas-fir forests in the Pacific Northwest. Absorption of carbon dioxide through the stomates during the process of photosynthesis requires simultaneous loss of water through the process of transpiration. However, when water availability becomes limited during the hot, dry growing season in the Pacific Northwest, stomata must regulate transpiration losses to prevent reduction of hydraulic conductance and potential cavitation (Bond and Kavanagh, 1999). This regulation of water loss limits forest productivity.

Accurate simulation of net primary production of a given forest stand therefore requires an understanding of the local physiological and climatic conditions and their control of water use and photosynthesis. Characteristic drought during the growing

season has been has been shown to reduce both photosynthetic activity and levels of stomatal conductance in Douglas-fir (Black, 1979; Emmingham and Waring, 1976; Price et al., 1986). Studies have found even under sufficient soil water availability, stomatal conductance has been observed to be inversely related to vapor pressure deficits (Waring and Franklin, 1979; Waring et al., 2008). As soil moisture decreases over the growing season the reduced available water supply lowers leaf water potential, and when coupled with increasing evaporative demands due to increasing vapor pressure deficit, stomata close as an adaptive response to minimize physiological damage (Oren et al., 2001; Jassal et al., 2009).

Throughout the forestry literature, varying forms of the Penman-Monteith equation have been employed to simulate evapotranspiration by relying on general concepts of energy balance, aerodynamic properties of plant/forest canopies, and physiological controls on water loss (Penman, 1956; Monteith, 1972). The original Penman equation, treated canopy level evapotranspiration as a large leaf and additionally combined energy and aerodynamic drivers into a single equation which could be run from weather data (Allen, 1986). Monteith further improved upon the original equation with inclusion of a more rigorous term for surface resistance (Allen, 1986).

While successful at coarse spatial scales, application of this approach for accurately estimating site-specific ET has been limited by lack of access to soil and climate data of sufficient spatial and temporal resolution (Calder, 1998). In addition, continuous monitoring of soil moisture simultaneously at many locations has been limited by the available technology until relatively recently. As a result, little validation of stand-level estimates of ET in response to variation in silvicultural regime and local stand structure has been achieved to date.

A study by Black found varying levels of success in validating measures of evapotranspiration against values from a soil water balance model at the stand level (1979). A one site outputs from the 2 models differed by only 1%, however, at the second site outputs differed by 12%. The difference in variability between sites was

attributed to a lack of accuracy in measurements required for the evapotranspiration on the second site (Black, 1979).

A common challenge encountered in application of coarse resolution models is obtaining accurate input variables required to run the soil moisture sub-models. In the growth model 3PG, the soil moisture sub-model interacts with vapor pressure deficits through the stomatal conductance term to modify total modeled productivity, requiring a measure of soil salinity to run properly (Morris and Collopy, 2001). The biome-scale model Biome BGC requires input of daily resolution climate data, soil moisture at field capacity, critical water potential, and initial soil water (Running and Hunt, 1993). The current physiological models would be of greater use in forest management if variables for input were more easily obtainable by quick and efficient field techniques or by accessing comprehensive databases provided by soil and climate scientists.

The general objective of this project is to simulate daily and seasonal evapotranspiration (ET) at the stand level through utilization of detailed soil and climate data that were available for a small watershed in the Oregon Coast Ranges. Specific objectives included: 1) develop a function for estimating stomatal conductance as a function of vapor pressure deficit; 2) select and parameterize a form of the Penman-Monteith equation for estimating daily ET; 3) estimate daily and total seasonal ET for plots on the Panther Creek Watershed; 4) compare measured daily soil water loss to estimated daily ET at each sample plot; 5) compare measured total seasonal soil water loss to estimated total seasonal ET at each sample plot; and 6) assess the quantitative relationship between total seasonal water use and/or ET and periodic annual increment in stem volume as a surrogate for net primary production.

Materials and Methods

Study Area

Data utilized for this project were collected during the summer of 2012 at the Panther Creek Watershed. The watershed is located in the northern portion of the Oregon

Coast Ranges within Yamhill County (Figure 4-1). Panther Creek covers an area of 2580 hectares and includes a combination of public and private ownership. Elevation across the watershed ranges between approximately 170 and 700m. Dominant vegetation includes Douglas fir (*Pseudotsuga menziesii*), western hemlock (*Tsuga heterophylla*), western red cedar (*Thuja plicata*), big leaf maple (*Acer macrophyllum*), and red alder (*Alnus rubra*), forming stands that, in general, are under active management for timber production.

Soils in the Coast Ranges are strongly related to their geomorphic surfaces and are generally either volcanic or sedimentary in origin (Balster and Parsons, 1966). In areas of volcanic parent material, the underlying basalt layer is commonly overlaid with soil textures in the lower third of the soil texture triangle (Natural Resources Conservation Service). In areas of sedimentary origin, sandstones and shales are typically overlaid with soil textures in the lower left corner of the soil texture triangle.

Climate within the study area can be characterized as having cool, wet winters and hot, dry summers. Periodic drought is common during summer months. Total precipitation is 1600 mm annually with average minimum January temperatures ranging from -2 to 2^{o} C and average maximum July temperatures from 20 to 25^{o}C (ClimateWNA).

Research plots across the watershed were established in two phases, Phase I for LiDAR ground-truthing and Phase II for soil research. Plots were circular with a 16m radius. For this project research was confined to 27 Phase II plots with Douglas-fir comprising $\geq$ 80% of total plot basal area. This compositional threshold was established to focus on plots as close to pure Douglas-fir as possible. Leaf area index had been previously been estimated for the subject plots to facilitate estimation of ET (see Chapter 2 of this thesis), and soil moisture was monitored continuously as described below to characterize the daily rate of water use.

Douglas-fir age on individual plots ranged between 21- and 139-years-old at breast height. Plot basal area and tree density ranged from 25.9 to 104.7 m^2/ha and 223 to 1255 trees/ha, respectively (Table 4-1). Twenty-four of the 27 plots were naturally regenerated after clearcut harvesting, and the three remaining plots were planted.

Available Data

Detailed soil data were collected to NRCS specifications at 26 of the 27 sampled soil research plots. A mini-meteorological station was established at each soil research plot and was equipped to record soil volumetric water content (m^3/m^3) and temperature at two-hour intervals throughout the day (Figure 4-2). Decagon EC-5 soil moisture sensors were installed at depths of 5 cm and 50 cm from the top of mineral soil at each mini-met station and data from the sensors were stored on a Decagon EM-50 Analog Data Logger and manually downloaded on a three-month cycle. Downloaded data was returned to the lab and graphically assessed for errors and missing observations (Figure 4-3). Volumetric water content was converted to an average daily value using the arithmetic mean.

At seven soil research plots sensors had missing data at 5 cm, 50 cm or both depths and were therefore not used in this analysis, leaving a total of 20 plots.

In addition to each mini-meteorological station, a larger weather station was also established at Panther Creek (Figure 4-4). Readings of climate data were taken on an hourly resolution. Measured climate data used in the current analysis included total precipitation (mm), temperature (^oC), vapor pressure deficit (kPa), relative humidity (%), and photosynthetically active radiation (uE). Data were collected from the weather station every three months and returned to the lab for quality control. Average daily values were computed from the hourly climate data as the arithmetic mean.

Data for this analysis were limited to the summer growing season between July 1st and September 30th. A start date of July 1st was selected to simplify simulations of stand

water use by focusing on the period with virtually no soil water recharge from precipitation (Figure 4-5).

Leaf Area Index

Leaf area index (LAI) was estimated for each plot by estimating foliage mass on felled trees, developing tree-level equations that predicted foliage mass as a function of DBH and live crown length, and applying an average specific leaf area of 53.3 cm^2/g to the foliage mass estimates (see Chapter 2 of this thesis). Values of plot-level LAI ranged from 2.65 to 11.47 (Table 4-1).

Statistical Analysis

Stomatal conductance

Estimates of stomatal conductance were derived from values of daily vapor pressure deficits, assuming an inverse relationship between the two variables (Waring and Franklin, 1979). A reverse sigmoid function was fit to the data presented by Waring and Franklin (1979) to facilitate daily predictions of stomatal conductance from measured vapor pressure deficits.

Evapotranspiration

Daily evapotranspiration was simulated using the Penman-Monteith variant applied by Tan et al (1978) for a thinned Douglas-fir stand in British Columbia, with estimates of LAI based on foliage mass predicted from DBH and live crown length (Chapter 2 of this thesis). The model was of the form:

[1] $$E = \frac{\rho C_p}{L\gamma} \frac{LAI_i VPD_i}{r_{si}}$$

Where E is daily evapotranspiration ($g \cdot cm^{-2} \cdot sec^{-1}$), ρ is the density of moist air (1.2×10^{-3} $g \cdot cm^{-3}$), C_p is the specific heat of moist air (1.01 $J \cdot g\text{-}1 \cdot {}^{o}C^{-1}$), L is the latent heat of vaporization of water (2450 J/g), γ is the psychrometric constant (0.66 mb), *VPD* is

daily vapor pressure deficits (mb), *LAI* is leaf area index ($m^2 \cdot m^{-2}$), and r_s is daily stomatal resistance ($sec \cdot cm^{-1}$).

The inverse of stomatal conductance ($sec \cdot cm^{-1}$) was taken to represent stomatal resistance. Final simulations of daily evapotranspiration were converted from $g \cdot cm^{-2} \cdot s^{-1}$ to $g \cdot m^{-2} \cdot day^{-1}$. Cumulative evapotranspiration for each plot was the summed daily value of evapotranspiration for all days since the starting date of July 1, 2012. Cumulative evapotranspiration was multiplied by the density of water ($g \cdot cm^{-3}$) assuming standard air temperature (4ºC) and converted to units of m^3/m^3.

Validation of Evapotranspiration

Plot level evapotranspiration simulated with the Penman-Monteith equations was visually compared to the corresponding measurement of soil water loss. Validation statistics were also calculated to further compare the two estimates. Statistics computed included mean difference, mean squared difference, mean absolute difference, and mean relative difference.

Comparison of Evapotranspiration to Stand Growth

The link between total seasonal evapotranspiration and stand productivity was assessed by comparing three-year periodic annual increment computed from plot measurements in 2009 and 2012. PAI was expressed as a function of initial basal area, initial stand age, and total seasonal water loss using multiple linear regression.

Results

Stomatal Conductance

The equation developed to simulate daily stomatal conductance was of the form:

[2] $$g_{s_i} = \frac{\beta_{20}}{1+exp^{\beta_{21}(VPD_i - \beta_{22})}} + \varepsilon_{2i}$$

where g_s is stomatal conductance (cm·sec^{-1}) on the *i*th day, *VPD* is vapor pressure deficit (mb) on the *i*th day, β_{2k}s are parameters to be estimated from the data, and ε_{2i} is the error term with $\varepsilon_{2i} \sim N(0,\sigma_2^2)$. Predicted stomatal conductance followed the same general trend as the curve used by Waring and Franklin (1976) to estimate evapotranspiration (Figure 4-6). The model slightly over estimated g_s at low VPD and slightly underestimated g_s at high VPD.

Evapotranspiration

Daily estimates of evapotranspiration varied tremendously from plot to plot (Figure 4-7). Plots with the highest leaf area index had the highest evapotranspiration. Total seasonal estimates of evapotranspiration likewise varied proportional to estimated plot LAI (Figure 4-8).

Validation of Simulated Evapotranspiration

Daily and total seasonal evapotranspiration (m^3/m^3) simulated from the Penman-Monteith equation in the form applied by Tan et al. (1978) were each graphically and numerically assessed against daily and total seasonal soil water loss (m^3/m^3) (Figure 4-9 – Figure 4-12, Table 4-2). The plot-to-plot variability in simulated evapotranspiration was greater at the seasonal resolution.

A graph of daily evapotranspiration vs. daily soil water loss at the watershed scale fit with a 1:1 shows estimates of evapotranspiration consistently overestimated in comparison to soil water loss (Figure 4-12). Mean relative difference was greater for the seasonal resolution than the daily resolution (Table 4-3a, b).

Comparison of Evapotranspiration to Stand Growth

The tested equation used to predict PAI was of the form:

[3] $$PAI_i = \beta_{30} + \beta_{31}BA_i + \beta_{32}Age_i + \beta_{33}WL_i + \varepsilon_{3i}$$

where *PAI* was net periodic increment on plot *i* between 2009 and 2012, BA_i was basal area on plot *i*, *Age* was average age at breast height on plot *i*, WL_i was cumulative water loss over the 2012 growing season on plot *i*, β_{3k}s were parameter estimated from the data, $\varepsilon_{3i} \sim N(0, \sigma_3^2)$. A plot of model fitted vs. residual values supported the assumption of constant variance (Appendix, Figure 5). The model produced an R^2 of 0.205. Only parameters for plot age and the intercept were significantly different from zero (p=0.0451 and 0.0008, respectively) (Table 4-4).

Discussion

Stomatal Conductance

Stomatal conductance is an essential process in evapotranspiration, regulating the movement of water vapor from leaves in response to changes in ambient environmental conditions and soil water availability (Oren et al., 2001; Addington et al., 2004). However, for this analysis a simple approach was developed to represent stomatal conductance with the objective of sacrificing some accuracy to eliminate the need to measure stomatal conductance directly.

A key component in stomatal conductance not addressed in this study is the coupling of soil moisture deficits and vapor pressure deficits. While both deficits are recognized to regulate stomatal closure of leaves, the switching point for dominance of one over the other, or if a switching point occurs, is largely unknown (Wijk et al., 2000;Oren et al., 2001; Addington et al., 2004). Estimates of stomatal conductance which account for the combined and possibly interactive effect of these two deficits would undoubtedly improve our ability to improve simulation of forest ET.

Evapotranspiration

An objective of this project was to simulate daily and seasonal evapotranspiration from a form of the Penman-Monteith equation. The equation utilized by Tan et al. (1978) for thinned Douglas-fir was selected for its simple form and limited number of physiological inputs. The variables driving evapotranspiration, including vapor

pressure deficits, stomatal conductance, and leaf area index, were either measured from the on-site weather station or estimated with regression equations. Sensitivity of ET estimates to these variables and the uncertainty in estimating them makes it difficult to evaluate the efficacy of the Penman-Monteith equation for estimating differences in ET among stands of varying structure within a narrow geographic range.

A variable commonly cited as a driver of evapotranspiration, net radiation, was not included in the model form from Tan et al. (1978). In coniferous forests where canopy conductance is greater than individual leaf conductance, VPD is believed to be the main influence on evapotranspiration, and LAI, which varies by plot, should be proportional to intercepted radiation, justifying the substitution of measured net radiation for the sake of simplification and practicality (Weiskittel et al., 2011; Waring and Running, 1998).

Penman-Monteith forms of greater complexity have been developed and used in variety of forestry contexts. A study by Whitehead and Kelliher (1991) incorporated additional terms into their Penman-Monteith equation for available energy flux into canopy, aerodynamic conductance of canopy, and water storage within the canopy for a given time period; Allen (1986) addressed a Penman-Monteith form which required an input of heat flux into the soil; and Ventura et al. (1999) incorporated wind speed as a variable in their Penman-Monteith equation. While inclusion of additional parameters has the potential to add vital information and improve simulations for intensive study sites, the goal of the Panther Creek study was to explore the utility of this equation for distinguishing ET differences among stands with varying structure attributable to silvicultural regime. For application in forest management, the number and variety of stands and soils necessitates a tradeoff between operational simplicity and physiological precision.

Validation of Evapotranspiration

Due to the responsiveness of stomatal conductance to ambient environmental conditions and soil water status, evapotranspiration is a dynamic process on the diurnal and seasonal scales, so essentially drives forest productivity. The variability seen from plot to plot in total daily simulated evapotranspiration can be attributed to plot-level LAI, while the large daily fluctuations at a given plot reflect the daily variation in vapor pressure deficit and stomatal conductance at the watershed level. Estimation of stomatal conductance and vapor pressure deficit at the plot-level would no doubt introduce additional plot-level variability in daily fluctuations of estimated ET.

Variability in soil water loss at a daily and seasonal resolution can be attributed to variability in soil textural and structural attributes (Brady and Weil, 2008). Additionally, influx of soil water from hydraulic redistribution adds variability to each plot, as does the influence of competing vegetation and other tree species (Price et al 1986; detailed discussion of variability in soil water loss from plot to plot can be found in Chapter 3).

The largest discrepancy between soil water loss and evapotranspiration occurs at the end of the growing season (Figure 4-8, 4-10). Timing of discrepancies suggests a term for soil moisture is needed in the Penman-Monteith equation to constrain evapotranspiration values as soil dries over the growing season.

Comparison of Evapotranspiration to Stand Growth

The low predictive power of the model created to predict periodic annual increment as a function of initial stand age, initial stand basal area, and seasonal water loss can be attributed in part to use of preliminary data for the analysis. Estimates of PAI were based on raw data from a current tree inventory still requiring additional quality control. Further, plots used in this study were constrained to a basal area of Douglas-fir 80% or greater. Inclusion of a covariate which addresses basal area in the other

tree species may help account for additional variability. Finally, water loss was used as a simple proxy for plot productivity. However, as can be seen in Chapter 3 of this thesis, improvements are required to estimate water use more accurately and to account for possible differences in water use efficiency.

Next Steps

This research provides a firm stepping stone for further analysis in hydraulic processes and their relationship to productivity of intensively managed Douglas-fir forests. Next steps for consideration include direct measurement of stomatal conductance and gas exchange, including that of water vapor during evapotranspiration. Stomatal conductance is a challenging parameter to estimate without direct measures of evapotranspiration or hydraulic conductance (Bond and Kavanagh, 1996; Weiskittel et al., 2011). Conversely, evapotranspiration is difficult to measure without estimates of stomatal conductance (Tan et al., 1978; Whitehead and Kelliher, 1991; Allen, 1986; Ventura et al., 1999). Simple equations developed to predict stomatal conductance and evapotranspiration with parameter estimates appropriate for the Pacific Northwest would facilitate application of water relations to simulation of Douglas-fir productivity. Ultimately, it may be important to account for the effect of wide variation in canopy structure among managed stands, in contrast to the "big leaf" approach implied by the Penman-Monteith equation. Further study into the complexities of soil moisture and fine root distribution and dynamics would also help improve mechanistic models of water availability and stand productivity.

Conclusions

Water lost to evapotranspiration was estimated from a simple Penman-Monteith for twenty plots and compared to measurements of soil water loss. Both ET and soil water loss varied widely from plot to plot at daily and seasonal resolutions. Relative mean difference suggested that estimated ET was more closely related to measured soil water loss at a daily resolution. However, estimates from the Penman-Monteith equation were not well validated by measures of soil water loss. While ET, soil water

loss, and net primary production must logically be closely related, further work is required to bring all three in line before they can be fully utilized in forest management.

Literature Cited

Addington, R. N., Mitchell, R. J., Oren, R. & Donovan, L. A. Stomatal sensitivity to vapor pressure deficit and its relationship to hydraulic conductance in Pinus palustris. *Tree Physiol* 24, 561–569 (2004).

Allen, R. A Penman for All Seasons. *Journal of Irrigation and Drainage Engineering* 112, 348–368 (1986).

Balster, C. A., Parsons, R. B., 1968.Service, U. S. S. C. & Station, O. S. U. A. E. *Geomorphology and soils, Willamette Valley, Oregon*. (Corvallis, Or. : Agricultural Experiment Station, Oregon State University.

Black, T.A., 1979. Evapotranspiration from Douglas-fir stands exposed to soil water deficits. *Water Resources Research* 15, 164-170.

Brady, N.C. and Weil R.R., 2008. The Nature and properties of soils; Fourteenth Edition. Fourth Edition. Pearson Prentice Hall, Inc., Upper Saddle River, New

Bond, B. J. & Kavanagh, K. L. Stomatal behavior of four woody species in relation to leaf-specific hydraulic conductance and threshold water potential. *Tree Physiol* 19, 503–510 (1999).

Calder, I. R., 1998. Water use by forests, limits and controls. *Tree Physiol* **18,** 625–631.

Emmingham, W.H. and Waring, R.H., 1977. An index of photosynthesis for comparing forest sites in western Oregon. *Canadian Journal of Forest Resources* 7, 165-174.

Jassal, R. S. *et al.* Components of ecosystem respiration and an estimate of net primary productivity of an intermediate-aged Douglas-fir stand. *Agricultural and Forest Meteorology* 144, 44–57 (2007).

Monteith, J. l., 1972 Solar Radiation and Productivity in Tropical Ecosystems. *Journal of Applied Ecology* 9, 747.

Morris, J.D. and Collopy, J.J. 2001. Validating plantation water used predictions from the 3PG forest growth model. The Australian National University International Congress on Modeling and Simulation Proceedings. 427-442.

Oren, R. *et al.* Sensitivity of mean canopy stomatal conductance to vapor pressure deficit in a flooded Taxodium distichum L. forest: hydraulic and non-hydraulic effects. *Oecologia* 126, 21–29 (2001).

Penman, H. L. Natural Evaporation from Open Water, Bare Soil and Grass. *Proc. R. Soc. Lond. A* 193, 120–145 (1948).

Price, D. T., Black, T. A. & Kelliher, F. M. Effects of salal understory removal on photosynthetic rate and stomatal conductance of young Douglas-fir trees. *Canadian Journal of Forest Research* 16, 90–97 (1986).

Running, S.W. and E.R. Hunt, Jr., 1993. Generalization of a forest ecosystem process model for other biomes, BIOME-BGC, and an application for global-scale models. Pp. 141-158 *In* J.R. Ehleringer and C.B. Field (eds.) Scaling Physiological Processes: Leaf to Globe. Academic Press, Inc. New York.

Tan, C. S., Black, T. A. & Nnyamah, J. U. A Simple Diffusion Model of Transpiration Applied to a Thinned Douglas-Fir Stand. *Ecology* 59, 1221–1229 (1978).

Valentine, H. T. & Mäkelä, A., 2005. Bridging process-based and empirical approaches to modeling tree growth. *Tree Physiology* 25, 769–779

Waring, R. H. & Franklin, J. F. Evergreen coniferous forests of the Pacific Northwest. *Science* 204, 1380–1386 (1979).

Waring, R. *et al.* Why is the productivity of Douglas-fir higher in New Zealand than in its native range in the Pacific Northwest, USA? *Forest Ecology and Management* 255, 4040–4046 (2008).

Waring, R.H. and Running, S.W., 1998. Forest cosystem analysis at multiple scales; Second Edition. Academic Press. San Diego, California. 370 p.

Weiskittel, A.R., Hann, D.W., Kerhsaw Jr., J.A., Vanclay, J.K. 2011. Forest Growth and Yield Modeling. Wiley. 424 p.

Whitehead, D. & Kelliher, F. M. Modeling the water balance of a small Pinus radiata catchment. *Tree Physiol* 9, 17–33 (1991).

Wijk, M. T. V. *et al.* Modeling daily gas exchange of a Douglas-fir forest: comparison of three stomatal conductance models with and without a soil water stress function. *Tree Physiol* 20, 115–122 (2000).

Wilson, K. B., Hanson, P. J., Mulholland, P. J., Baldocchi, D. D. & Wullschleger, S. D. A comparison of methods for determining forest evapotranspiration and its components: sap-flow, soil water budget, eddy covariance and catchment water balance. *Agricultural and Forest Meteorology* 106, 153–168 (2001).

Table 4-1. Attributes of the 20 plots sampled associated with soil pits on the Panther Creek Watershed.

Plot	Number of Trees		DBH (cm)		Height (m)		Douglas-fir Basal Area (m^2) per HA	LAI
	> 10cm	≤ 10cm	Mean	Range	Mean	Range		
200101	40	22	34.21	2.60 - 108.60	26.00	3.90 - 63.10	97.057	11.152
200102	26	1	51.36	8.7 - 131.10	35.90	4.30 - 57.20	86.793	8.385
200105	57	0	25.98	12.10 - 45.70	26.18	13.10 - 33.70	41.464	3.540
200106	26	0	27.42	9.20 - 53.00	22.44	3.80 - 38.10	40.229	4.316
200108	30	0	44.54	23.50 - 74.6	37.15	27.70 - 46.10	62.591	5.910
200109	17	2	64.30	5.50 - 118.90	45.28	5.40 - 60.90	87.912	10.328
200111	31	0	42.35	13.50 - 74.30	32.20	14.60 - 43.60	63.482	6.775
200201	101	2	27.72	6.80 - 72.20	27.02	7.70 - 43.70	89.011	6.985
200206	56	1	34.13	7.80 - 52.30	26.94	6.90 - 35.90	69.384	6.196
200207	21	1	41.94	3.10 - 65.40	32.26	2.40 - 42.4	40.543	4.034
200208	37	0	39.70	10.30 - 71.50	30.88	6.70 - 44.90	66.914	6.603
200209	29	5	33.88	2.50 - 90.90	27.84	3.20 - 53.40	47.655	5.564
200302	52	0	26.78	14.00 - 41.40	25.12	14.80 - 31.50	38.301	3.623
200303	18	0	70.81	23.30 - 113.00	42.93	14.30 - 57.10	104.708	11.470
200304	38	0	31.56	13.70 - 60.80	29.18	12.30 - 39.80	41.176	3.953
200305	54	0	33.91	18.7 - 51.20	34.36	25.50 - 40.20	64.269	5.530
200310	56	6	21.93	6.50 - 46.50	15.48	1.60 - 21.90	31.011	3.159
200311	44	0	38.49	16.9 - 89.90	33.21	16.60 - 43.80	74.791	6.558
200312	40	4	30.62	2.9 - 61.80	25.75	3.40 - 32.80	46.983	4.128
200313	32	2	27.60	3.70 - 42.50	21.83	4.50 - 27.70	25.913	2.649

Table 4-4. Cumulative soil water loss and cumulative ET by plot.

Plot	Cumulative Soil Water Loss (m^3/m^3)	Cumulative ET (m^3/m^3)
200101	0.1668	0.9633
200102	0.0732	0.7243
200105	0.1038	0.3058
200108	0.1074	0.4241
200111	0.1611	0.5852
200201	0.0884	0.6034
200206	0.0973	0.5352
200207	0.2706	0.2675
200208	0.1254	0.5704
200209	0.1319	0.3993
200302	0.1745	0.3130
200303	0.1026	0.9908
200304	0.1040	0.3415
200305	0.1076	0.4777
200310	0.1345	0.2729
200311	0.0635	0.5665
200312	0.2256	0.3566
200313	0.1774	0.2280

Table 4-3 a. Validation statistics calculated for soil water loss and ET at a daily resolution.

Statistic	Value
Mean Difference	-4.0685E-03
Squared Difference	3.4051E-05
Absolute different	4.5255E-03
Relative Difference	-5.8983E-01

Table 4-3 b. Validation statistics calculated for soil water loss and ET at a seasonal resolution.

Statistic	Value
Mean Difference	-3.6164E-01
Squared Difference	1.8883E-01
Absolute different	3.6199E-01
Relative Difference	-6.5339E-01

Table 4-4. Parameter estimates, standard errors and associated p-values for estimating stomatal conductance (Equation [2]) and PAI (Equation [3]).

Response	**Parameter**	**Estimate**	**Standard Error**	**P-Value**
g_s	β20	0.4799	0.0363	< 0.0001
g_s	β21	0.0994	0.0363	< 0.0001
g_s	β22	21.7665	1.8986	< 0.0001
PAI	β30	299.2520	72.8170	< 0.0001
PAI	β31	26.4640	20.2350	0.2094
PAI	β32	299.3480	316.5630	0.3584
PAI	β30	-2.7740	1.2770	0.0452

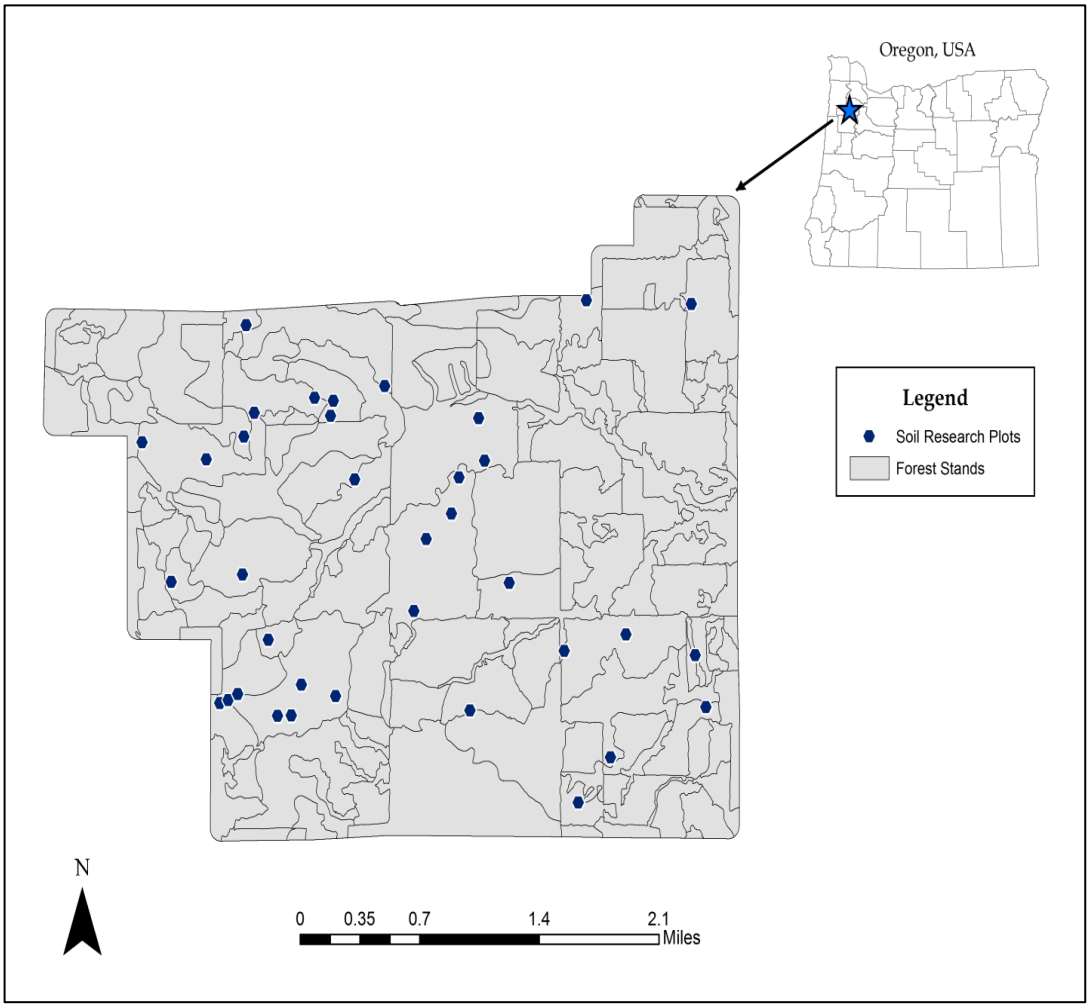

Figure 4-1: Map of the Panther Creek Watershed with location of soil research plots and delineation of individual forest stand

Figure 4-2. Plot mini-meteorological weather station established to collect soil volumetric water content (m^3/m^3) at 5 and 50 cm below the surface of mineral soil.

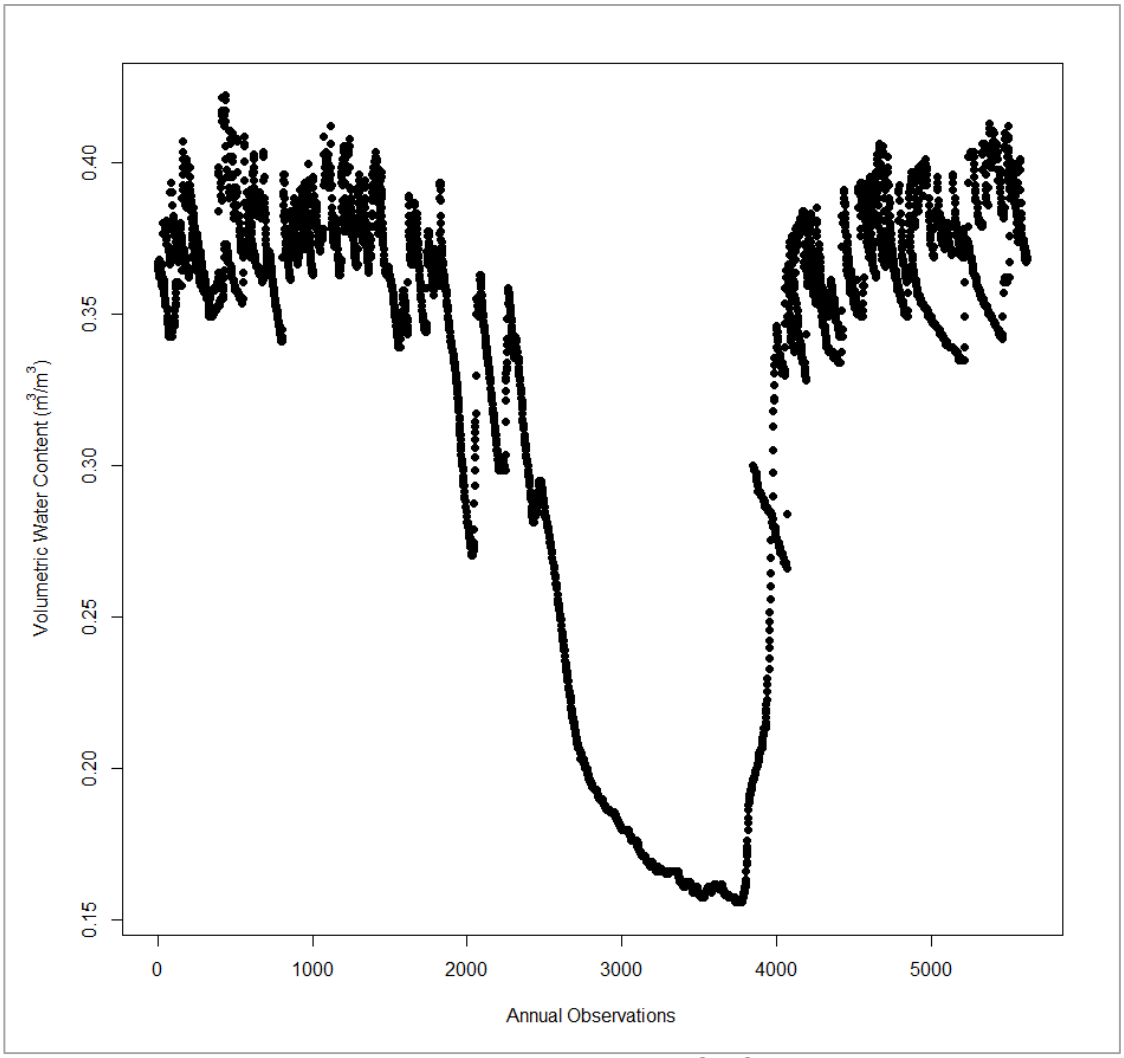

Figure 4-3: Raw soil volumetric water content data (m^3/m^3) collected at two-hour intervals from mini-meteorological station at each plot in 2012.

Figure 4-4: Mega-meteorological station established at Panther Creek for collecting detailed climatic data.

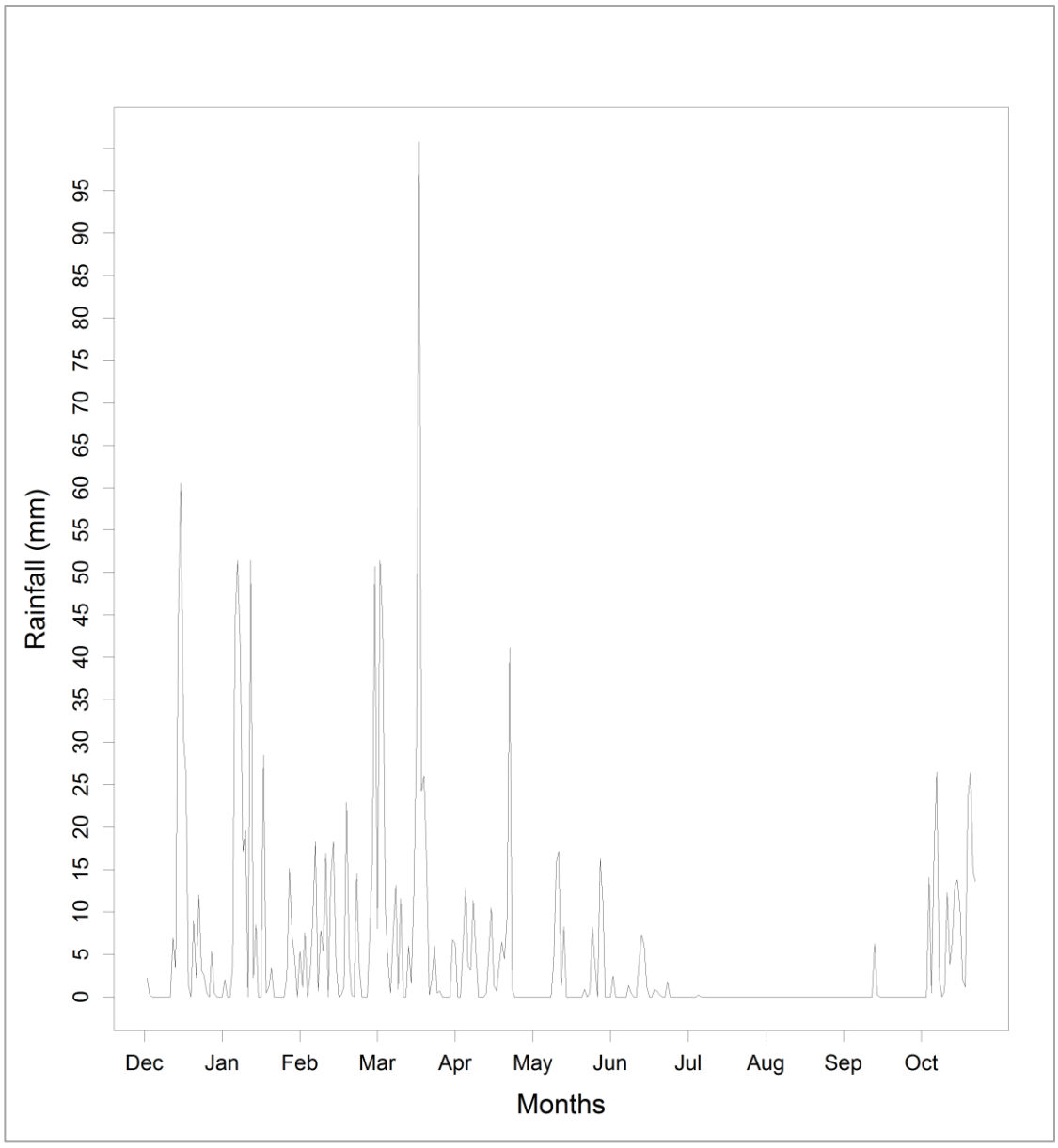

Figure 4-5. Daily total precipitation measured at the Panther Creek mega-meteorological weather station between December 2011 and October 2012.

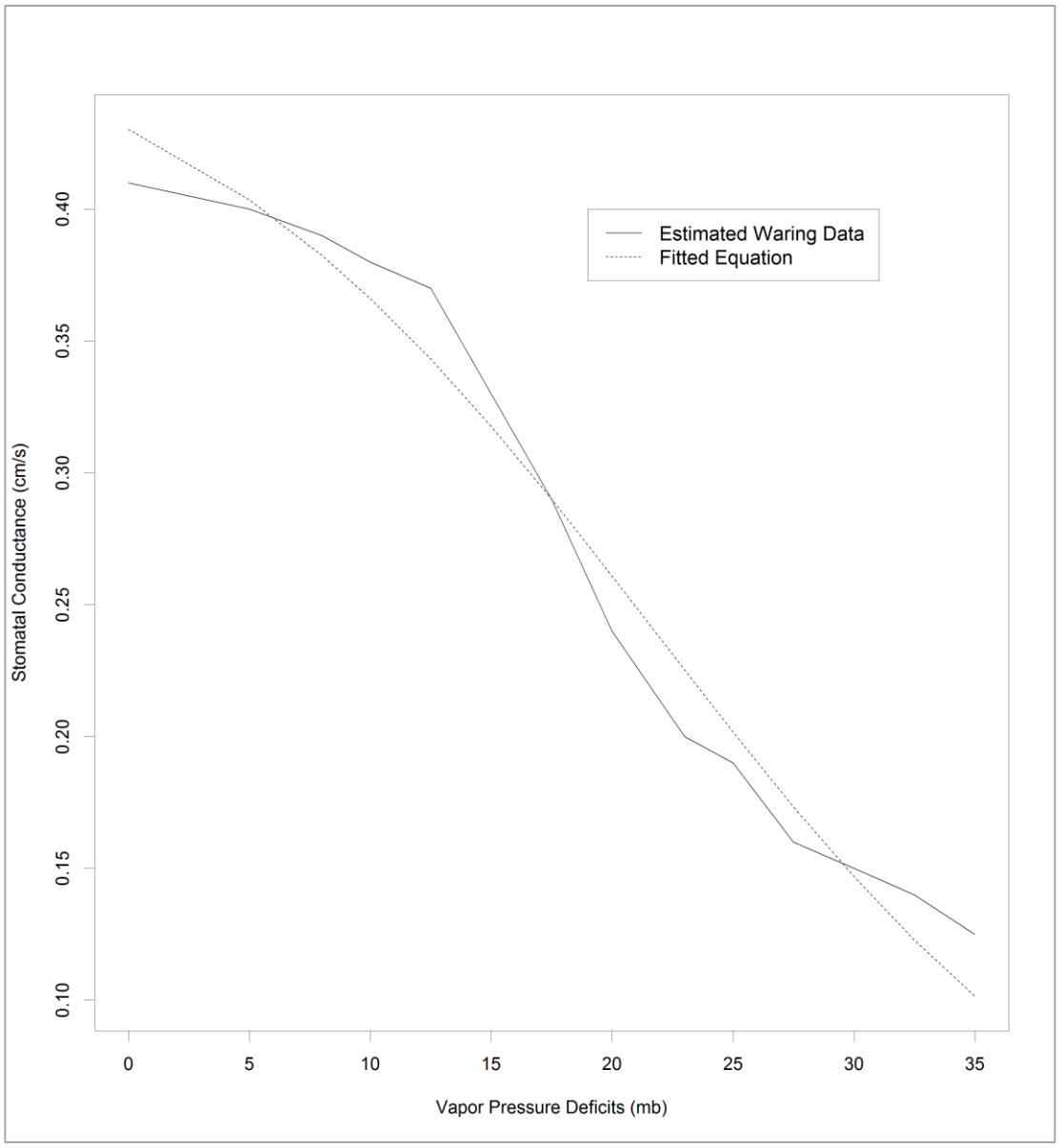

Figure 4-6. Modeled daily stomatal conductance against measured daily vapor pressure deficits.

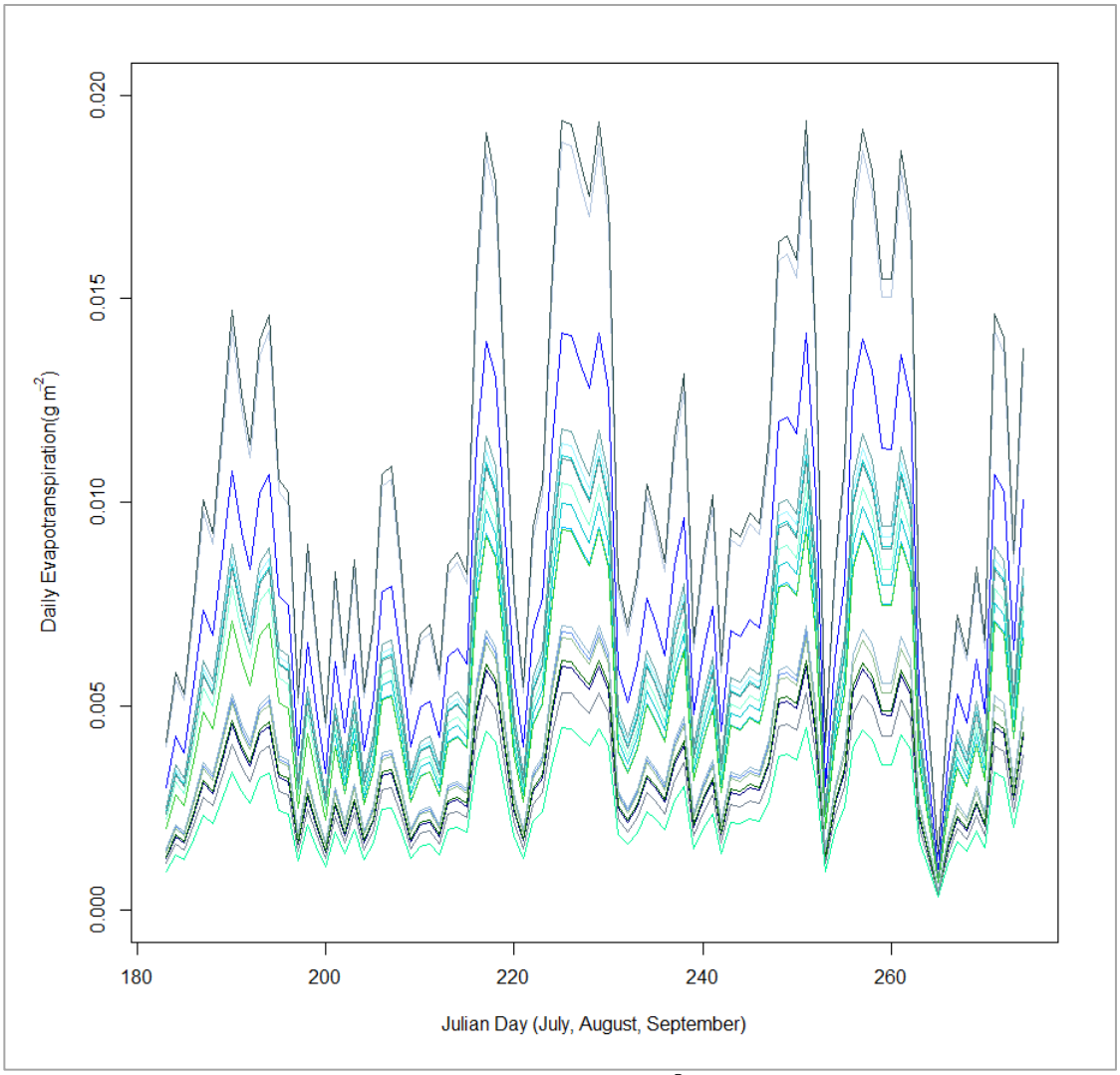

Figure 4-7. Daily simulated evapotranspiration (g m^{-2}) on each of 20 plots on the Panther Creek Watershed.

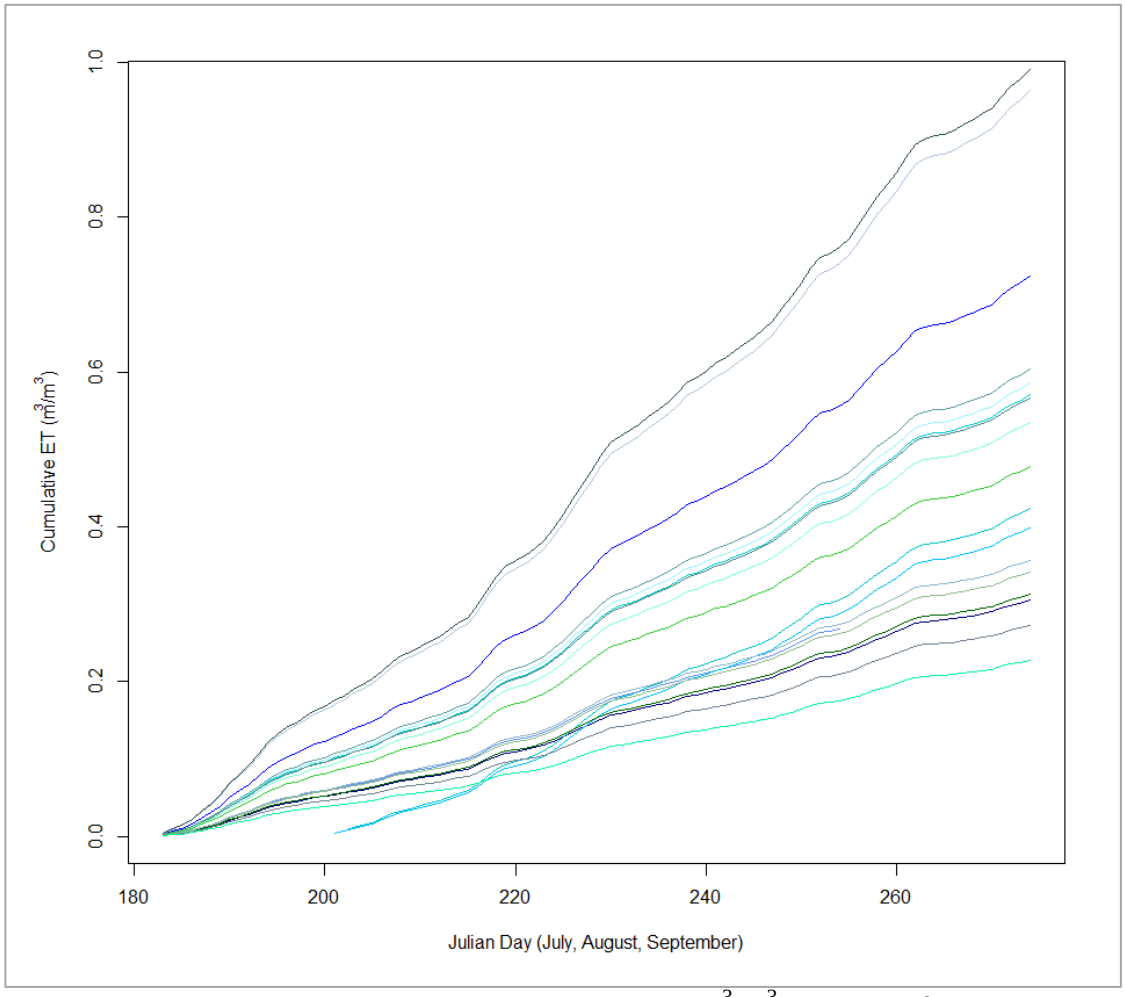

Figure 4-8. Simulated cumulative evapotranspiration (m^3/m^3) on each of 20 plots on the Panther Creek Watershed.

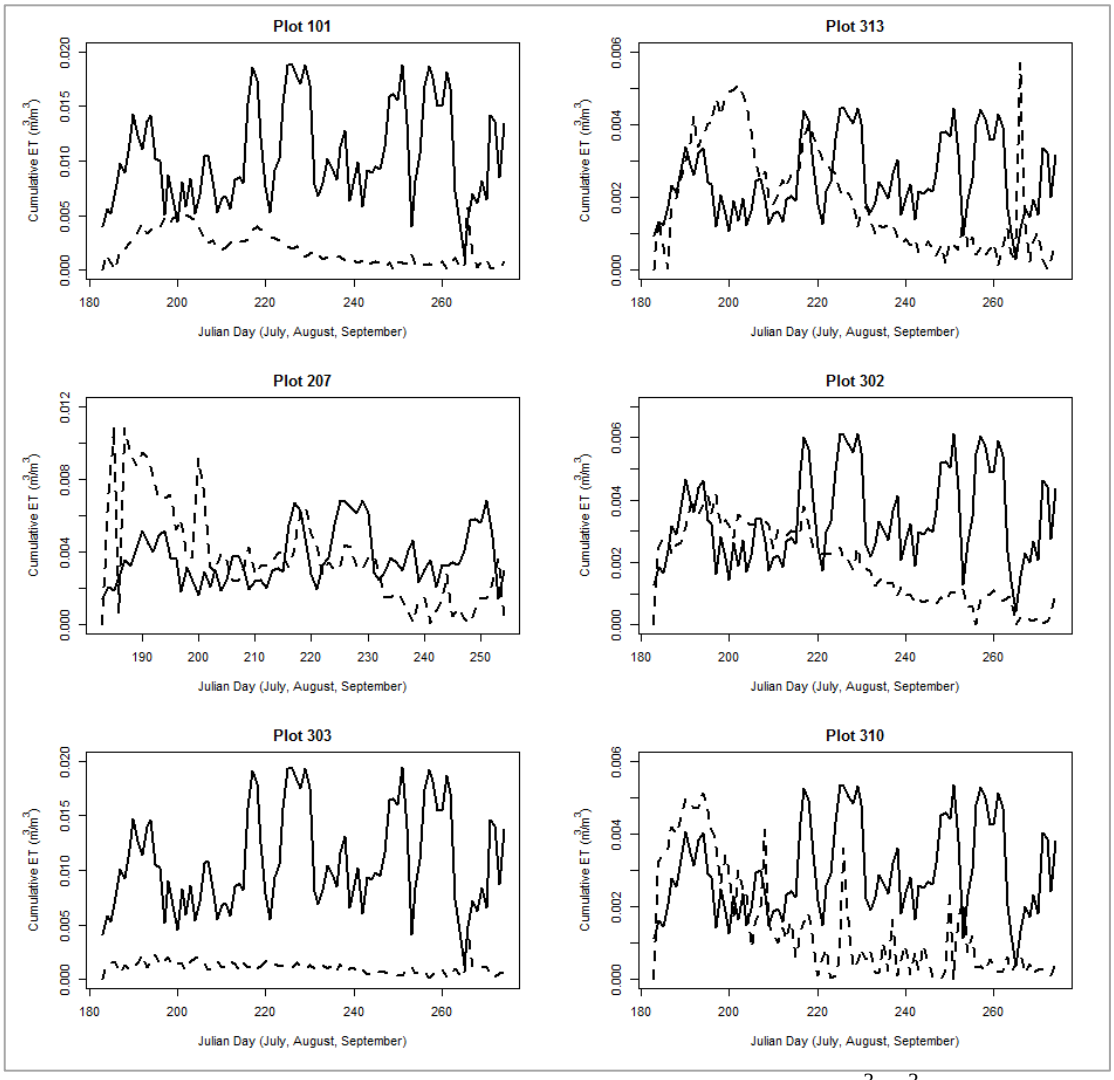

Figure 4-9. Comparison of cumulative daily evapotranspiration (m^3/m^3) estimated by the Penman-Monteith equation and cumulative daily soil water loss measured in soil at each plot

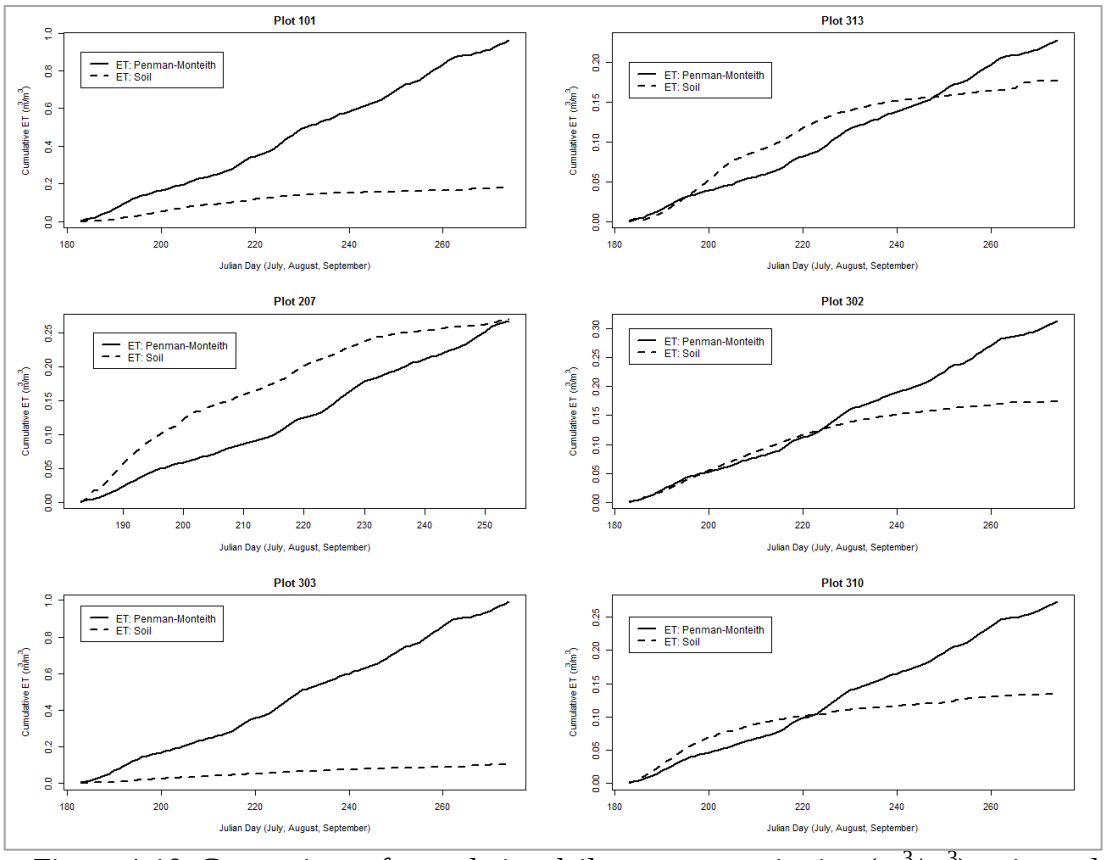

Figure 4-10. Comparison of cumulative daily evapotranspiration (m^3/m^3) estimated by the Penman-Monteith equation and cumulative daily soil water loss measured in soil at each plot.

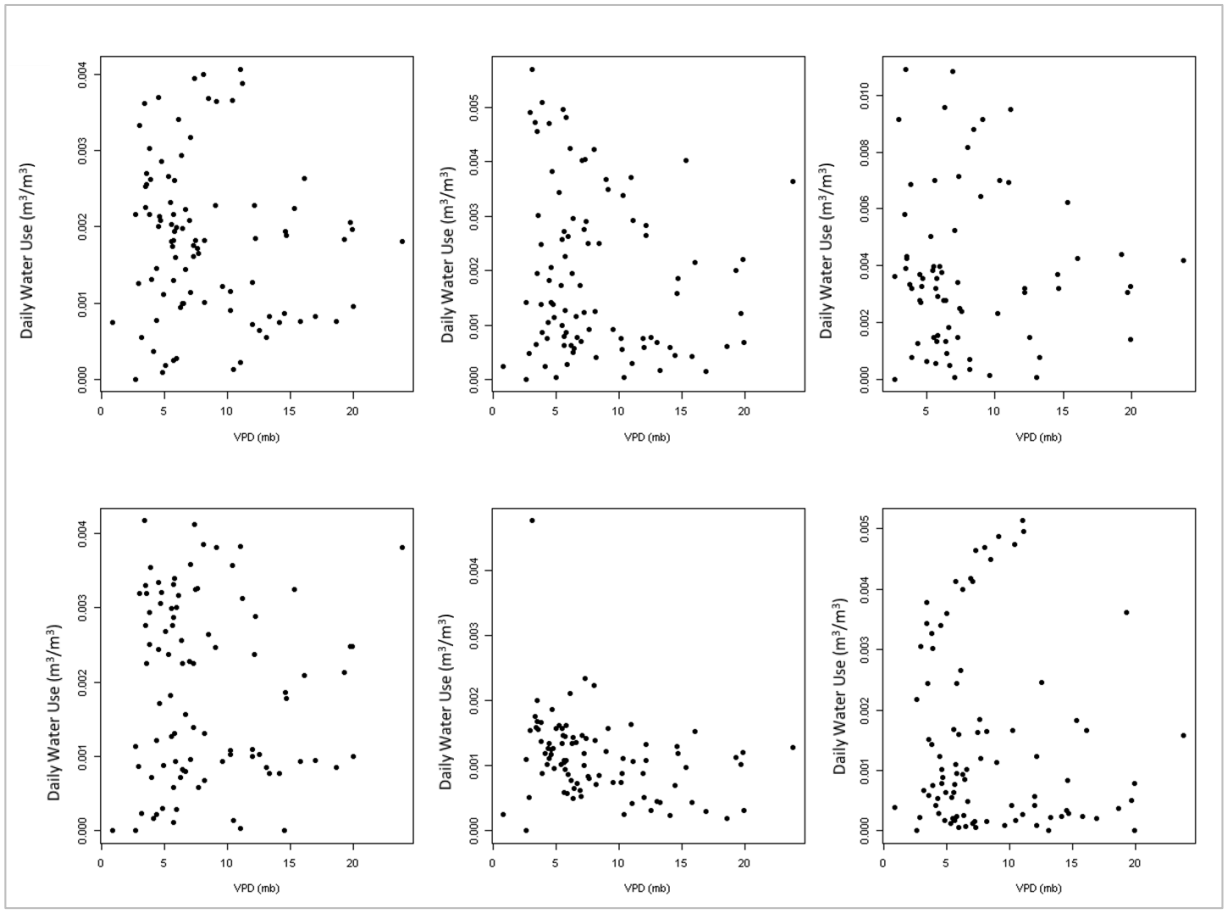

Figure 4-11. Comparison of daily water use (m^3/m^3) vs. daily vapor pressure defecits (mb).

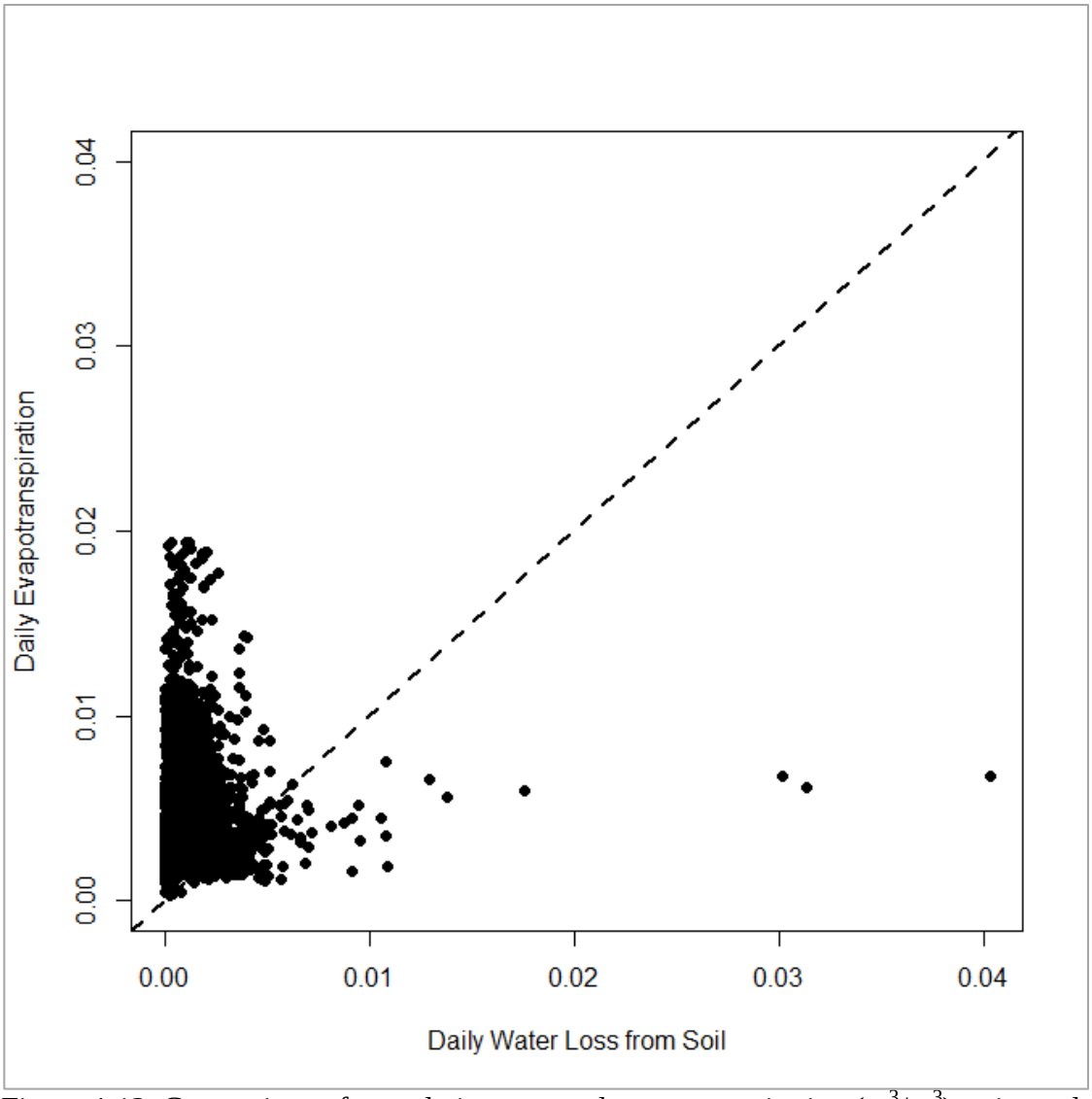

Figure 4-12. Comparison of cumulative seasonal evapotranspiration (m^3/m^3) estimated by the Penman-Monteith equation and cumulative seasonal soil water loss measured in soil at each plot

CHAPTER 5: CONCLUSIONS

This research provides a framework for assessing the ability of stand structural parameters, soil attributes, and climatic factors to predict forest evapotranspiration at the stand level. While many models have been developed to estimate forest evapotranspiration at regional and larger scales, forest hydraulic processes have significant potential if they can be adapted to scales relative to forest management. Important components of evapotranspiration were examined within Panther Creek, a relatively small watershed located in the eastern Oregon Coast Ranges.

Leaf area index (LAI) has been directly linked to productivity as it provides the surface over which water and carbon dioxide are exchanged between the plant and the atmosphere, and it is the surface area over which solar radiation is absorbed. As a result, any mechanistic models of forest productivity will be very sensitive to values of LAI. Improvements in estimation of this important parameter are essential to improvements in our ability to simulate gas exchange and photosyntheis.

The analysis completed in Chapter 2 compared estimates of leaf area index from three different but commonly employed methods. Two indirect estimates included estimation of LAI through light attenuation as measured by the Li-Cor 2200 Plant Canopy Analyzer, and application of leaf area to sapwood area ratios. LAI was also estimated with allometric relationships published in the literature and others developed specifically for trees within the Panther Creek Watershed. Indirect estimates were compared to LAI estimated from the foliage mass equations developed by destructively sampling a set of Douglas-fir trees at Panther Creek, with these latter estimates closest to true values.

Wide variability was apparent between indirect estimates of LAI and LAI estimated from foliage mass measured directly on Panther Creek sample trees. Li-Cor estimates differed from direct estimates by up to 40%. Underestimations by the Li-Cor instrument were attributed to departure from the assumption of randomly distributed

foliage assumed in values yielded by the instrument. Overestimation of LAI from the Li-Cor instrument probably resulted from occasionally heavy vine maple cover and inevitable shading by non-photosynthetic material. Calibration of the Li-Cor device will probably be necessary for practical application in stands of varying structure.

LAI estimated from sapwood area allometrics were consistently lower than from direct measurement of trees at Panther Creek. The best performing sapwood allometric was a simple conversion ratio of 0.66 m^2 of foliage for each cm^2 of sapwood area at crown base. The sapwood conversion ratio estimated LAI reasonably close to LAI estimated by destructive sampling, except at LAI estimates of eight or greater. Underestimation by sapwood allometrics for plots at the higher LAI may be attributable to more variable LA:SA ratios associated with structural differences associated with the older ages and taller heights on those plots.

In Chapter 3, soil moisture sensors associated with research plots characterized soil moisture draw down over the summer growing season among intensively managed Douglas-fir stands. Sensors measured soil volumetric water content (VWC) at 5cm and 50cm daily based on dielectric constant of the soil. To determined average daily VWC of the top 50 cm of the mineral soil, VWC at 25cm was linearly interpolated between 5cm and 50cm on each plot and for each day between July 1st and September 30th. Daily water loss from a given plot was the calculated as the difference between average VWCs on successive days. Daily water loss was generally regarded as a surrogate for daily evapotranspiration. Cumulative seasonal water loss was the cumulative daily water loss over the entire growing season.

Three models were fit to the data to help understand patterns in water loss. Two models were fit at a daily resolution, the first a model predicting daily water loss as a function of climate data measured from the on-site weather station. The second model fit daily water loss as a function of stand structural properties, soil attributes and climate data calibrated to each site through the Stage (1976) slope-aspect transformation. At a seasonal level water loss was predicted as a function of stand

structural attributes and soil properties. Predictive power was highest for daily water loss modeled by stand structural attributes, soil properties, and calibrated climate data. However, predictive power was low for all models due to a combination of relatively simplistic model forms and missing explanatory variables that would influence on soil water loss such as abundance of other tree species and competing vegetation. Likewise, VWC from the Decagon moisture sensors was not corrected for rock content.

In Chapter 4, daily and seasonal water loss calculated in Chapter 3 was compared to estimates of evapotranspiration simulated with a simple Penman-Monteith equation adapted by Tan et al. (1978) for a thinned Douglas-fir stand in British Columbia. Estimates were compared to determine if simulated evapotranspiration could be validated against soil water loss.

To use the equation developed by Tan et al. (1978), LAI was based on destructively sampled trees at Panther Creek (Chapter 2) and a simple estimate of daily stomatal conductance was derived from the reverse sigmoid relationship with daily vapor pressure deficits described by Waring and Franklin (1979).

Comparisons between evapotranspiration simulated with the Penman-Monteith equation and soil water loss over the growing season exhibited differences that varied greatly from plot to plot at both the daily resolution and seasonal resolution. The wide differences in water use estimated by the two methods suggested that additional work is needed to improve estimates of ET, estimates of soil water loss, or both.

In conclusion, simulated evapotranspiration with a simple Penman-Monteith equation was not adequate for estimating differences in soil water loss among plots in the Panther Creek watershed. Future work will seek to improve both estimates of gas exchange and estimates of soil water use at a scale that is useful for understanding forest productivity and how silvicultural regimes should be tailored to sites with specific combinations of soil and climatic conditions.

Appendix

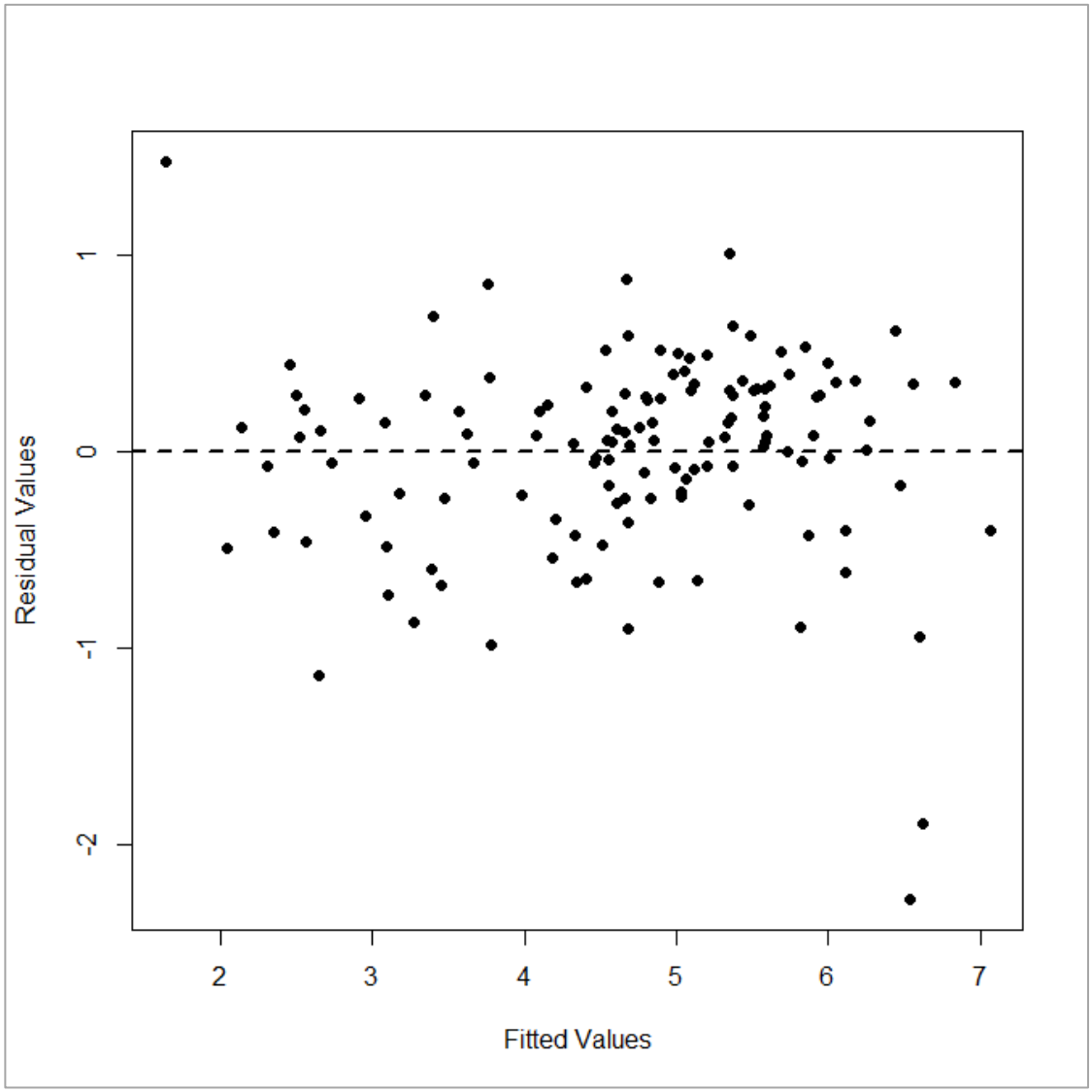

Figure 1. Fitted vs. residual plot for modeled daily water loss from climate variables (Chapter 2, Equation [3])

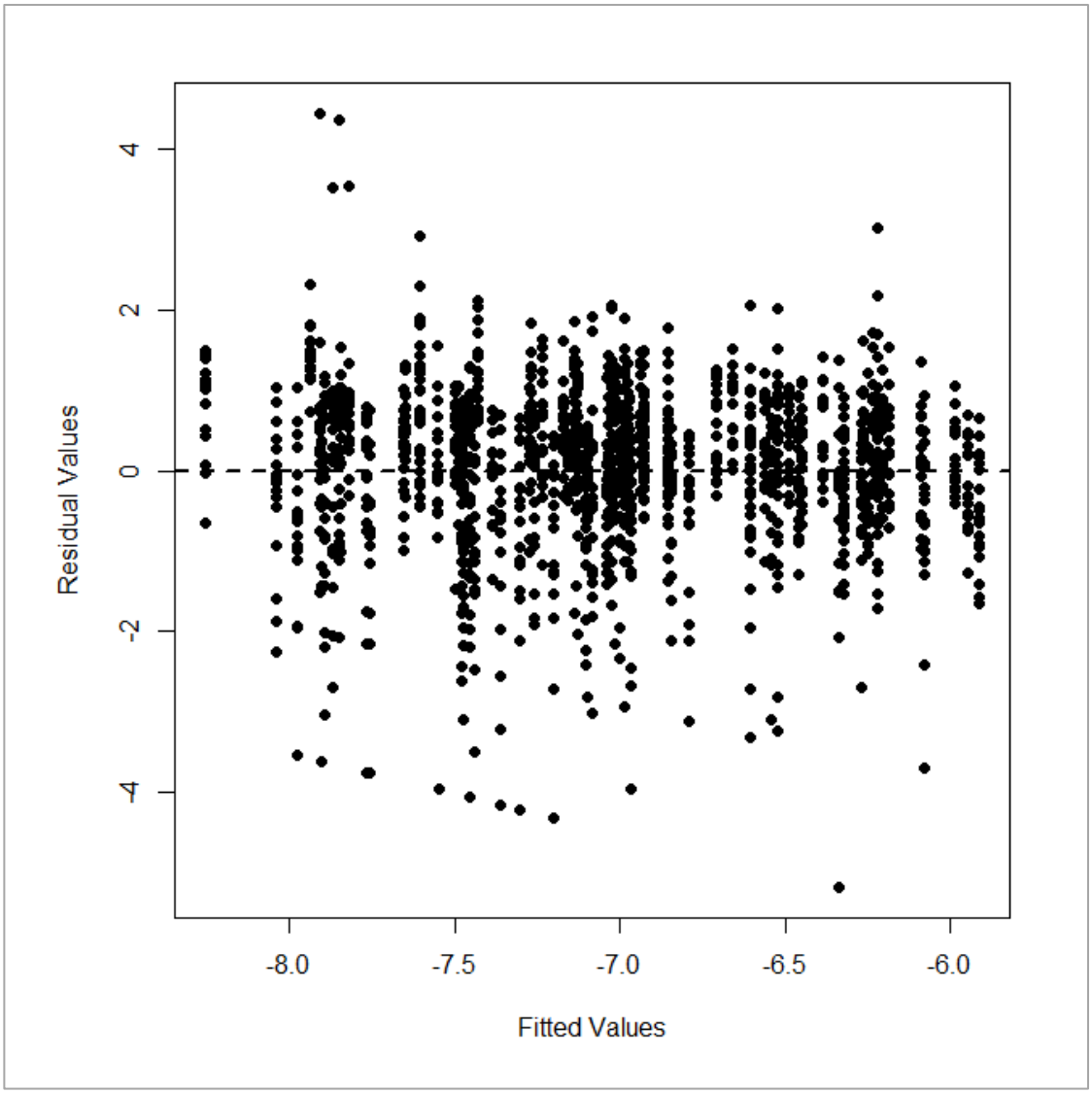

Figure 2. Fitted vs. residual plot for modeled daily water loss from climate variables (Chapter 3, Equation [2])

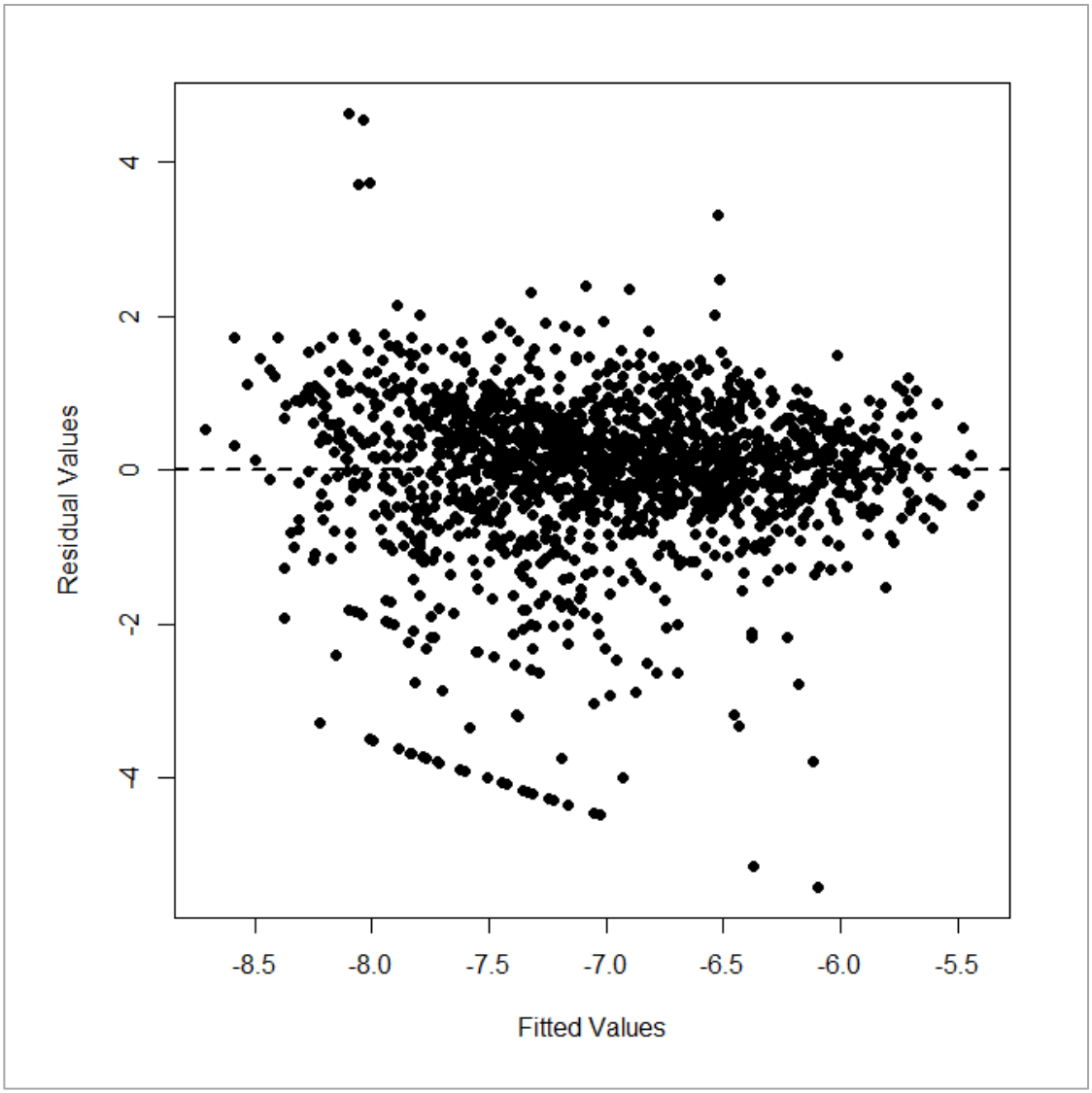

Figure 3. Fitted vs. residual plot for modeled daily water loss from climate, stand structural, and soil attributes (Chapter 3, Equation [2])

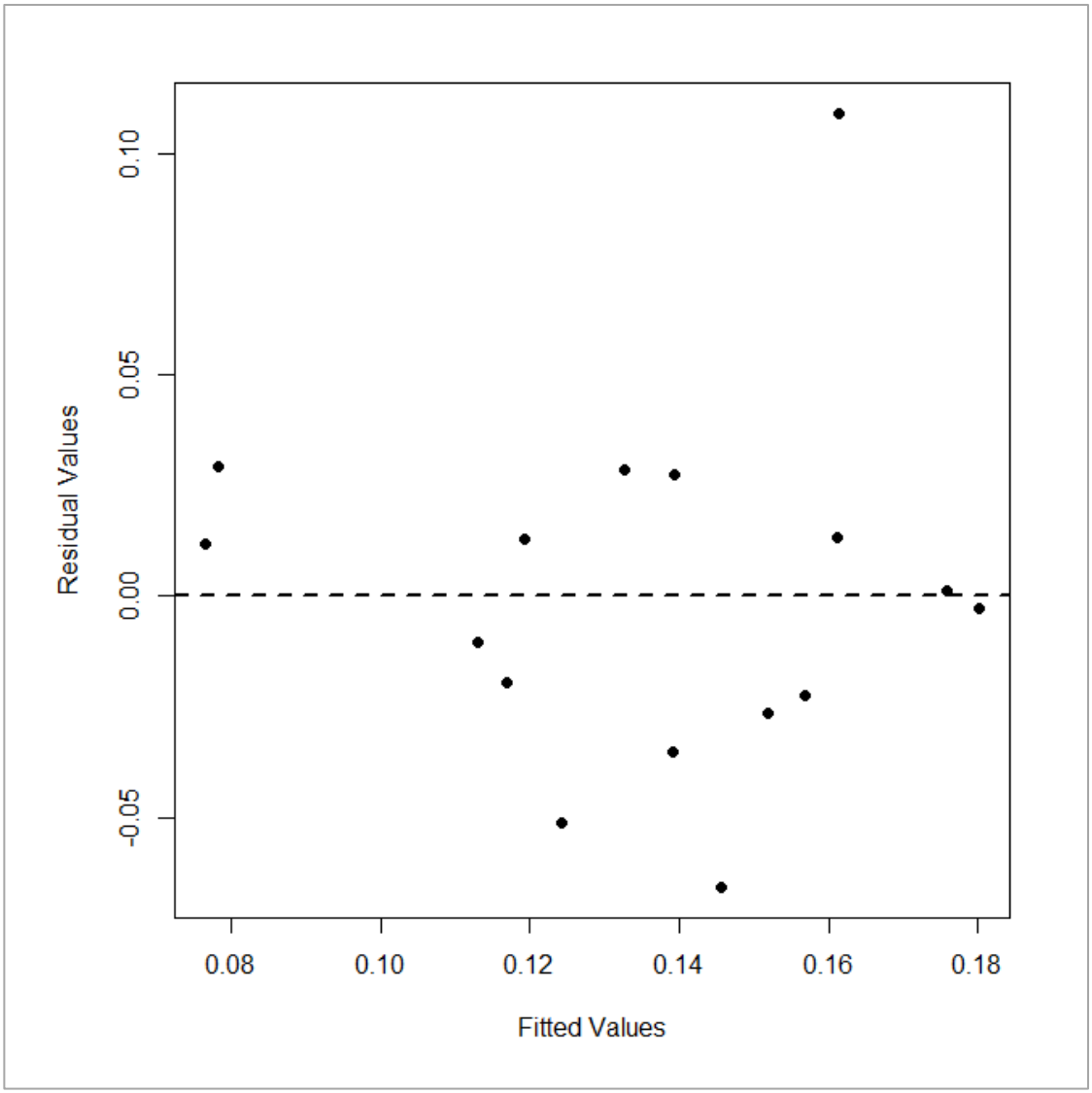

Figure 4. Fitted vs. residual plot for modeled cumulative water loss (Chapter 3, Equation [4])

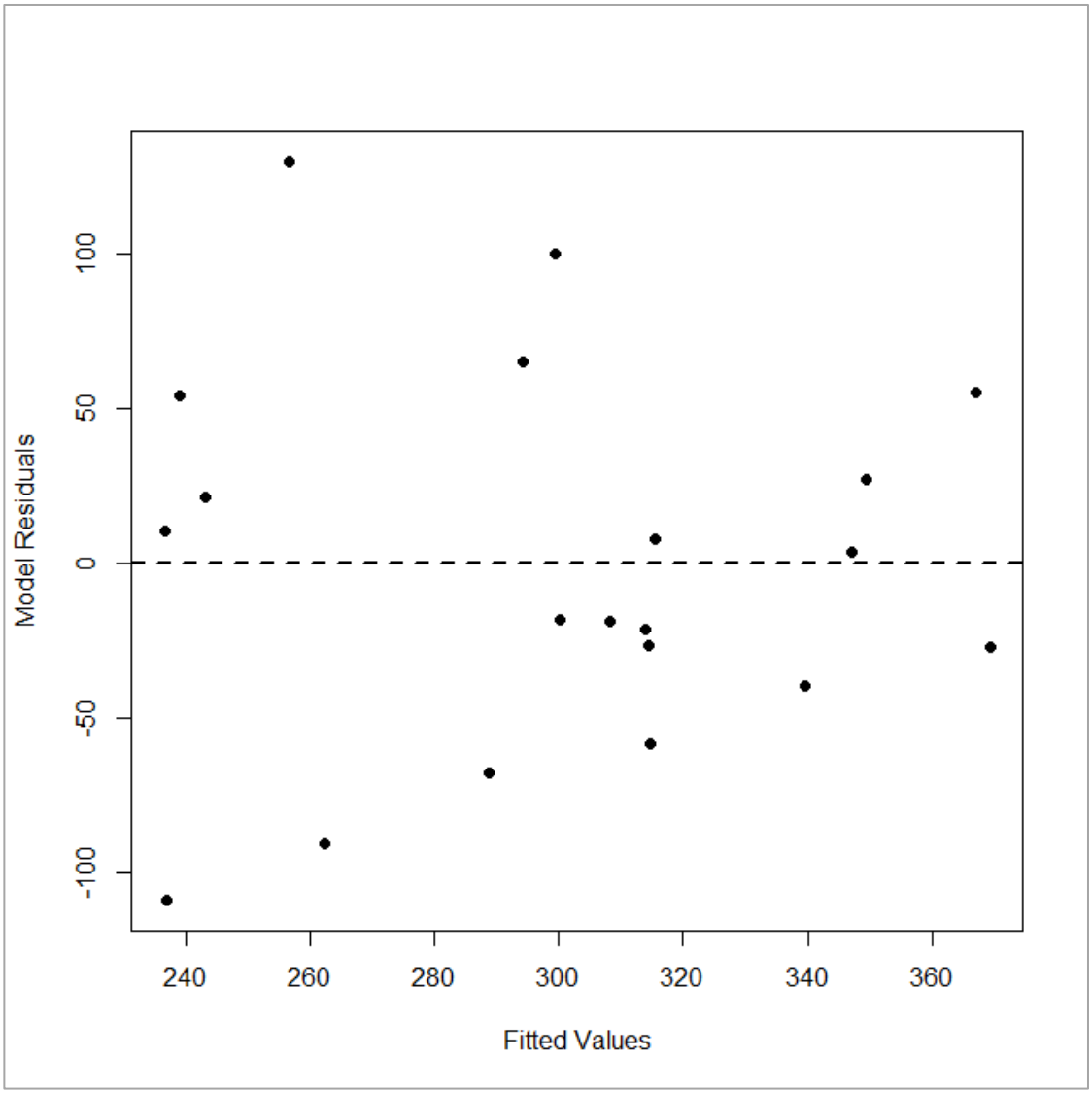

Figure 5. Fitted vs. residual plot for modeled PAI (Chapter 4, Equation [3])